Record 2002/08

Geological and morphological framework of the Norfolk Ridge to Three Kings Ridge region

George Bernardel, Leesa Carson, Sébastien Meffre
Phil Symonds and Alain Mauffret

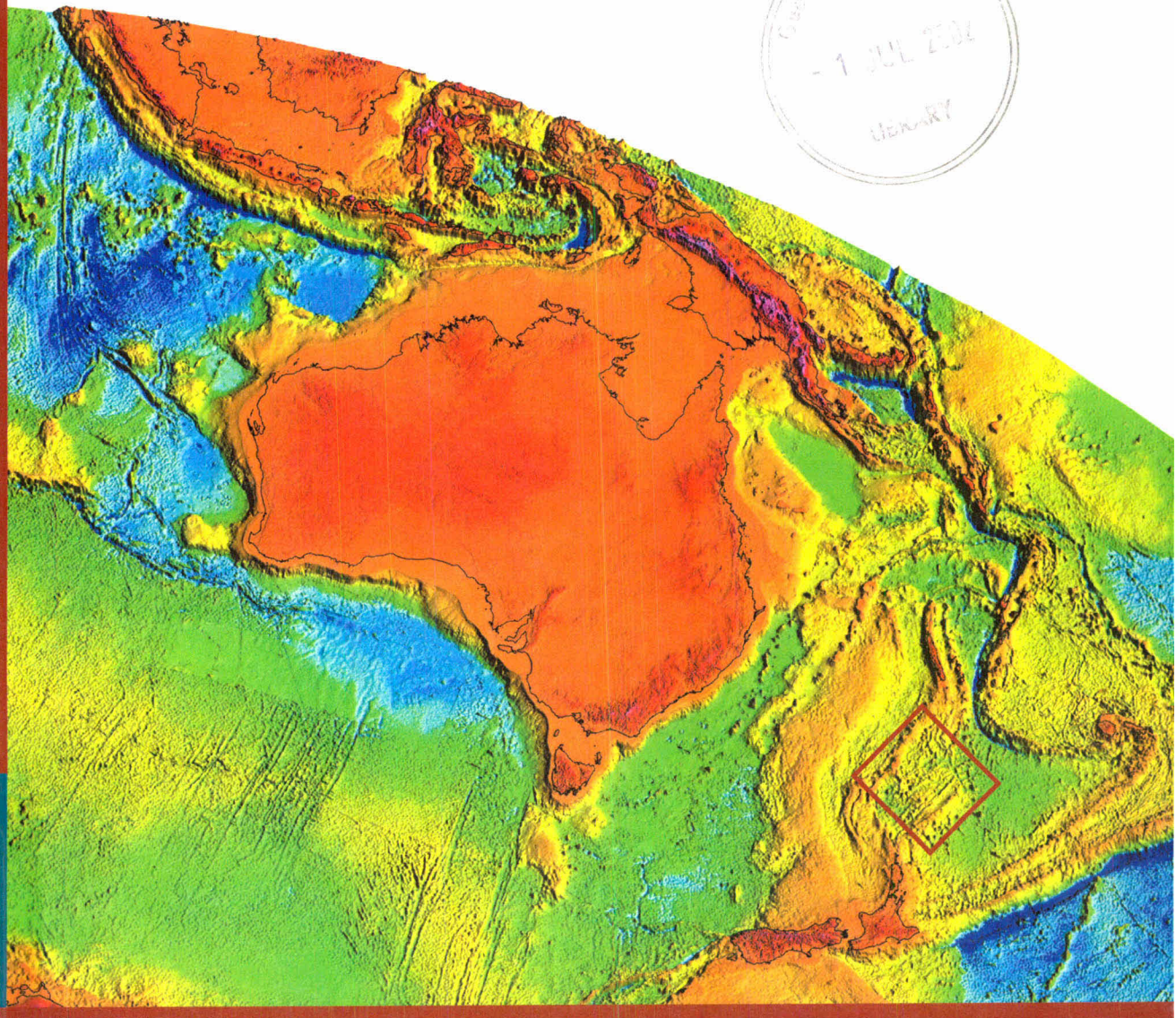

GEOSCIENCE Australia

SPATIAL INFORMATION FOR THE NATION

GEOSCIENCE AUSTRALIA

DEPARTMENT OF INDUSTRY, TOURISM & RESOURCES

GA Record 2002/08

Geological and morphological framework of the Norfolk Ridge to Three Kings Ridge region

George Bernardel, Leesa Carson, Sébastien Meffre[1]
Phil Symonds and Alain Mauffret[2]

Petroleum & Marine Division, Geoscience Australia,
GPO Box 378, Canberra ACT 2601

Canberra 2002

[1] *School of Earth Science, University of Tasmania, GPO Box 252-79, Hobart, Australia*
[2] *Université Pierre et Marie Curie, Paris VI, Paris, France*

Department of Industry, Tourism & Resources

Minister for Industry, Tourism & Resources: The Hon. Ian Macfarlane, MP
Parliamentary Secretary: The Hon. Warren Entsch, MP
Secretary: Mark Patterson

Geoscience Australia

Chief Executive Officer: Neil Williams

ISSN: 1039-0073
ISBN: 0 642 46737 4

Bibliographic reference: Bernardel, G., Carson, L.J., Meffre, S., Symonds, P.A. and Mauffret, A., 2002. *Geological and morphological framework of the Norfolk Ridge to Three Kings Ridge region*, Geoscience Australia Record, 2002/08.

Contents

List of Tables

Executive Summary

The marine geophysical survey FAUST-2 conducted in late 1999 was the second of two collaborative surveys involving the Australian Geological Survey Organisation (now Geoscience Australia) and the Institut Français de Recherche pour l'Exploitation de la Mer. The aim of the FAUST-2 survey was to study the seafloor morphology, underlying geological framework and tectonic evolution of the area east of Norfolk Island. The derived interpretations will clarify the extent and nature of possible Australian and French extended Continental Shelf beyond the respective Exclusive Economic Zones to support claims under the United Nations Convention on the Law of the Sea.

The FAUST-2 survey area refers to the part of the southwest Pacific largely bounded by longitudes 166°E to 175°E and by latitudes 25°S to 31°S, lying midway between New Caledonia to the north and New Zealand to the south. This area stretches from the Norfolk Ridge to the west, across to the Three Kings Ridge and South Fiji Basin to the east, and includes parts of the intervening North and South Norfolk Basins. The FAUST-2 survey acquired about 186 000 km^2 of multibeam bathymetry and 12 500 km of high-resolution seismic data as well as a suite of rock samples from three dredge sites.

Seven morphological provinces are distinguished within the FAUST-2 survey area largely on the basis of depth and their relationship to large-scale tectonic features and boundaries: the Three Kings Ridge Province over the elevated Three Kings Ridge feature; the Forster Province over a deep and relatively featureless oceanic basin; the Cagou Trough Province over an elongate trench-like feature along the western edge of the Three Kings Ridge feature; the Norfolk Province over a zone of mostly subdued seafloor to the east of Norfolk Ridge; the Nepean Province over an extended spur- and saddle-like feature of the Norfolk Ridge; the Cook Province over the Cook Fracture Zone and adjoining faulted seafloor; and the Kingston Province covering a large area of seafloor characterised by a zone of elevated seafloor split by two major elongate and broad depressions.

The FAUST-2 survey area has complex geology reflecting the tectonic evolution of Eocene subduction and collision followed by Oligocene extension and seafloor spreading. A first-pass interpretation of widespread volcanism, rift, deep-extensional and other faulting and the presence of several seismic sequences indicate a period of rapid extension involving seafloor spreading and intra-plate re-adjustments following a period of island-arc collision. The presence of mantle-derived rocks in the FAUST-2 dredges supports the idea of rapid post-orogenic collapse.

The combination of interpretations of the FAUST-2 geophysical and geochemical data with data from previous studies has enabled a revised tectonic model for the Norfolk Ridge – Three Kings Ridge area. The model proposes an east-dipping subduction of a probable Cretaceous basin, which was floored by oceanic or transitional crust. Cessation of subduction along the Three Kings Ridge in the Oligocene was followed by a major extensional phase associated with seafloor spreading in the North Norfolk Basin.

Introduction

We report here a study of the morphological and geological framework of the FAUST[1]-2 survey area and adjoining seafloor. The FAUST-2 survey area refers to that part of the southwest Pacific largely bounded by longitudes 166°E to 175°E and by latitudes 25°S to 31°S, lying midway between New Caledonia and New Zealand to the north and south, respectively (Figs 1-5). The survey area stretches from the Norfolk Ridge, in the west, across to the Three Kings Ridge and South Fiji Basin, in the east, and includes parts of the intervening North and South Norfolk Basins.

The FAUST-2 survey area is situated in a broad zone of the Indo-Australian Plate along a convergent boundary with the Pacific Plate. This zone reflects a complex multi-stage cyclic process of compressional and extensional tectonics related to the fragmentation of eastern Gondwana from the Jurassic through to the present. The fragmentation process is reflected regionally in the parallel ribbon-like development of vast tectonic provinces (Figs 1 & 2). The survey area is about 500 km distant from the nearest plate boundary section. The geological relationships in the survey area developed in response to this complex tectonic process in the period from the Cretaceous to the Oligocene and continues to be affected by the dynamics of regional macro- and micro-plate adjustments.

The designation "FAUST-2" for the survey area is given in recognition of the large quantity of geophysical data acquired in 1999 on a multibeam bathymetry and geophysics survey[2] (Mauffret & Symonds et al., 2001). This was the second of two collaborative surveys resulting from an agreement reached between the Australian Geological Survey Organisation (AGSO; now Geoscience Australia) and the Institut Français de Recherche pour l'Exploitation de la Mer (IFREMER) in Canberra, Australia, in October 1998. The first survey, FAUST-1[3] (Lafoy et al., 1998; Bernardel et al., 1999), acquired some 4600 km of deep-seismic data across the entire region from the eastern Australian margin to the New Hebrides Trench. The FAUST-2 survey concentrated on acquiring about 186 000 km^2 of multibeam bathymetry and 12 500 km of high-resolution seismic data, as well as a suite of rock samples from three dredge sites largely in the area directly to the east of Norfolk Island (Fig. 3). Satellite-derived gravity (Sandwell & Smith, 1997), and geophysical data acquired by AGSO Survey 177 (Ramsay et al., 1997), show that this area has complex bathymetry and geology.

The broad objectives of the FAUST-2 survey were two-fold:

1. to obtain a clearer understanding of the morphological setting, geological framework, tectonic evolution, resource potential, and future environmental and resource management issues within the region bounded by the Norfolk Ridge to the west and the Three Kings Ridge to the east; and

[1] FAUST refers to the collaborative France-Australia program "France-AUstralia Seismic Transect".
[2] For GA database purposes the FAUST-2 multibeam survey is known as GA Survey 221.
[3] For GA database purposes the FAUST-1 seismic survey is known as GA Survey 206.

2. to examine the extent and nature of possible Australian and French extended Continental Shelf to the east and southeast of their respective Exclusive Economic Zones.

The broad objectives of the earlier AGSO Survey 177 were also two-fold:

1. to better understand the complex bathymetry and underlying geology of the wider southern Lord Howe Rise to south-eastern South Fiji Basin region; and

2. to examine the extent and nature of possible Australian and New Zealand extended Continental Shelf to the east and north-to-northeast of their respective Exclusive Economic Zones.

In response, this report will focus on the following five major objectives:

1. to detail the seabed physiography revealed by the multibeam data, which was partly presented in Mauffret & Symonds et al. (2001);

2. to examine the seismic data for tectono-stratigraphic sequences;

3. to characterise the area into structural lineaments and provinces;

4. to examine the dredge samples for geochemical and chronological markers; and

5. to propose a model for the tectonic evolution of the wider region.

The new data sets provide a means to reveal the structural framework of the surveyed area, as the sediment cover is relatively thin and readily responds in form to basement movements. The high-resolution swath-track seismic data, in conjunction with the detailed bathymetry, allows for a detailed structural interpretation. The deep-crustal view of the AGSO Surveys 177 and 206 seismic, along with the petrology, geochemistry and isotopic dating of the FAUST-2 dredge samples, provide additional indicators for the presence of deep crustal material at the seafloor. An interpretation of the wider geological setting is not possible without using other regional geological and geophysical data in conjunction with ideas developed in the literature.

The area between New Caledonia and northern New Zealand has many indicators of an early collision and later separation event between the Three Kings Ridge and Norfolk Ridge systems. This has to be viewed in the overall tectonic setting for the wider southwest Pacific which involves a complex spatial and temporal interplay of various stages of probable continental/oceanic rifting, collision, island-arc and back-arc basin development, subduction, obduction and major transcurrent motions. The general tectonic setting for New Caledonia and northern New Zealand is well developed. However, the tectonic setting of the study area remains largely conjectural. This report, therefore, represents the first attempt at modelling the tectonic evolution for this region using the new AGSO and IFREMER collaborative data sets.

The discussion below commences with a general review of the literature presenting the evolution of ideas for both the survey area and wider regional setting. This discussion is followed by: a short description on the data and interpretative methodologies used; a detailed physiographic description of the newly-mapped seafloor; a discussion on tectono-stratigraphic markers; a discussion on the geological structures in the newly-surveyed area; a detailed analysis of the FAUST-2 dredge samples; a new tectonic evolution model; and a brief discussion on resource potential.

Previous Work

The Norfolk Ridge – Three Kings Ridge region was sparsely covered by marine scientific surveys prior to 1996. The New Zealand Oceanographic Institute 1966 cruise collected bathymetry and magnetic data to interpret the structure and geological history of the Lowe Howe Rise – New Caledonia Basin – Norfolk Ridge area (van der Linden, 1967). Shor et al. (1971) interpreted the northern sector of the Norfolk Ridge from refraction velocities. Geophysical studies (seismic reflection, seismic refraction, magnetics and gravity) collected by the Mobile Oil Corporation and Bundesanstalt für Geowissenschaften und Rohstoffe, covered the southern and central areas of the Norfolk Ridge (Eade, 1988). Zhu and Symonds (1994) and Herzer et al. (1997) undertook gravity modelling from the West Norfolk Ridge across to the Reinga Basin, at the southern end of the Norfolk Ridge.

More recent seismic data acquired in the survey area include: GEORSTOM, AUSTRADEC, Lamont-Doherty Vema and Deep-Sea Drilling Project (DSDP) GLOMAR CHALLENGER data (Launay et al., 1982; Kroenke & Dupont, 1982; Kroenke & Eade, 1982). In 1996, as part of the collaborative program to support marine jurisdiction claims, AGSO and the New Zealand Ministry of Commerce acquired over 4000 km of deep-seismic, gravity, magnetic and echosounder bathymetry data in the region (Ramsay et al., 1997). The collaborative France/Australia FAUST-1 survey in 1998 surveyed the northern parts of the Lord Howe Rise – Norfolk Ridge region collecting four deep-seismic lines and other geophysical data (Lafoy et al., 1998; Bernardel et al., 1999).

Direct geological information on the survey area is limited. The geology of the northern and southern regions of the Norfolk Ridge is known from studies on New Caledonia (eg Paris, 1981; Brothers & Lillie, 1988), and Northland, New Zealand (eg Spörli & Kear, 1989). The central region of the Norfolk Ridge is limited to geological and geophysical interpretations and gravity measurements on Norfolk Island (Jones & McDougall, 1973; Abell & Taylor, 1981; Williams & Murray, 1985). Mortimer et al. (1998) have undertaken detailed petrology, geochemistry and isotopic studies on 18 rocks dredged from the southern Norfolk Ridge – Three Kings Ridge area.

Geological Setting

The geological interpretation and tectonic evolution of the Norfolk Ridge – Three Kings Ridge region remains contentious. The study area cannot be understood in isolation from the wider geological setting of the southwest Pacific and eastern Australia. The region has undergone a complex process of continental margin development, from crustal compression and accretion, through passive margin extension, breakup and seafloor spreading, to present-day convergence (Symonds et al., 1996, 1999). A summary of the tectonic events for the southwest Pacific and eastern Australia is tabulated in Appendix 2.

Regional setting

An extensional terrane developed through eastern Australia in the Late Jurassic – Palaeogene in response to the fragmentation and dispersal of Gondwana. Rifting between Australia and Antarctica, and probably onto Lord Howe Rise occurred in the Late Jurassic – Early Cretaceous (Symonds et al., 1999). The transition from convergence to divergence was characterised by extensional/transtensional magmatism near the locus of the future Tasman breakup during the Barremian – Cenomanian (~120-95 Ma; Symonds et al., 1999). A major rift system developed along the eastern Australia continent in the Cenomanian – Campanian (~95-80 Ma), with the Lord Howe Basin, Middleton Basin, Tasman Basin, New Caledonia Basin and possibly the South Loyalty Basin starting to open (Symonds et al., 1999; Auzende et al., 2000). During the Campanian – Eocene (~80-52 Ma) extension continued with the Challenger Plateau, Lord Howe Rise, Norfolk Ridge and North Island, New Zealand separating from Australia (Gaina et al., 1998). Following the break up, most of the rift basins off eastern Australia received sag-phase sediments, and many were affected by compressional reactivation episodes due to changes in intraplate stress fields (Symonds et al., 1999). Convergent tectonism (ie collision, obduction, subduction and associated back-arc spreading) re-commenced along the eastern margin of the Australian plate from New Guinea through New Caledonia to New Zealand during the Eocene – mid Oligocene (Symonds et al., 1999). A change in the Indo-Australia Plate and Pacific Plate motions in the mid to late Eocene (~ 43 Ma) may have been sufficient to initiate the Tonga-Kermadec arc activity.

FAUST-2 survey area setting

The Norfolk Ridge is a major submarine feature extending from New Caledonia south to Northland, New Zealand (Eade, 1988). There is general consensus that the Norfolk Ridge represents rifted Gondwana continental crust (Eade, 1988; Willcox et al., 1989; Eissen et al., 1998; Mortimer & Herzer, 2000). The breakup of the eastern margin of Gondwana occurred during the Late Cretaceous to Early Eocene (Eade, 1988; Black, 1996, Symonds et al., 1996). Other hypotheses on the evolution of the Norfolk Ridge include an arc system (Dubois et al., 1974; Kroenke, 1984) and arc migration with marginal basin development (Karig, 1970; Packham & Falvey, 1971).

During the Early Eocene to Oligocene, convergence at the plate boundary occurred along the Norfolk Ridge (Eade, 1988, Symonds, et al., 1996). New Caledonia is thought to have been shaped by a collision between a thinned continental margin and an island-arc at an east-dipping subduction zone (Meffre et al., 1993; Aitchison, et al.,

1995; Cluzel, 1998). The attempted subduction of the island arc resulted in the obduction of an ophiolitic nappe from the northeast during the Late Eocene (42-36 Ma). The development of the collision zone can be traced southwards to New Zealand (Aitchison et al., 1995). In Northland, New Zealand, sedimentary rocks and ophiolites are obducted from the northeast in the late Oligocene (25-22 Ma) to form the Northland Allochthon (Malpas et al., 1992). Partly overlapping the obduction in Northland is Miocene arc volcanism (22-16 Ma; Herzer, 1995).

The Three Kings Ridge is considered to be a product of arc volcanism (Kroenke & Dupont, 1982; Davey, 1982; Herzer & Mascle, 1996). Rocks dredged from the Three Kings Ridge have been identified as subduction-related basalts and shoshonites (Mortimer et al., 1998). Shoshonite and basalt Ar-Ar radiometric ages established a firm Early Miocene age (~20 Ma) for igneous activity, however the duration of arc activity is unknown (Mortimer et al., 1998). The Loyalty Ridge to the north is thought to be a continuation of the Three Kings Ridge, which was separated by sinistral displacement along the Cook Fracture Zone (Lapouille, 1977). Mortimer and Herzer (2000) suggest that the Three Kings Ridge is a continuation of the Northland arc.

Other interpretations of the Three Kings Ridge include an extinct mid-ocean ridge (van der Linden, 1967), a remnant arc that the Lau Ridge was rifted off as the South Fiji Basin formed (Launay et al., 1982) and a submarine ridge ("third arc") that formed due to crustal compression behind a volcanic ridge (Karig, 1970).

The North and South Norfolk Basins are interpreted as a back-arc basin to the Three Kings Ridge (Launay et al., 1982; Herzer & Mascle, 1996). Dolerites and basalts dredged from the North and South Norfolk Basins are mineralogically and chemically compatible with them forming in a back-arc basin setting (Mortimer et al., 1998). Eade (1988) suggested that a remnant piece of the Cretaceous Pacific Plate was trapped between the Norfolk Ridge and the Three Kings Ridge, which extended along the eastern margin of the Norfolk Ridge from New Caledonia to Northland, New Zealand and included the North and South Norfolk Basins and the South Loyalty Basin.

The southern margin of the South Norfolk Basin is marked by a continental-ocean transform fault, termed the Vening-Meinesz Fracture Zone (Fig. 3). The Vening-Meinesz Fracture Zone is a zone of northwest-striking stepped faults acting as a dextral-slip transform associated with the opening of the North and South Norfolk Basins and the eastward migration of the Three Kings Ridge (Herzer & Mascle, 1996). The North Norfolk Basin and the Three Kings Ridge are terminated abruptly in the north by the northwest-trending Cook Fracture Zone, which is described as a sinistral strike-slip fault (Tajima & Okal, 1995).

The age of the North and South Norfolk Basins is speculative. A Late Cretaceous age is suggested based on magnetic anomalies 34 and 33 over the basins, the depth to basement and the age of obducted crust in Northland, New Zealand (Launay et al., 1982; Eade, 1988). Kroenke (1984) speculated that the basins formed during the Late Eocene. An Early – Late Miocene back-arc spreading event in the South Norfolk Basin is proposed by Herzer and Mascle (1996) and Herzer et al. (1997). Radiometric dating of an intraplate seamount (ie dredge GO345 – see Table 4) supports the

argument that the South Norfolk Basin was opening or opened by at least 18-20 Ma (Mortimer et al., 1998).

There are a number of models proposed for the evolution of the Norfolk Ridge – Three Kings Ridge region.

One model proposes that the Three Kings Ridge is the volcanic arc product of Late Oligocene or Miocene west-dipping subduction (Herzer & Mascle, 1996 and Mortimer et al., 1998, respectively). Herzer and Mascle (1996) described the Three Kings Ridge as being connected to the Norfolk Ridge with South Fiji Basin crust subducting westwards below the ridge. The Vening-Meinesz Fracture Zone facilitated the opening of the back-arc basin (ie South Norfolk Basin) and the southeast migration of the Three Kings Ridge (Herzer & Mascle, 1996). Herzer (1995) interpreted the obduction of the Northland allochthon and arc volcanism along Northland, New Zealand as resulting from southwest-dipping subduction of the South Fiji Basin. Mortimer and Herzer (2000) suggest a rapid opening of the back-arc basins (ie Norfolk and South Fiji Basins) associated with trench retreat of a west-dipping subduction zone.

Lapouille (1977, 1978) proposed that the Three Kings Ridge and the Loyalty Ridge were the result of two successive episodes of subduction. An early Tertiary eastward subduction of the Indo-Australian Plate beneath the Pacific Plate was followed by an Early Miocene westward subduction of the Pacific Plate. Malpas et al. (1992) supported the subduction flip for the case of a short-lived east-dipping subduction changing to a west-dipping subduction.

Several authors have proposed an east-dipping subduction zone with the Three Kings Ridge representing an island-arc (Lapouille & Dugas, 1975; Kroenke & Eade, 1982; Smith, 2000). Topographic changes along the Three Kings Ridge may indicate that subduction in the north changes to obduction along the southern half of the ridge (Kroenke & Eade, 1982). A significant proportion of the North and South Norfolk Basins had been subducted under the Three Kings Ridge, while the obduction destroyed trench morphology and resulted in intense deformation and overthrusting of the forearc basin (Kroenke & Dupont, 1982; Kroenke & Eade, 1982). The obduction of New Caledonia in the north choked the subduction zone, and the continued convergence resulted in the development of a new west-dipping subduction zone (proto-Tonga-Kermadec Trench) to the east (Sdrolias, 2000; Smith, 2000). The suggested active age of the subduction ranges from Cretaceous to mid-Eocene (Launay et al., 1982; Meffre, et al., 1993; Smith, 2000).

Physiographic Setting

The major submarine physiographic features in the southwest Pacific region are, from west to east (Fig. 1): the Tasman Basin, the Lord Howe Rise, the New Caledonia Basin, the Norfolk Ridge, the South Norfolk Basin, the North Norfolk Basin (also referred to as Kingston Basin; Van der Linden, 1967), the Three Kings Ridge, the South Fiji Basin, and, further to the east, the Tonga-Kermadec arc system. In the north, the northwest-trending Cook Fracture Zone separates the Loyalty Ridge and the South Loyalty Basin from the Norfolk Ridge – Three Kings Ridge system. The Vening-Meinesz Fracture Zone in the south forms a major northwest-trending

escarpment separating the South Norfolk Basin and the Three Kings Ridge from Northland, New Zealand and the Reinga Ridge.

The Tasman Basin separates the Lord Howe Rise from eastern Australia. This triangular-shaped ocean basin is about 1100 km wide in the south, between Tasmania and New Zealand, and narrows to about 150 km in the north. The basin floor lies at about 4800-5100 m depth, and varies from flat to extremely rugged. The linear north-south oriented Tasmantid seamount chain extends from the northern Tasman Basin to about latitude 37°S, where it bifurcates. The seamounts and guyots rise to 2500 m above the seabed.

The Lord Howe Rise is the largest feature in the region, covering approximately 1 100 000 km^2. It extends for about 2000 km from the Coral Sea, southwest of New Caledonia to Challenger Plateau in the south, adjacent to New Zealand.

The northern segment of the Lord Howe Rise trends northwest and merges with a complex region that includes features such as the Chesterfield Plateau, Kenn Plateau, Mellish Rise and the Fairway Ridge (Dubois et al., 1974). The north-trending central segment of the rise extends for 1100 km from about latitudes 24°S to 34°S. The northwest-trending southernmost segment of the rise is almost contiguous with the Challenger Plateau adjacent to the New Zealand continental margin. The north-south oriented Bellona Trough, at about latitude 39°S, partly separates the Lord Howe Rise from the Challenger Plateau (J. Sayers, *pers comm* 2002). On the western flanks of the rise is the north-trending Lord Howe seamount chain, which includes isolated islands and banks. Excluding this chain, the shallowest part of the rise is in the east, where crestal water depths range from 1000-1500 m.

The morphology of the western flank of the Lord Howe Rise province is complex. Along the central segment of the rise, the 3000-4000 m deep Lord Howe and Middleton Basins separate the Dampier Ridge (crestal water depths of 2000-2500 m) from the rise. The 3000 m deep northwest-trending Monawai Sea Valley, and the slightly shallower Monawai Spur, form the western flank of the rise in the south.

The New Caledonia Basin lies to the east of the Lord Howe Rise. This basin extends from the continental margin of the North Island, New Zealand to west of New Caledonia. The basin is about 2000 km in length with an average width of about 150 km. The basin is characterised by northwest-trending segments in the north and south, separated by a north-south-trending central segment. The seafloor lies at a depth of about 3000 m and is generally flat-lying.

The Norfolk Ridge is a complex system of ridges and basins that extends from New Caledonia to Northland, New Zealand. To the west of the Norfolk Ridge lies the New Caledonia Basin and to its east lies the North and South Norfolk Basins and the Loyalty Ridge – Basin system in the north. The northern north-trending segment is a steep-sided, narrow submerged continental ridge. It is approximately 70 km wide with crestal water depths ranging between 500-1500 m (Hill, 1993). The only exposed parts of the central portion of the ridge are Norfolk and Philip Islands. The Norfolk and Philip Islands were formed by 3.1-2.3 Ma volcanic activity (Jones & McDougall, 1973; Aziz-ur-Rahman & McDougall, 1973). A chain of seamounts (Norfolk Seamount Chain) punctuates the western flank of the ridge (Rigolot, 1989). The

southern sector of the ridge comprises a northwest-trending 250 km wide complex system of ridges and basins, which merge with the New Zealand continental shelf (Eade, 1988). The southern part of the ridge complex includes West Norfolk Ridge, Wanganella Basin, Wanganella Ridge, Reinga Basin, Reinga Ridge and South Maria Ridge. The water depths range from 300-1000 m on the ridges to 1500-2000 m in the intervening basins. The southern segment of the Norfolk Ridge is offset to the west with respect to the northern Norfolk Ridge, along a possible continuation of the Vening-Meinesz Fracture Zone.

The Vening-Meinesz Fracture Zone is a large-scale northwest-trending escarpment that is interpreted as a dextral-slip continental-oceanic transform (Herzer & Mascle, 1996). The fracture zone separates the South Norfolk Basin and Three Kings Ridge to the north from the continental crust of the Reinga Ridge and Northland, New Zealand to the south (Herzer et al., 1997).

The Loyalty Ridge and South Loyalty Basin lie in the north of the survey area. The northwest-trending Loyalty Ridge is about 80 km wide and 1100 km long (Meffre, 1995). A linear chain of seamounts and islands surmounts the ridge. The South Loyalty Basin is a narrow trough, which parallels the Loyalty Ridge. The basin has a maximum depth of more than 3500 m in the north, shallows to 1500 m southeast of New Caledonia and deepens to 3000 m at its southern extent (Eade, 1988).

The South Fiji Basin lies to the north and east of the Three Kings Ridge and is bounded by the Lau-Colville Ridge in the east (Eade, 1988). A topographic high referred to as the Central Ridge divides the basin into two distinct regions, which are sometimes referred to as the Minerva Abyssal Plain to the north and the Kupe Abyssal Plain to the south (Packham & Terrill, 1975). The South Fiji Basin is a large basin, which formed as a back-arc basin to the Tonga-Kermadec subduction system during the Oligocene (Tajima & Okal, 1995). The 4000 m deep basin is generally flat-lying with isolated seamounts and ridges. The margin of the South Fiji Basin with the Three Kings Ridge is very complex and contains numerous large seamounts (Sarah Seamounts) that rise to less than 2000 m depth (Kroenke & Eade, 1982). A line of elongate seamounts extends into the centre of the southern South Fiji Basin (Davy, 1982). The basin is interpreted to contain two seafloor-spreading triple junctions that were active within 34-25 Ma (Sdrolias, 2000).

Along the eastern edge of the South Fiji Basin lies the Tonga-Kermadec arc system, which forms the southwestern-most portion of the circum-Pacific "Ring of Fire". This system includes, from east to west: the Tonga-Kermadec Trench, the Tonga-Kermadec Ridge (active arc), the Havre Trough-Lau Basin (back-arc basin) and the Colville-Lau Ridge (remnant arc). The Tonga-Kermadec Trench is a west-dipping subduction zone, that generally trends north-northeast (Dupont, 1988; Ballance et al., 1999). The Tonga-Kermadec Ridge forms a linear high. The only exposed areas are the Tonga Islands in the north and the active volcanic islands of the Kermadec Islands in the south. Many of the active volcanoes are located in the southeastern portion of the ridge (Ballance et al., 1999). The Lau Basin is an active back-arc basin while the Havre Trough in the south is still in the rifting stage of opening (Fujiwara et al., 2001). The Colville Ridge is entirely submarine and is the southern extension of the Lau Ridge, which includes the Lau Islands.

Duncan et al (1985) dated two episodes of volcanism on Eua Island (Tonga Islands), the oldest is middle to late Eocene (46-40 Ma) and a later eruption in the early Oligocene (33-31 Ma). Crawford et al., (in press) suggests the Tonga-Kermadec arc activity commenced in the mid Eocene. However, the Eocene arc-type rocks contain no evidence of subduction polarity and may be related to northeast-dipping subduction near New Caledonia (Ballance et al., 1999). Ballance et al., (1999) indicates a late Oligence (~28 Ma) for Tonga-Kermadec arc activity.

There is a marked change in the morphology and trend of the Tonga-Kermadec arc system across a west-northwest-trending 'tectonic' line termed the "32°S Boundary" (Ballance et al., 1999). North of this line the seafloor is shallow (less than 3000 m) and characterised by high sediment-fill with broad ridges. In contrast, the area south of 32°S is characterised by narrow asymmetric ridges, steep escarpments, low sediment-fill and is more than 3000 m in depth (Ballance et al., 1999).

The complex province directly to the east of the Norfolk Ridge is the main focus of the FAUST-2 survey area. The area includes, primarily, the Three Kings Ridge, North Norfolk Basin, South Norfolk Basin and the Cook Fracture Zone. These regions are briefly discussed below and will be described in more detail in a later section.

The northern part of the Three Kings Ridge is about 100 km wide and trends north-south, while in the south the ridge broadens and is more north-northeast-trending. The ridge is surmounted by seamounts and guyots, which rise to less than 500 m depth. The western flank of the Three Kings Ridge consists of gentle slopes, whereas the eastern flank is irregular, steep and marked by numerous seamounts (Kroenke & Eade, 1982). The increased width in the south is largely due to two terrace-like features at about 3000 m and 2000 m depth along the western flank – the Lower and Upper Three Kings Terraces (Herzer & Mascle, 1996). In the north, a broader terrace feature lies between the Three Kings Ridge to the east and a subdued ridge on its western margin. This "double ridge" system has been compared to the Loyalty Basin and Ridge system in the north (Packham & Terrill, 1975; Launay et al., 1982). The similarities between the Loyalty Basin – Loyalty Ridge and Three Kings Ridge systems are highlighted by seismic and satellite gravity data (Figs 1, 2 & 3; Meffre, 1995; Symonds et al., 1999).

The North Norfolk Basin and the South Norfolk Basin lie between the Norfolk Ridge to the west and the Three Kings Ridge to the east. The South Norfolk Basin is bound by the Venning-Meinesz Fracture Zone to the south. The Cook Fracture Zone forms the northern margin of the North Norfolk Basin. The basins are separated by a shallow stretch of seafloor, which seems to be an eastward extension of the Norfolk Island platform. This shallow area is thought to be underpinned by another major fracture zone, termed the "Norfolk Fracture Zone" (see Strike-slip Faults section below). Volcanic and seismic activity close to Norfolk and Philip Islands may be associated with this discontinuity (Aziz-ur-Rahman & McDougall, 1973; Launay et al., 1982; Herzer & Mascle, 1996; Mortimer et al, 1998).

The North Norfolk Basin is poorly understood. It is about 60-100 km wide and 350-400 km long (Launay et al., 1982). The basin includes broad rises and highs at about 2500 m water depth and volcanic seamounts. The South Norfolk Basin is 200 km

wide and about 500 km long, with an average depth of 4000 m (Launay et al., 1982). The South Norfolk Basin is deeper and has a smoother, more regular topography than the North Norfolk Basin (Launay et al., 1982).

Little is known about the Cook Fracture Zone, which is described as a strike-slip fault. The Three Kings Ridge and North Norfolk Basin terminate abruptly against it in the north, where it adjoins the western part of the South Fiji Basin.

Geophysical Data and Approaches

For this interpretative study several geophysical data sets were examined, including reflection seismic, bathymetry, gravity and magnetics. Refraction seismic data were acquired on AGSO Survey 177, but were not interpreted. Interpretation of the data sets involved several approaches, which are discussed below.

Geophysical Data Sets

Reflection Seismic

The seismic data used are spatially referenced in Figure 3.

For AGSO Survey 221 (ie FAUST-2) seismic profiles 2 to 77 were examined, which represents about 10 000 km of two-dimensional coverage. These data were acquired in 1999 using a 300 m long 6-channel streamer with a source of two air guns operating at a pressure of 2000 psi. The resulting onboard processed 3-fold stack data were migrated and provide good detail down to about two seconds two-way time penetration in sedimentary strata (eg Three Kings Basin).

For AGSO Survey 177 all of seismic profiles LHRNR-B,-C,-D and NZ-D were examined. Parts of LHRNR-BA over the Norfolk Ridge and NZ-E,-F,-G,-H,-I which cross onto the Three Kings Ridge, as well as TL-01 along the axis of the southern New Caledonia Basin, were examined. These lines represent a total of about 3600 km and were acquired in 1996 using a 4000 m long 320-channel streamer with a source of 20 air guns at 1800 psi. The seismic data were 48-fold stacked and migrated, which have limited resolution in the shallow sedimentary section, but enable imaging of reflectors, in places, down to 11 s two-way time (see SPs 2500-4000 on profile LHRNR-B across the Cagou Trough).

For AGSO Survey 206 those parts of seismic profiles 206-03 and 206-04 crossing the entire western New Caledonia Basin province across to the eastern edge of the Loyalty Ridge were examined, which represents about 1000 km. The survey parameters were similar to those adopted on AGSO Survey 177. The seismic data have very good detail into the thick Norfolk Ridge and Loyalty Basin sedimentary sequences.

For AGSO Survey 114, those parts of seismic profiles 114-02 and 114-04 crossing into the South Norfolk Basin from the New Caledonia Basin to its southwest were

examined, which represents about 900 km of two-dimensional coverage. These data were acquired in 1992 using a 3000 m long 120-channel streamer with a source of 20 air guns operating at 1800 psi. The seismic data were 30-fold stacked and migrated, and provide good resolution into the sedimentary sections of the South Norfolk Basin and southern New Caledonia Basin.

Several older vintage seismic lines crossing the FAUST-2 survey area and the South Norfolk Basin were also examined. These were: line diagrams of interpreted AUSTRADEC survey profiles AUS-202, AUS-203, GEORSTOM survey profiles GEO-311 and GLOMAR CHALLENGER Leg 21 profile GC-21 across the region between the Norfolk Ridge and Three Kings Ridge presented in Kroenke and Dupont (1982), Launay et al., (1982) and Rigolot (1989); part of Sonne survey profile SO-7-001 from the Wanganella Ridge into the South Norfolk Basin in Rigolot (1989); and profiles MO-143, RE-8 and RE-3 in Herzer and Mascle (1996).

Bathymetry

The bathymetric data examined are presented as colour-coded images in Figures 3 and 4 and with contours in Figure 5. These figures integrate a merged grid of several multibeam data sets with satellite-derived predicted bathymetry (Smith et al., 1997).

Multibeam bathymetric mapping produces a high-resolution view of the seafloor. The primary data set used in this study is the FAUST-2 multibeam data set, acquired by the N/O *l'Atalante* (Mauffret & Symonds et al., 2001), which is concentrated in the area broadly outlined by Norfolk Island, the Three Kings Ridge and the Cook Fracture Zone. Including the transit swaths to and from Noumea, New Caledonia, this data set represents about 186 000 km^2 of seafloor coverage, at an average depth-sounding resolution of about 250 m. The wider region is covered by: a single track of the N/O *l'Atalante* down the western side of the Norfolk Ridge (TRANSNOR[4] survey); a single track across the North Norfolk Basin and South Fiji Basin by the R/V *Melville*; and a single track, with some concentrated mapping, in the South Norfolk Basin by the N/O *l'Atalante* (ie at the end of the Resolution Ridge[5] survey).

Predicted bathymetry is used to represent seafloor where multibeam bathymetry is absent. It is of coarser resolution as it is derived from the inversion of widely-spaced satellite-altimeter marine gravity measurements (Smith & Sandwell, 1997). Predicted bathymetry spatially locates large-scale bathymetric features, but provides poor depth control. It is beneficial for defining large-scale tectonic features – for example, compare the swath-mapped Cook Fracture Zone in Figure 3 with its predicted bathymetry signature in Figure 1.

[4] Transit by N/O *l'Atalante* from Noumea, New Caledonia, to complete the TASMANTE survey south of Tasmania, via Auckland, in 1994.

[5] N/O *l'Atalante* survey conducted in February, 2000, over Resolution Ridge, southwest of the South Island, New Zealand.

Gravity

Satellite-derived gravity (Sandwell & Smith, 1997) is a valuable tool in identifying the location both of large-scale bathymetric features and deep-seated large-scale crustal features. The gravity data set (Sandwell & Smith, 2000) is spatially gridded and imaged for the southwest Pacific region in Figure 2.

More detailed ship-based gravity measurements were made during the collection of seismic data on AGSO Surveys 177 and 206, as well as along all FAUST-2 ship tracks. The FAUST-2 gravity data are gridded and imaged in Figure 6a.

Magnetics

Total-field magnetic data was collected on AGSO Surveys 177 and 206 and along all FAUST-2 profiles. For the AGSO seismic surveys it is generally examined as two-dimensional continuously-varying values. The dense line spacing of the FAUST-2 magnetic data allow for spatial interpolation (Fig. 6b). Anomalous high values are generally indicative of volcanic bodies, as is readily identified by correlation with seamounts on the bathymetric data sets.

Interpretative Approaches

The bathymetry and seismic data sets were the primary tools for interpreting the physiography and tectonic development of the study area.

The physiographic descriptions rely on examining the gridded bathymetry for the region as 2-dimensional and 3-dimensional images, where the colour used is based on a mapping to elevation in relation to sea-level (Fig. 3). In addition, contour-based maps were generated. For the area covered by the more accurate FAUST-2 multibeam bathymetry slope and aspect grids (see Figs 7 & 8, respectively) were generated to better aid in characterising the seafloor form.

For the survey area, the seismic data reveal a geological basement covered by sedimentary strata of thickness generally less than the amplitude of gross basement movements. This suggests that the seafloor physiography may reflect regional and local basement structures. Furthermore, the data provide information on sedimentary sequences and structural geology. The high-resolution FAUST-2 seismic data records of 7-8 seconds two-way time provide very good detail for the sedimentary sequences and the form of the top of the underlying basement, although this was found to be difficult in areas affected by interbedded lava flows, such as near seamounts. Further information into the nature of basement is provided by the 16-second two-way time deep-seismic data from AGSO Surveys 177 and 206. This is most notable for lines LHRNR-C, LHRNR-BA, 206/03 and 206/04 across the Norfolk Ridge, LHRNR-B across the terrain leading eastwards into the Cagou Trough and LHRNR-D over the Cagou Trough and adjoining Three Kings Basin, where continuous reflection events are visible several seconds of two-way time below seismic basement.

The gravity and magnetic data were only examined as an aid to the structural interpretations. These data reveal anomalies such as the areal extent of lava flows based on a magnetic signature and vicinity to a volcanic source and indicate whether a

large gravity anomaly is likely to be due to a seamount, or other bathymetric variations, rather than large-scale basement features.

The geophysics-based structural/tectonic interpretation presented was broadly based on the following sequence of three operations:

1. all the seismic data were interpreted for major faults and, where discernible, for the horizon defining the base of the relatively unstructured sedimentary pile;

2. all faults were posted on a map of colour-coded gridded bathymetry; and

3. the underlying bathymetry map was used to examine whether seafloor expression correlated with the faults interpreted on the FAUST-2 seismic data.

The results of this interpretative flow are discussed below.

Geological Samples and Approaches

Studies of the rocks from the three FAUST-2 dredges (see Fig. 3 for locations) were undertaken to enhance the understanding of the geological and tectonic evolution of the Three Kings Ridge. Igneous rocks emplaced or erupted in different tectonic settings are likely to differ in their petrography and chemistry. Therefore, it is possible to determine the tectonic setting of the dredged samples by comparing their petrography and chemistry with that of rocks in a well-constrained tectonic setting. The chemistry is also useful for regional correlations with similar rocks from New Zealand, New Caledonia and the southwestern Pacific island arcs. Radiometric dating was also undertaken to provide chronological markers to the evolution of the region.

Rocks Sampled

The 64 rock samples examined from the three FAUST-2 dredge sites can be grouped into the following 7 rock types based on their chemical and petrographic characteristics:

1. Peridotite, including altered lherzolite, harzburgite and dunite;
2. High-Ca boninite;
3. Medium-Ti arc-related basalt;
4. Alkaline intraplate basalt;
5. High-K intrusive rocks;
6. Sandstone, siltstone and conglomerate containing igneous clasts and benthic foraminifera; and
7. Back-arc basin basalt, dolerite and basaltic glass.

The petrology and chemistry of these rocks were studied in detail to determine the tectonic setting of the Three Kings Ridge and establish regional correlations with rocks from New Caledonia, New Zealand and the wider southwest Pacific setting.

Analytical Approach

All of the dredged material stored at Geoscience Australia was examined and 64 samples were chosen for further study, with radiometric dating being performed on several. Samples chosen included the complete range of rock types present in all three dredges, although igneous rocks were targeted in particular. All selected rock samples were made into thin-sections at the University of Tasmania and 39 samples were then selected for chemical analysis. The chemistry of the rocks was determined using a number of techniques including the following:

- X-ray fluorescence analysis (XRF) for whole-rock trace and major element chemistry;
- Solution Inductively Coupled Plasma Mass Spectrometer analysis (ICPMS) for whole-rock low-level trace elements;
- Electron microprobe (EMP) analysis to determine the major element composition of minerals and glass;
- Laser-ICMPS analysis to determine the trace element composition of minerals and glass; and
- Potassium-Argon (K-Ar) isotopic analysis to determine the age of plagioclase and glass.

More detailed petrological and geochemical analyses are discussed, along with dating, in a later section.

Morphological Setting

The seafloor morphology of the FAUST-2 survey area is presented in Figures 3, 4 and 5. Figures 6 and 7 show colour-coded images of seafloor slope and aspect for the survey area. Seven provinces are defined on the basis of spatial extent and similarity in physiographic character (Fig. 5). These provinces are: Three Kings Ridge, Cagou Trough, Kingston, Nepean, Cook, Norfolk and Forster. The naming of features in some of these provinces, particularly in the area previously named North Norfolk and Kingston basins, has been changed to reflect the improved definition of seafloor morphology following the FAUST-2 survey.

Three Kings Ridge Province

The Three Kings Ridge Province is the easternmost physiographic province and includes the Three Kings Ridge on the eastern margin, a central perched terrace, a smaller ridge along the western margin and a portion of the South Fiji Basin in the northeast sector. The province is located within longitudes 172°E and 173°30'E and

latitudes 27°25'S and 30°S. It is flanked to the west by the Cagou Trough and to the east by the South Fiji Basin.

The dominant feature in the province is the Three Kings Ridge, centred approximately along longitude 173°E. The southern two-thirds of the ridge maintains an approximate north-northeast trend, while north of 28°S the ridge curves around to a northwest strike as the ridge approaches the Cook Fracture Zone. The ridge is capped by seamounts and guyots, whose general axis trends approximately north-south. At the northern end of the ridge the seamounts are generally smaller. There are three main clusters of seamounts/guyots: a north- and northeast-trending lenticular grouping of seamounts and guyots along the eastern margin; a random scattering of very small seamounts in the north; and a northwest alignment of seamounts in the west. The central region of the ridge is characterised by two large guyots. The guyots are centred at about 172°55'E, 28°36'S and 172°57'E, 28°44'S with summits averaging 330 m and 360 m depth, respectively. The encircling slopes of the seamounts and guyots are characterised by 18°-27° slopes near the summit and 4°-18° slopes in the lower reaches.

The western margin of the Three Kings Ridge is broad with flat to gentle radiating slopes of 0°-4°, dipping towards the northwest to southwest. The surface is characterised by an irregular ripple-like appearance. Numerous canyons dissect the slopes with the deeper canyons displaying a rough east-northeast strike. The eastern flank of the ridge is rugged with steep slopes, escarpments, ridges and canyons and is punctuated by numerous small seamounts. Slopes range between 2°-13° towards the southeast to northeast, with steeper areas associated with escarpments and seamounts.

A perched terrace region, herein named Three Kings Terrace, lies between the Three Kings Ridge and the smaller ridge along the western margin. The broad rectangular-shaped terrace trends about north-northeast. The bathymetry along the Three Kings Terrace is relatively uniform ranging from about 2600 to 2900 m depth. The terrace floor is slightly uneven, and in areas displays rough northeast-trending linear features. The terrace shallows to about 2700 m at latitude 29°S where it forms a small east-trending rise. Canyons and channels from the surrounding ridges erode areas adjacent to the terrace margins. The western margin is quite linear compared to the broad sigmoidal character of the eastern margin, which is largely due to the radiating seamount slopes of the Three Kings Ridge volcanic axis. The flanks of the terrace are generally gentle ranging from 0°-4° with some areas up to 4°-8°.

A narrow north-trending ridge forms the western margin of the Three Kings Ridge Province. The ridge is characterised by higher relief areas in the northern and southern extremities. In the northern half of the ridge there are distinct northeast-trending features, which are emphasised in the aspect image (Fig. 8). Along most of the western flank of the ridge the slope on average dips towards the northwest to southwest at 4°-18°, and in some areas increases to 18°-22°. The eastern slopes of the ridge dip about 2°-13° towards the southeast to northeast onto the terrace region.

The northern sector of the western ridge is characterised by a group of three medium-sized seamounts centred at 172°03'E, 27°22'S, 172°09'E, 27°27'S and 172°8'E, 27°35'S, with an average summit depth of 1750 m, 1600 m and 1800 m, respectively.

Several small volcanoes lie adjacent to the two easternmost seamounts. Directly south of this area, at latitude 27°42'S, is a wide (~14 km) valley feature that truncates the ridge. The valley is dissected by a sinuous-like canyon and has an overall gradient of generally 2°-8°.

The central western ridge region has an irregular rough surface and is less prominent towards the south. A distinct elevated basin at latitude 28°40'S dissects the ridge. The basin is featureless and bounded by northeast-trending parallel escarpments. Further south, the ridge is cut by a northwest-trending broad (~11 km) valley, which descends into the Cagou Trough. The eastern portion of the ridge narrows towards the south into a spur. The western portion broadens into the southern extent of the ridge. The ridge has an irregular undulating surface with several channels. A small elevated circular-shaped depression lies between the ridge and a distinct wedge-shaped plateau. The plateau is centred at 172°10'E, 29°45'S with a summit at a depth of about 1600 m. It has a gentle northwest- to southwest-dipping slope of 0°-4° that is dissected by a linear canyon. The steeper northeast- to southeast-facing slopes of 4°-13° are punctuated by several canyons.

In the northeast sector of Three Kings Ridge Province lies a portion of the South Fiji Basin. The basin is flanked to the west by the rugged eastern margin of the Three Kings Ridge. Broad ridges and elevated areas extend from the Three Kings Ridge into the South Fiji Basin. The basin is characterised by an undulating irregular surface dotted with small seamounts. The seafloor lies at a depth between 2900-3600 m, with the seamounts rising to depths between 2500-2800 m. It has a flat to gentle gradient of 0°-2° towards the northeast to southeast. Minor 2°-4° slopes reflect poorly defined northeast-trending ridging.

Cagou Trough Province

The Cagou Trough Province comprises the well-defined north-south oriented Cagou Trough, which lies directly west of the Three Kings Ridge Province. The Cagou Trough is centred approximately along longitude 171°52'E, and consists of a series of basins that can be broadly divided into three main regions: northern, central and southern. Overall, the trough shallows to the south with the minimum depth of 2940 m reached in the southern region.

The western margin (with the Kingston Province) is a series of well-defined arcuate-shaped and steep slopes in the north that become more irregular towards the south. The western slopes are predominantly 18°-27° in the north that become progressively more variable towards the south, with slopes ranging between 4°-13°. The eastern margin is relatively linear with slopes of 8°-13° along most of the margin, however, these decrease to 4°-8° in the south.

The northern region of the province consists of several basins. In the northern extreme are two basins with a north-northwest axial trend. The basins have irregular undulating floors and are separated by a northeast-trending rise. These basins lie at depths of 3600-3750 m and are offset to the west from the adjacent southern basin. To the south is a distinct northeast-trending oval-shaped basin, with a relative smooth to almost featureless floor. This oval basin is separated from the northern basins by a

northeast-trending escarpment and from the southern basins by a northeast-trending ridge. The deepest part of the Cagou Trough occurs within this basin, which reaches a maximum depth of about 4260 m. The southernmost basin of this region is a wedge-shaped basin with a curved western margin. The southeast margin is defined by a northeast-trending ridge and a broad sedimentary fan from the Three Kings Ridge Province that spreads out across the floor of the basin. The basin is the deepest to the north at about 4000 m and shallows to the south to about 3600 m. The basin floor is irregular and has a central high. The basin margin is defined by 8°-22° slopes, reaching 22°-27° in the south. The southeastern margin of the basins tends to be broader with gentle slopes of 4°-8°.

The central region is separated from the northern region by a northeast-trending scarp and a rise formed by a sedimentary fan. The basin narrows to the south and is truncated by a southeast-trending escarpment. The eastern margin is relatively linear with slopes of 8°-18°. The western margin ranges from arcuate to irregular with northeast-trending spurs protruding into the basin. The margin has a stepped appearance, characterised in the north by slopes of 8°-18° separated by broad flat areas, whereas the stepped slopes of the southern areas average between 4°-18°. The basin has a relatively smooth floor and reaches depths of approximately 3800-3900 m. An east-west oriented ridge bisects the basin at latitude 28°31'S.

The southern region is separated from the central region by a major broad southeast-trending ridge that protrudes from the Kingston Province. This basin is noticeably shallower than the central region. It appears to be slightly offset to the west relative to the central region. The basin floor is relatively smooth rising slight to the south. The northern end of the basin lies at about 3200 m depth and progressively shallows to the south to a depth of about 2900 m. The eastern margin varies from being less pronounced with slopes of 2°-4°, to better defined with slopes of 8°-13°. The western margin is irregular with slopes of 4°-18° with ridging extending into the province floor.

Kingston Province

The Kingston Province is a triangular-shaped region that extends from longitudes 169°E to 171°44'E and latitudes 26°54'S to 29°55'S. The province is characterised by a northeast-trending trough that separates a wedge-shaped plateau in the southeast from a broad undulating plateau region in the west.

The wedge-shaped plateau (herein named Bates Plateau) extends northwards from the high that separates the North and South Norfolk Basins. The plateau is characterised by an undulating surface that narrows to a sigmoid-like ridge in the north. The surface of the plateau has a rippled or crenulated appearance. Depths along the main plateau region range between 2100-2600 m. A distinct east-southeast-trending linear saddle traverses the plateau at latitude 28°51'S. Small seamounts punctuate its central and western areas. The western margin of the plateau is irregular with numerous embayments and gentle slopes of 2°-8° towards the north to west descending into the adjacent broad depression. The eastern flanks of the plateau are rugged with northeast- to southeast-dipping slopes of 13°-18° and several spurs protrude into the adjacent Cagou Trough.

A characteristic feature of the Bates Plateau is the rough north-south alignment of several large guyots, seamounts and well-defined ridges along the eastern margin. In the southeast corner lies a seamount and a guyot centred at 171°36'E, 29°44'S and 171°39'E, 29°35'S with summits reaching approximately 840 m and 800 m depths, respectively. The seamount is elongated in an east-southeast direction and is separated from the guyot by a saddle at a depth of about 1700 m. The guyot is elongated in a north-south direction and is characterised by a well-defined north- to northeast-trending ridge. To the north are several north-, northeast- and east-southeast-trending discontinuous ridges. Further north is a smaller seamount centred at 171°40'E, 29°07'S with a summit at about 1400 m depth. Extending from the seamount is a northeast-trending ridge. A large oval-shaped seamount, elongated in an east-west direction, is centred at 171°40'E, 28°52'S with a peak at approximately 1400 m depth. Well-defined north-south oriented ridges extend to the north and south from the seamount. Several well-defined sinuous ridges extend to the northern part of the plateau. All encircling slopes of the seamounts and guyots average 8°-22° with some reaching 22°-27°.

A roughly northeast-trending trough (herein named Philip Trough) separates the two plateau regions of the province. The trough has an irregular shape that trends northeast in the south and swings more to a north-south orientation in the north. The trough is arc-shaped at the northern extent and rectangular in the central region. In the south, it is initially narrow, broadening to the south with a distinct circular basin in the southwest. The basin floor lies at a depth of about 3400-3500 m in the north and central regions, rising to 3000-3300 m in the south.

The southeastern margin of the central trough is irregular and characterised by numerous embayments. In the northeast, the trough is separated from the Cagou Trough by a narrow sinuous escarpment-bounded ridge with 18°-27° northeast- to east-dipping slopes and 0°-8° north- to northwest-dipping slopes. The western flanks of the trough are well-defined with slopes ranging between 2°-13° towards the east and south. The margin is irregular in the south being linear in the central region and curved in the north. At about longitude 171°11'E there is a distinct offset of the margin to the east, which marks a broadening of the trough floor to the south.

Overall, the trough floor is broadly undulated with predominantly north to west dips. The northern extent is characterised by a small seamount centred at 171°43'E, 27°13'S with a summit at about 2900 m depth and an elongate depression along the eastern margin. To the south are a pair of seamounts centred at 171°42'E, 27°35'S and 171°45'E, 27°34'S with summits at 2700 m and 2900 m, respectively. South of 28°S is a distinct north- to northeast-trending scarp that raises the seafloor by about 200 m. Further south, between latitudes 28°34'S and 28°44'S, is a well-defined southeast-trending series of volcanoes lying at about 2700 m depth. The trough floor in this region is rough with irregular rises and volcanoes. The southern region is gently undulating with a scattering of small seamounts.

Centred at about 169°57'E, 29°30'S is a circular basin with an approximate diameter of 25-30 km. The basin has well-defined margins on the north, south and west sides,

and is characterised by northeast- to southeast-dipping slopes of about 4°-18°, with some reaching 18°-27°. The eastern margin is more open with gentle slopes of 2°-8° towards the northwest to southwest. The basin floor is at an average depth of 3500 m and is generally featureless.

The plateau in the western half of the province (herein named Kingston Plateau) lies directly to the east of the North Norfolk Basin and to the north of the Nepean Province. It has an irregular undulating surface marked by depressions, seamounts and volcanic edifices. Bathymetry is variable along the plateau and ranges within 2200-2900 m with seamounts that rise above 2100 m depth. The surface of the plateau has a similar crenulated appearance as the Bates Plateau. The southwest margin is characterised by 8°-18° southwest- to northwest-dipping slopes that descend into the adjacent deeper seafloor of the North Norfolk Basin. The slopes along the eastern margin of the plateau generally dip 2°-8° towards the northeast to south, with areas in the central region marked by escarpments having 13°-22° slopes.

Seamounts and volcanoes dominate in the southern half of the Kingston Plateau. Two larger seamounts are centred at approximately 169°46'E, 28°41'S and 169°51'E, 28°33'S with summits at about 1600 m and 1200 m, respectively. Along the southwest margin, bordering the Nepean Province, are a series of north- to northeast-trending discontinuous ridges. A north-northeast-trending rectangular basin with well-defined margins extends, and gradually deepens, between latitudes 29°05'S and 29°24'S. The northern half of the plateau is characterised by a further series of north-northeast-, north- and northeast-trending discontinuous ridges with a few scattered volcanic edifices. A distinct narrow northwest-trending basin bisects the plateau between latitudes 27°42'S and 28°S.

Nepean Province

The Nepean Province incorporates the Nepean Saddle, a spur of the Norfolk Ridge to the east of Norfolk Island, and a portion of the South Norfolk Basin. The province stretches from longitudes 168°12'E to 170°21'E and latitudes 29°3'S to 30°29'S. It is characterised by an irregular surface with several large seamounts, ridges and basins.

The Norfolk Ridge defines the westernmost boundary of the province. A broad spur off the Norfolk Ridge (southeast of Norfolk Island) descends from about 1200 m depth eastwards onto the Nepean Saddle at about 2200 m depth. Slopes average 4°-13° and dip largely towards the northeast to east and towards the southeast to south. The southern portion of the Norfolk Ridge is characterised by a northeast-trending escarpment with 8°-18° east- to south-dipping slopes and well-developed northwest-, east- and northeast-trending deep canyons. The northern portion of the Norfolk Ridge is characterised by slopes of 4°-13°, predominantly northeast- to east-dipping and is dissected by several canyons.

The Nepean Saddle separates the North Norfolk Basin to the north and the South Norfolk Basin to the south. The saddle is approximately 39 km wide adjacent to the Norfolk Ridge and widens eastwards along two distinct broad ridges, the southern ridge trending east-southeast and the northern ridge trending east-northeast.

The saddle is undulating with gentle 4°-8° slopes to the northeast to east, descending into the North Norfolk Basin, and is dotted by small seamounts. The southern margin of the Nepean Saddle has a distinct east-west oriented lenticular seamount centred at 168°51'E, 29°42'S with a summit at about 700 m depth. The encircling slopes of the seamount are 18°-27° near the summit and 4°-18° in the lower reaches. Many small volcanic cones dot the eastern flank of the seamount.

The southern ridge of the Nepean Saddle is characterised by an east-southeast-trending lenticular seamount (herein named Blackbourne Seamount) centred at 169°10'E, 29°50'S with a peak at about 800 m depth. The encircling slopes average 8°-18° with some slopes reaching 18°-27° descending into the South Norfolk Basin. Several small volcanic edifices punctuate the seamount. East of the seamount, the ridge broadens and forms an irregular crenulated surface with several small volcanic edifices in the south and a small oval-shaped basin in the north. The main ridge region ranges from 2100-2600 m depth. The ridge gently dips (0°-4°) east to southeast into a depression and the South Norfolk Basin. In the north, a northwest-trending scarp with northeast- to east-dipping slopes of 4°-13° descends into a small oval-shaped basin, centred at about 169°36'E, 29°40'S, lying at a depth of about 2700 m.

At the eastern extremity of the province is a large lenticular guyot (herein named Faust Guyot), centred at 170°04'E, 29°44'S, that culminates at about 600 m depth. This east-southeast-trending guyot rises above the surrounding seafloor that lies at depths of 3000-3500 m. The encircling slopes of the seamount are 18°-27° near the summit and 8°-18° in the lower reaches. A small circular depression occurs at the eastern end of the guyot and the surrounding slopes are dotted with small volcanoes.

The northern ridge of the Nepean Saddle is characterised by three parallel northeast-trending ridges and two moderate-sized east-west-trending seamounts. The southernmost northeast-trending ridge is dominated by volcanic ridges and groupings of volcanoes. The middle ridge is flank to the south by a narrow basin and to the north by a broad well-defined valley. The middle ridge has gentle southeast-dipping slopes and steep northwest-dipping slopes with a group of seamounts at the northern end and a few small volcanoes at the southern margin. The ridge narrows and changes strike at latitude 29°22'S to more a north-northeast trend. The northernmost ridge is a linear narrow feature with a small volcano at its northern end.

In the northeast corner of the province are two irregularly-shaped seamounts centred at 169°40'E, 29°26'S and 169°46'E, 29°18'S with peaks at 900 m and 1000 m, respectively. A saddle at a depth of about 2200 m separates the seamounts. The encircling slopes range within 8°-18° reaching 18°-27° in areas. Numerous small volcanoes punctuate the lower reaches.

A portion of the South Norfolk Basin is located in the southern part of the province. It is bound to the north by the linear east-southeast-trending scarp of the Nepean Saddle. The western margin is defined by the north-northeast-trending escarpment of the Norfolk Ridge. The basin floor in this area is undulating with a gradual increase in depth to the south, ranging within 2700-3700 m depth. A central high region along latitude 29°58'S is defined by two east-trending ridges dotted by small volcanoes and

an approximate northeast-trending grouping of volcanoes. These ridges lie at about 2500-3000 m depth.

Cook Province

The Cook Province lies along the northern extent of the survey area. It includes the Cook Fracture Zone, a plateau region in the west and adjacent areas of the North Norfolk Basin and the South Fiji Basin. The province is located within longitudes 169°E and 173°38'E and latitudes 25°24'S and 27°47'S.

The west-northwest-trending Cook Fracture Zone is the dominant feature across the province. It is characterised by a linear escarpment in the west and a gorge-like feature in the east. The fracture zone is a series of linear features, which are predominantly offset slightly to the southwest. In the westernmost extent of the province, the escarpment of the Cook Fracture Zone is less well-defined and the continuation of the fault trace is difficult to discern. In the east, the fracture zone appears to disappear into the South Fiji Basin. The escarpment in the west is characterised by south- to southwest-dipping slopes of 13°-27°. East of longitude 171°35'E the fracture zone is characterised by an axial trough. The maximum depth of about 4350 m is found within the trough between longitudes 172°20'E and 172°45'E. A large northeast-trending elongate seamount centred at about 171°54'E, 26°45'S cross-cuts the fracture zone.

An area between longitudes 172°13'E and 174°54'E bordering the Three Kings Ridge Province displays a series of roughly north-northeast-trending ridges. The ridges are bounded to the south by an east-southeast-trending elongate seamount and east-northeast-trending ridges.

In the west of the province lies a plateau region that can be divided into north and south plateaus by the escarpment created by the Cook Fracture Zone. The deeper south plateau is characterised by an undulating surface at about 3200 m depth with a large central irregular-shaped rise, centred at about 169°50'E, 26°S. This rise has a rugged surface with two seamounts at its northeastern and western ends with peaks at about 1600 m and 2100 m, respectively. The elevated western margin of the plateau is irregular with south- to east-dipping 2°-8° slopes. The eastern margin has slopes averaging 2°-4° descending south to east into the deeper part of the North Norfolk Basin. The elevated north plateau ranges from 2500-2700 m depth reaching 1900 m on highs and seamount summits. This plateau has an undulating rough surface characterised by two distinct east-trending scarps. The northeastern margin is distinguished by a series of northwest-trending ridges, several volcanic edifices and a small seamount. An elevated area in the north is characterised by several northeast-trending ridges and volcanoes. The eastern margin of the plateau extends eastwards as a broad spur with southeast-trending ridges and rugged slopes of 2°-18° towards the northeast to southeast into the South Fiji Basin.

A deeper portion of the North Norfolk Basin on the southern side of the Cook Fracture Zone lies between longitudes 170°27'E and 171°34'E (ie Forster Province). It is characterised by linear parallel ridges and troughs, which are truncated at the Cook Fracture Zone. The ridging is probably relic seafloor spreading fabric that trends

northeast within the basin and northwest within the fracture zone. In the vicinity of the Cook Fracture Zone the basin floor lies at about 4000-4100 m depth. The dominant feature is a large northeast-trending prominent ridge, centred at 170°51'E, 26°37'S, with a summit at 3200 m depth. The seafloor is randomly dotted with probable small volcanoes.

The South Fiji Basin covers the area north of the Cook Fracture Zone. It is characterised by distinct linear ridges, which may represent relic seafloor spreading ridges. The ridges trend northeast adjacent to the fracture zone, and progressively rotate to an east-northeast-trend away from the fracture zone. The ridges are abruptly truncated at the fracture zone. The overall surface of the South Fiji Basin is undulating with areas of higher elevation being irregular in shape. The depth of the basin averages 4200 m near the Cook Fracture Zone. Numerous volcanoes are scattered across the seafloor.

Norfolk and Forster Provinces

The Norfolk and Forster Provinces lie between the Norfolk Ridge to the west and the Kingston Province to the east. The provinces are interpreted using predicted bathymetry (Smith & Sandwell, 1997), which provides a good large-scale overview of seafloor features. Swath bathymetry tracks through the north, along the north and south margins and along the Norfolk Ridge/North Norfolk Basin margin provide some further insight into its morphology.

The Norfolk Province stretches largely from longitudes 167°49'E to about 169°38'E and latitudes 25°35'S to 29°19'S. The province incorporates the North Norfolk Basin and a northern plateau region. The southern margin of the province has gentle slopes of 2°-4° punctuated by several volcanoes. The western margin with the Norfolk Ridge is irregular with deep northeast-trending linear canyons. The margin appears to be stepped with slopes averaging 8°-13°, reaching 13°-22° in places. The North Norfolk Basin lies south of latitude 27°S and has an irregular appearance with a seamount centred at about 168°45'E, 28°14'S.

The northern plateau region is characterised by a distinct northwest-trending ridge/seamount complex separated by a deep trough. The trough appears to be offset to the west along an east-west oriented saddle. The northern margin has an irregular surface with northeast-trending ridges and an east-west elongated seamount. A FAUST-2 swath track across the area indicates an irregular undulating surface with both northeast- and northwest-trending ridges and west-northwest-trending scarps.

The Forster Province lies to the south of the Cook Fracture Zone and to the east of the Kingston Province. Its western and southern margins border the Norfolk Province. The province comprises an oval-shaped basin characterised by deeper bathymetry relative to the North Norfolk Basin. The basin (herein named Forster Basin) extends from longitudes 169°22'E to 171°6'E and latitudes 26°40'S to 28°6'S. A distinct feature in the basin is a large seamount centred at 169°58'E, 27°10'S.

Physiographic depth analysis

Bathymetry, or depth of the seafloor below sea-level, is the fundamental parameter acquired by the swath-mapping technique. The spatial view of seafloor depth is presented in Figures 1, 3 and 4 as colour-coded terrain images. Table 1 presents a statistical overview of the depth regime for the seafloor covered by the FAUST-2 swath data in the area east of Norfolk Island (ie transit tracks are not included). The numbers tabulated are calculated from the representative grid with an un-projected cell size of 0.001°.

Minimum:	-140 m
Maximum:	-4528 m
Mean:	-2814 m
Standard deviation:	670 m

Depth range (m)	% of total	Comments*
140 – 500	0.07	summits of large Three Kings Ridge seamounts
500 – 1000	0.6	summits of seamounts of the Three Kings Ridge, Nepean Saddle and eastern margin of the Kingston Province
1000 – 1500	2.77	upper slopes of seamounts, northern areas of the Nepean Province and eastern flanks of the Norfolk Ridge
1500 – 2000	6.48	upper slopes of the Three Kings Ridge, northwest areas of the Forster Province
2000 – 2500	21.38	plateau regions of the Kingston Province and Nepean Province, lower regions of the Three Kings Ridge Province
2500 – 3000	31.47	basin regions of the Three Kings Ridge Province and Kingston Province
3000 – 3500	21.95	basin floor regions of the Nepean Province and Kingston Province
3500 – 4000	12.56	floor regions of the South Fiji Basin, Nepean Province and Cagou Trough Province
4000 – 4528	3.72	eastern end of the Cook Fracture Zone, South Fiji Basin and Nepean Province

* refers to those areas where the depth ranges dominate (see Fig. 5).

Table 1. Statistical analysis of terrain depth over the FAUST-2 survey area covered only by the FAUST-2 survey swath bathymetry data.

Physiographic slope analysis

Slope is a primary attribute of terrain and is calculated from a regularised cell representation of bathymetry. Slope details the gradient, or rate of change, in depth across the terrain. Figure 7 depicts a colour-coded image of slope across the survey area. Table 2 presents a statistical overview of the slope regime for the seafloor covered by the FAUST-2 swath data in the area east of Norfolk Island. The numbers tabulated are calculated from the representative grid with an un-projected cell size of 0.001°.

	Minimum:	0.0°
	Maximum:	41.32°
	Mean:	1.99°
	Standard deviation:	2.09°

Slope range (°)	% of total	Comments*
0 – 2	67.12	basin floors and plateaus
2 – 4	21.48	basin margins, lower slopes of ridges
4 – 8	9.12	lower slopes of seamounts and basin margins
8 – 13	1.85	flanks of seamounts and ridges
13 – 18	0.31	upper slopes of seamounts and Cook Fracture Zone
18 – 22	0.09	upper slopes of seamounts and Cook Fracture Zone
22 – 27	0.03	uppermost slopes of seamounts and Cook Fracture Zone

* refers to those areas where the slope ranges dominate (compare Figs 5 & 7).

Table 2. Statistical analysis of terrain slope over the FAUST-2 survey area covered only by the FAUST-2 survey swath bathymetry data.

Physiographic aspect analysis

Aspect is a primary attribute of terrain and is calculated from a regularised cell representation of bathymetry. It details the direction towards which a slope faces across the terrain. Figure 8 depicts a colour-coded image of aspect across the study area. Table 3 presents a statistical overview of the aspect of seafloor terrain covered by the FAUST-2 swath data in the survey area. The numbers tabulated are calculated from the representative grid with an un-projected cell size of 0.001°.

	Minimum:	0°
	Maximum:	360°
	Mean:	185°
	Standard deviation:	104.4°

Aspect range (°)	% of total	Comments*
000 – 045	11.8	eastern end of the Cook Fracture Zone
045 – 090	11.9	eastern flanks of Norfolk Ridge and Three Kings Ridge
090 – 135	12.4	eastern basin margin within the Kingston Province
135 – 180	11.8	Cook Province and northern extent of South Norfolk Basin
180 – 225	12.0	Cook Province and northern extent of South Norfolk Basin
225 – 270	12.8	basin margins of the Three Kings Ridge, Cagou Trough and Kingston Province
270 – 315	14.2	basin margins of the Three Kings Ridge, Cagou Trough and Kingston Province
315 – 360	13.1	basin margins of the Three Kings Ridge, Cagou Trough and Kingston Province

* refers to those areas where the aspect ranges dominate (compare Figs 5 & 8).

Table 3. Statistical analysis of terrain aspect over the FAUST-2 survey area covered only by the FAUST-2 survey swath bathymetry data.

Tectono-stratigraphic Indicators

There are no drillholes in the area between the Norfolk Ridge, Three Kings Ridge, Cook Fracture Zone and Vening-Meinesz Fracture Zone. However, Deep Sea Drilling Project (DSDP) drill sites 205, 206 and 285 are found in the wider region (see Fig. 3) and so provide some evidence for the dating of tectonic events.

DSDP holes 205 and 285 are located in the northern part of the South Fiji Basin some 300-500 km to the east of the northern end of the Three Kings Ridge (Fig. 3). DSDP 205 drilled about 350 m of sediment above oceanic crust dated as early Late Oligocene (Burns et al., 1973). DSDP 285 drilled about 560 m of sediments above oceanic crust dated as early Mid Miocene (Andrews et al., 1975). However, these distances and the sampling of rocks post-dating the Late Eocene regional collision provide limited information for the tectonic development in the FAUST-2 area.

DSDP hole 206 is located about 400 km to the southwest of Norfolk Island, in the middle of the southern New Caledonia Basin. It is located on an apparent basement high and penetrated about 730 m of middle Paleocene and younger nannofossil ooze with variable amounts of foraminifera and volcanic ash (Burns et al., 1973). No basement rocks were encountered, thereby limiting the value of the site in providing a continuous stratigraphic record of New Caledonia Basin sequences post-dating its formation.

The relationships between the seismic sequences in the seismic profiles may provide markers for the effects of tectonic activity on the stratigraphic record and may, therefore, furnish ideas on the geological evolution of the region.

Apart from the North Norfolk Basin, the Cagou Trough and a sedimentary basin underlying the Three Kings Terrace (herein named the Three Kings Basin), much of the FAUST-2 area is covered by a relatively uniform thickness of sediments averaging about 200-500 ms two-way time (TWT) (see Fig. 9). The North Norfolk Basin is traversed by profile GEO-311 and crossed by the northern ends of FAUST-2 profiles 6, 7 and 8. The basin contains up to 1.5 s TWT of sediment (Fig. 10). The FAUST-2 profiles 33-36 and 38b obliquely traverse the Cagou Trough. The seismic data shows a variable sedimentary thickness along strike with a maximum of 1.5 s TWT. The Three Kings Basin is covered by a large suite of FAUST-2 profiles along with lines LHRNR-B and LHRNR-D. The seismic data shows a complex succession of sequences at least 2 s TWT thick. These three areas are likely to contain tectono-stratigraphic units and provide an upper age limit for the underlying basement as well as some evidence for the history of tectonic deformation.

North Norfolk Basin Seismic Sequences

The northern end of FAUST-2 profile 7 provides the best high-resolution seismic penetration of North Norfolk Basin sedimentary sequences. Line GEO-311 provides a complete transect of the North Norfolk Basin (see Fig. 3), however, it was only available as an interpreted line diagram (Launay et al., 1982) and as a highly-reduced reproduction (Rigolot, 1989), thereby providing little information on seismic reflection character and inter-relationships. Figure 10 presents profile 7 from shot-

points (SPs) 2700-3400, as it strikes from north-northeast to east-southeast, and from seabed to just below basement at about 6 s TWT. Four seismic horizon events are identified within a sedimentary package averaging 1.5 s TWT thickness above basement and are labelled, from top to bottom, as 'A', 'B', 'C' and 'D'. Although their mapped extent on profile 7 is limited, the events may represent sequence boundaries and, therefore, may be related to regional tectonic events. Furthermore, they provide some age constraint for the underlying North Norfolk Basin basement.

Seismic event 'A'

Event 'A' is marked by a change from an underlying sequence of moderate amplitude and continuous reflectors to an overlying sequence of similar continuity, but stronger amplitude (Fig. 10). It lies at about 150 ms TWT below seafloor. Towards the south, the sequence beneath event 'A' has less continuous reflectors of strong amplitude (ie south of SP 2800 profile 7). This loss of seismic character in the underlying section, along with the proximity of seamounts and many minor volcanic developments in the Nepean Saddle region, suggests that it comprises lava flows that have spread into the North Norfolk Basin.

Examination of all the seismic data indicates that this event is not discerned in the Three Kings Ridge, South Fiji Basin or South Norfolk Basin sequences. However, a strong onlap reflector at 100-200 ms TWT below seafloor is interpreted in the northern Forster Rift Zone (see below; eg SPs 500-1000 FAUST-2 profile 21) and in the Highly-Extended Zone (see below; eg SPs 3000-4000 FAUST-2 profile 31) within the North Norfolk Basin. Further to the north, within the Loyalty Basin, a reflector showing a similar onlap style to a strongly-continuous reflector package is found at about 100-200 ms TWT below seafloor. This package appears to be associated with sag-phase sediments (eg SPs 400-1000 FAUST-2 profile 66c).

Correlation with regional and local tectonic events (Appendix 2) suggests several possibilities for event 'A'. Recent ~3 Ma volcanism on nearby Norfolk and Philip Islands (Jones & McDougall, 1973) may provide the youngest age for event 'A'. However, an onlap event distant from volcanic sources suggests a fault related origin associated with regional tectonic events. Possible events include ~5 Ma New Hebrides island-arc commencement, ~6 Ma Lau Basin opening (Ballance et al, 1999; Müller et al., 2000) or effects associated with ~11 Ma Loyalty Ridge intraplate volcanism (Eissen et al., 1998). The absence of an event 'A' style reflector within the South Fiji Basin does not support a more regional tectonic influence. Therefore, we relate event 'A' to an event associated with ~3 Ma volcanism.

Seismic event 'B'

Event 'B' is marked by a subtle transition from an underlying sequence of moderate-strong amplitude parallel and continuous reflectors to an overlying package of greater amplitude variability (Fig. 10). It lies about 600 ms TWT below seafloor. Event 'B' is associated with chaotic strong amplitude zones of reflectors at ~SP 3150 and south from SP 2950 to the northern edge of the Nepean Saddle. This zone of reflectors is considered to represent lava flows from volcanic sources on the Nepean Saddle descending into the North Norfolk Basin.

'Basement' in the South Norfolk Basin on profiles 15, 16 and 19 has a reflection character indicative of lava flows. It is found at about 500-600 ms TWT below seafloor. Shallower reflectors indicating lava flows at about 400 ms TWT, which are probably due to later volcanic pulses from surrounding volcanic zones and seamounts.

The Forster Rift Zone is covered by about 300-600 ms TWT of sedimentary strata overlying a highly faulted and structured volcanic substrate. Several areas in this zone are characterised by a slightly deeper sequence with an onlap reflector above 'basement' (eg SPs 600-1000 on FAUST-2 profile 21).

The 'basement' reflector within the central zone of the Highly-Extended Zone and the Bates Plateau has a strong-amplitude chaotic character indicative of lava flows. The sediment cover is onaverage 400-600 ms TWT thick. Further to the west, about 600 ms TWT of sediment is found along the locus of Forster Basin breakup (eg SPs 450-700 on FAUST-2 profile 66d and the southern end of FAUST-2 profile 66a).

Correlation with regional and local tectonic events (see Appendix 2) suggests two possibilities for event 'B'. The dating of lava from a seamount in the South Norfolk Basin at 18 Ma (Sample GO345; Mortimer et al., 1998; see Table 4) provides an age for intraplate volcanism. Profile SO-7-001 indicates about 900 ms TWT of sediment overlying the base of the seamount's flanks and resting on probable lava flows. This thicker sediment cover, however, may be related to the greater shedding of sediments off the Vening-Meinesz Fracture Zone scarp to the south. Therefore, event 'B' may reflect intraplate movements associated with this volcanic pulse. The second possibility is that the overlying sediment cover on event 'B' is equivalent to that overlying the western ?rifted edge of the Forster Basin, which dates the breakup and opening of the Forster Basin. Based on the dating of basalt from FAUST-2 dredge 3, the opening of Forster Basin is probably no younger than ~27 Ma (see FAUST-2 Dredge 3 section below), and possibly as early as the age of South Fiji Basin formation at ~33 Ma (Sdrolias, 2000). Therefore, largely based on the widespread cover of a similar 500-600 ms TWT thickness of sediment over the volcanic 'basement' in the Forster Rift Zone, we favour event 'B' as dating the breakup of the Forster Basin around 27-33 Ma (ie Early to Mid Oligocene).

Seismic event 'C'

Event 'C' is marked by a strong transition from an underlying sequence of weak amplitude and moderately continuous reflectors to an overlying package characterised by more consistent strong amplitude (Fig. 10). It lies at about 800-1000 ms TWT below seafloor. The event shows a strong onlap surface where it expresses some relief (ie at about SP 3350, Fig. 10). There is some evidence for erosion indicated by the truncation of several underlying reflectors (ie SPs 3200-3250). Because of the masking effect of overlying volcanics (ie event 'B' above) this event is difficult to discern along the basin edge with the Nepean Saddle.

South of the western end of the Cook Fracture Zone 800-1000 ms TWT of sediment cover is found along FAUST-2 profiles 72-75 (Fig. 9) above a platform composed of lava flows. The potential for large sediment input off the Cook Fracture Zone scarp may not allow a valid correlation of this sequence with the depositional cycles in the southern North Norfolk Basin.

A regional outlook provides evidence for the widespread presence of a strong reflector showing relief and onlap with some erosional truncation. Survey 114 profile 114/02 and Survey 177 profiles LHRNR-C and TL-01 across the southern New Caledonia Basin show a very strong and continuous reflector at 1-1.5 s TWT below the seafloor. In particular, profile 114/02 shows an across-basin strong reflector about 1.5 s TWT below seafloor with strong onlap and some minor truncation clearly evident on the bounding flanks with the Lord Howe Rise (ie SPs 11200-11500) and West Norfolk Ridge (ie SPs 13000-13700). This reflector was widely mapped in the southern Lord Howe Rise and New Caledonia Basin region by Stagg et al. (in press). The reflector is interpreted as a Late Eocene – Early Oligocene regional unconformity probably due to the collision and subsequent obduction event in New Caledonia (Stagg et al., in press). Although distant, this reflector may also be represented by a strong onlap event at about 1.2 s TWT below seafloor at the western end of LHRNR-C, along the eastern flank of the New Caledonia Basin. On the basis of overlying sediment cover and the presence of strong onlap, we propose that event 'C' equates with the Late Eocene collision of the combined Three Kings Ridge and Loyalty Ridge complex with New Caledonia and Norfolk Ridge to the north.

Seismic event 'D'

Event 'D' is marked by a strong transition from an underlying sequence of moderate amplitude and moderately continuous reflectors to an overlying package characterised by weaker amplitude and continuity (Fig. 10). It lies at about 1000-1200 ms TWT below seafloor and shows onlap where it expresses some relief. Due to the masking effect of overlying volcanics (ie event 'B' above) this event is difficult to interpret close to the basin edge with the Nepean Saddle.

The southern New Caledonia Basin may provide some evidence for the nature of event 'D'. A strong reflector with onlap lies about 1.5 s TWT below seafloor along the northern part of profile TL-01. Further to the south the reflector traverses the New Caledonia Basin on profile 114/02 as a very strong event at 2 s TWT. It clearly shows onlap relationships towards the flanks of the basin and against major asymmetric folds, which are related to basement thrust faults. This event was widely mapped in both the southern Lord Howe Rise and southern New Caledonia Basin region by Stagg et al (in press). It is considered to be a Late Paleocene to Early Eocene compression event coincident with the cessation of spreading in the Tasman Sea and subsequent plate boundary readjustment (Stagg et al., in press; see Appendix 2). Therefore, on the basis of the surface structure and strong onlap it is proposed that event 'D' marks this regional compression event.

North Norfolk Basin basement

The North Norfolk Basin basement is evident on FAUST-2 profile 7 from about SP 2800 to the end of line (Fig. 10). It is defined by a band of short strong amplitude reflectors offset by normal faulting. This short profile provides no clear evidence as to the nature of the basement: continental, oceanic or transitional. If event 'D' is as old as Late Paleocene then the basement underlying the North Norfolk Basin may be Late Cretaceous, or older, as argued for the New Caledonia Basin to the west (Uruski & Wood, 1991).

Cagou Trough Seismic Sequences

The Cagou Trough contains up to 1.5 s TWT of sediments (Fig. 9) over volcanic basement. Although this thickness is equivalent to that of the sediments within the southern North Norfolk Basin, an equivalent age is not inferred. The thick sedimentary sequence may represent slumping and debris flows shedding off the bounding steep flanks (Mauffret & Symonds et al., 2001).

An onlap surface marking a major change in reflector style is ubiquitous throughout the trough. It is found at about 150 ms TWT below seafloor. This reflector correlates well with the event 'A' discussed above and may express the presence of the same tectonic event within the trough. The overlying strong amplitude reflector package appears to thicken in a small fault-bounded basin, which is the sigmoidal depression centred at approximately 171°55'E, 27°23'S in the northern part of the trough (see Fig. 5; SPs 1500-2000 FAUST-2 profile 34). The form of this depression suggests transtensional movement along the trough and may provide further evidence that event 'A' is associated with a regional-scale tectonic event.

The seismic sequence beneath event 'A' is defined by a relatively chaotic package of weakly continuous and variable-amplitude reflectors. It is difficult to interpret any sequence boundaries. This package may represent the rapid accumulation of sediments into the trough after an extensional phase probably dating from the time of Forster Basin breakup.

Three Kings Basin Seismic Sequences

The Three Kings Basin contains at least 2 s TWT of sedimentary strata and is enclosed in a north-south oriented depocentre centred along longitude 172°20'E. Basement is not well-imaged in the seismic data, due to its depth and the presence of lava flows extending westwards from the central volcanic chain of the Three Kings Ridge, and for this reason is not mapped on Figure 9. Based on evidence that the Three Kings Ridge was the southwards extension of the Loyalty Ridge volcanic arc, the Three Kings Basin is probably equivalent to the Loyalty Basin. The interpretation of Cretaceous sediments within the Loyalty Basin (Auzende et al., 2000) suggests a Cretaceous age for basement in the Three Kings Basin.

A band of strong amplitude and continuous reflectors lying at about 600-1000 ms TWT below the seafloor is widespread across the basin. The uppermost reflector shows onlap, particularly along the flank of the basin. This band is associated with a chaotic zone of reflectors descending from the seamounts to the east (eg ~SP 2000 FAUST-2 profile 44) and is interpreted as a series of lava flows or interbedded volcaniclastics and sediments. The volcanic interpretation and depth below seafloor suggests a possible equivalence with event 'B' (see above) interpreted in the southern North Norfolk Basin. This band may mark a pulse of volcanic activity along the Three Kings Ridge at some time in the Oligocene and may be associated with Forster Basin breakup to the west. However, the dredging of a 19-22 Ma basalt further to the south (dredge site S574 – see Fig. 3; Mortimer et al., 1998) provides strong evidence that the latest volcanic event may be Early Miocene in age.

A large elevated block occurs along the western edge of the Three Kings Basin, centred at approximately 172°10'E, 29°45'S (see FAUST-2 profiles 37a and 38a and LHRNR-D). The relationship of seismic sequences along the eastern flank of the block provides some evidence for its development. Profiles 37a and 38a clearly show at least four seismic sequences, characterised by upper onlap surfaces, abutting the buried eastern edge of the block from about 3.5 s TWT to about 5.5 s TWT depth (see FAUST-2 profile 37a, Fig. 11). The two topmost packages overlie a seismic sequence containing possible lava flows, which is probably related to ~20 Ma volcanism along the Three Kings Ridge to the east (Sample S574; Mortimer et al., 1998; see Table 4). Therefore, the large thickness of the lowermost fourth sequence constrains the 'emplacement' of the block to no later than the Early Miocene and probably much earlier. This is confirmed by an initial K-Ar dating of around 22 Ma on dredged rocks (see Dredge 2 description below; Table 6).

Structural Interpretation

The Norfolk Ridge – Three Kings Ridge region reflects the dynamics of episodic crustal collision, extension and regional plate re-adjustments that have occurred in the southwest Pacific since the Cretaceous. This dynamic setting resulted in superimposed extensional and compressional structural features and associated widespread volcanism.

A first-pass analysis of the newly-surveyed seafloor east of Norfolk Island reveals a complex geological setting, which is strongly characterised by volcanic edifices and lava flows, and which underlies a complex bathymetric form (Mauffret & Symonds et al., 2001). Figure 12 presents a preliminary classification of both faulting types and structural domains for the area between the Norfolk Ridge and Three Kings Ridge, based on an interpretation of the 2-dimensional seismic data made in conjunction with an analysis of seafloor morphology. The presence of lava flows within and at the base of the sedimentary section limits the ability to interpret faults through to basement. The rationale behind the individual interpretations and a consideration as to their possible tectonic significance is discussed below. We expect that more detailed studies into all the available geological and geophysical data will place the interpretations discussed below into a more definitive chronological setting.

Normal Faults

Rift zones are interpreted from an en echelon arrangement of faults of mostly normal throw (Fig. 12). These faults control basement and extend upwards into the overlying sedimentary section in places. This style of faulting was previously suggested in the area by Launay et al. (1982) in interpreted line diagrams for profiles GEO-311 and AUS-203 within their "transition zone". The rifting is concentrated in the southern Loyalty Ridge and northern Three Kings Ridge, where the faults abut the Cook Fracture Zone, and in a complex zone centred along longitude 170°E and lying largely between the latitudes of 28°S and 30°S (see below).

Figure 12 also marks a series of normal faults with large throw. These faults are coincident with curvilinear prominent scarps or the edge of elevated seafloor. This is

seen in the southwards continuation of the elevated boundaries to the Forster Basin domain (see below) and the approximate north-south-trending normal faults flanking the adjoining Forster Rift Zone domain (see below). The marked normal faults are parallel to each other, which implies that they may have formed in a wide field stress domain consistent with rifted extension.

Seismic data indicate normal faults with large throws (eg ~SP 3950 profile LHRNR-B) along the steep western flank of the Cagou Trough. However, a similar set of faults is absent along the eastern flank of the trough, which probably indicates a mode of extension for the trough's formation other than pure rifting.

A prominent north-northeast-trending linear bathymetric scarp, as well as a set of west-dipping normal faults on profile GEO-311 (Rigolot, 1989), suggests a rifted margin along the south-eastern edge of the Norfolk Province (ie along longitude ~169°10'E; see Fig. 5). This margin is sub-parallel to the eastern flank of the Norfolk Ridge, which is characterised by a set of steep east-dipping normal faults (Rigolot, 1989).

Strike-slip Faults

A series of linear to slightly curvilinear strike-slip faults is marked on Figure 12. These faults are expected to reflect either major structural boundaries, such as the Vening-Meinesz Fracture Zone and Cook Fracture Zone, or fracturing resulting from transtensional or transpressional tectonism. The Cook Fracture Zone is marked as a strike-slip fault and is discussed in more detail below.

The strike-slip faults are largely interpreted from seismic data, where a more vertical sense to the fracture suggests movement other than a pure normal or reverse throw. Linear features on the seafloor provide some sense of the fault's azimuth. For example, the northwest-trending volcanic feature, centred at about 171°E, 28°40'S, suggests structural control during its formation and, thereby, provides some evidence for correlating fractures evident on the adjoining seismic profiles along a northwest direction.

Zones of buckled sediments near strike-slip faults are presented in Figure 12. These zones may also provide evidence for transtensional/transpressional motion along the faults.

East-northeast-trending strike-slip faults are mapped through the northern half of the Three Kings Ridge, which is largely based on the direction of various seafloor features, for example: volcanic spurs to the Three Kings Ridge seamount chain; and canyons descending into the South Fiji Basin. These faults may have formed in response to a stress-field associated with oblique strike-slip motion inferred to have commenced on the west-southwest-trending spreading arm of the Minerva Triple Junction in the South Fiji Basin in the Late Oligocene (Sdrolias, 2000).

The strike-slip faults mapped through the Bates Plateau, to the west of the Three Kings Ridge, are sub-parallel to the Cook and Vening-Meinesz fracture zones. These faults are based on the alignment of seafloor features: the volcanic lineament developed at 171°E, 28°40'S; the northeast-trending termination to the graben-like

feature at 169°20'E, 29°20'S; and the kink developed in the Cagou Trough at 172°E, 30°S.

A major west-northwest-trending fault is interpreted in the south of the survey area, which parallels the Cook and Vening-Meinesz fracture zones. It has a strong seafloor expression and clearly offsets basement (eg SP 2850 FAUST-2 profile 21 and SP 3100 FAUST-2 profile 23a). This fault may represent a major boundary accommodating differing movements between the northern and southern halves of the Norfolk Ridge – Three Kings Ridge region (?Norfolk Fracture Zone).

Indeterminate Faults

Faults that are not related to clear strike-slip motion, or are not interpreted to be related to a rifting mode of extension, are designated as indeterminate faults (Fig. 12).

A set of sinuous-like faults is mapped in the northern half of the Highly-Extended Zone (see below). Unfortunately, the strike of the FAUST-2 profiles does not provide a clear indication as to the sense of movement, although dip-profiles N and GEO-311 indicate that they have normal throws. We suggest that these faults may form part of an extended zone of crust not resulting from a pure rifting mechanism.

Obliquely joining the Cagou Trough at about latitude 29°S is a fault zone bounded by two indeterminate-style faults striking north-northwest. The faults appear to align with the trend of the eastern flank of the large block centred at about 172°10'E, 29°45'S. Furthermore, FAUST-2 profile 41 (see SPs 500-900) indicates that in profile view this zone is characterised by a major steeply-dipping slightly curvilinear fault (~SP 750) associated with a strongly buckled sedimentary section underlying a collapsed seafloor. We are uncertain about the cause of this faulting.

Volcanic Edifice Zones

Seamounts and other volcanic edifices within the Norfolk Ridge – Three Kings Ridge region are presented in Figure 12. The general shape and distribution may indicate structural control during periods of volcanism.

The approximate east-southeast to west-northwest alignment of several seamounts east of the Nepean Saddle and the Faust Guyot centred at about 170°04'E, 29°44'S parallel a major strike-slip fault lying midway between the Vening-Meinesz and Cook fracture zones (ie ?Norfolk Fracture Zone). This suggests the presence of a transfer zone, rather than a single fault, accommodating disparate movements between the North and South Norfolk basins.

The presence of many smaller volcanoes throughout the Forster Rift Zone appears to support the interpretation of a rift zone, and may delineate a complex set of leaky fracture zones forming the microplate boundaries to a rifted province in the process of breakup. This is possibly analogous to the volcanism developed in the Afar triangle of east Africa (Barberi & Varet, 1977).

A series of large seamounts is mapped along the western flank of the Cagou Trough between latitudes 28°S and 30°S, and may continue to the south as inferred by the

predicted bathymetry data set along longitude 171°30'E. FAUST-2 dredge site 1 (see Fig. 3) sampled one of these seamounts and found peridotite (see below).

Loyalty Ridge and Three Kings Ridge Rift Zones

Figure 12 highlights two triangular-shaped zones of approximate east-west directed en echelon normal faulting at the southern and northern ends of the Loyalty Ridge and Three Kings Ridge complexes, respectively. These faults align with a set of scarps at about 170°E, 25°50'S and the graben centred at about 172°10'E, 27°10'S.

The faults within these zones suggest east-west-trending rifts in response to a north-south sense of extension. This rift zone may have developed in response to propagating extension into the conjoined Three Kings Ridge and Loyalty Ridge island-arc system down the west-southwestern seafloor spreading arm of the Minerva Triple Junction developing in the northern South Fiji Basin (Sdrolias, 2000).

Forster Basin Rifting and Seafloor Spreading Zone

The Forster Basin rifting and seafloor spreading zone is shown on Figure 12. It is an elongate southwest-northeast-trending zone between the Cook Fracture Zone and an interpreted strike-slip fault at about 27°S, while south of 27°S the zone trends more north-south and is centred along longitude 170°E. The zone tapers-out in the middle of the South Norfolk Basin at about latitude 32°S. It is subdivided into 2 sub-zones: the Forster Basin and the Forster Rift Zone, north and south respectively of about latitude 28°S.

The Forster Basin is a bathymetric depression bounded by rifted margins. Strong ridging along the Cook Fracture Zone, adjacent to back-arc oceanic crust in the South Fiji Basin, is interpreted as seafloor spreading fabric developed sub-parallel to the rifted margins of the basin. The Forster Basin extends southwards to about 28°S where it shows a shallowing of the seafloor (Fig. 5). We interpret Forster Basin crust to be oceanic in origin and resulting from the propagation of newly-created seafloor down the west-southwestern trending Minerva Triple Junction spreading arm through the Loyalty Ridge and Three Kings Ridge rift zone (see above). The large seamount centred at approximately 169°58'E, 27°10'S is probably a later-stage hotspot event.

The Forster Basin Rift Zone is interpreted to be the southern extension of the Forster Basin seafloor spreading event. Between latitudes 28°S and 29°20'S the new FAUST-2 data reveals that it is characterised by rifted margins and a series of mostly north-south-trending horsts and grabens. However, further south into the South Norfolk Basin predicted bathymetry suggests the presence of several seamounts, while swath data shows a north-south elongate depression, of sub-parallel western and eastern flanks, centred at about 31°30'S. In addition, the interpretation of a set of symmetric normal faults on profile AUS-203 by Launay et al. (1982) supports the notion that this rift zone extends at least into the northern South Norfolk Basin.

Between latitudes 28°S and 29°20'S the bathymetry shows the southwards tapering of shallow graben-like features, suggesting the southwards propagation from the Forster Basin of a series of rifted arms (eg a north-south depression with rifted margins centred at about 170°10'E, 29°15'S). The bathymetry reveals a series of moderate

scale volcanic features, while the magnetics indicate the probable extent of buried lava flows (Fig. 6b). We postulate that the rifting loci were accompanied by incipient breakup volcanism and, therefore, that the underlying crust may be transitional between continental and oceanic rock.

Between latitudes 29°20'S and 31°S the bathymetry reveals a more complex seafloor. This complex morphology is due to the overprinting of structural events within the Highly-Extended Zone extending southwestwards from the east (see below).

An elongate depression with sub-parallel flanks centred along longitude 170°E and between latitudes 31°S and 32°S is interpreted as the southernmost extent of the Forster Rift Zone. This is probably the limit to which the rift locus associated with Forster Basin breakup and seafloor spreading propagated to the south. Therefore, this depression may represent the pivot of clockwise-directed extension, along the Cook Fracture Zone, of the complete pre-existing Three Kings Ridge and forearc collision complex to accommodate the opening of the Forster Basin. This form of extensional domain is analogous to the Danakil "crank-arm" model of kinematic opening proposed by Souriot and Brun (1992) for the Afar triangle in east Africa.

Highly-Extended Zone

The Highly-Extended Zone is shown in Figure 12. It trends from the south-southwest to the north-northeast from about latitude 31°S midway in the South Norfolk Basin to the Cook Fracture Zone. The zone extends across a broad shallow depression (ie the Philip Trough) bounded by several plateau-like seafloor features (ie the Kingston and Bates Plateaus). A large crescent-shaped plateau dominates the northern part of this zone, centred at about 171°20'E, 27°30'S.

Several interesting features are noted within the Highly-Extended Zone:

- the sub-parallel form to the flanks of the broad depression;
- the planimetric curvilinear form to faulting indicated by profile N to be antithetic to a major east-dipping fault along the western edge of the depression;
- the corrugated-like form to the seafloor along the western flank of the broad depression at about 171°E, 28°15'S;
- the parallel flanks of the northern crescent-shaped plateau with elevated crust to the west and the faulted western edge of the Cagou Trough to the east, suggesting extension; and, most significantly
- evidence of either crustal-scale shear zones related to collision, or east-dipping upper crust detachments, evident on profile LHRNR-B.

The sub-parallel margins of the broad depression are oriented perpendicular to the Cook Fracture Zone and extend into the northern part of the South Norfolk Basin. Profiles LHRNR-B, GEO-311 and N show that the western edge of the depression is

steeper and appears to be fault-controlled. Profile N (Davey, 1982) indicates that this western fault shallows to the east and acts as the footwall to a series of antithetic west-dipping faults within the depression and along its eastern edge. We suggest that this western bounding fault may represent a crustal-scale detachment.

Elevated sections of seafloor, some with corrugated surfaces, are widely recognised where seafloor spreading ridges and transform faults intersect (Severinghaus & Macdonald, 1988; Tucholke & Lin, 1994; Cann et al., 1997; Ranero & Reston, 1999). These topographic highs are modelled as exhumed lower-crust and upper-mantle along low-angle detachments. The corrugated surfaces are en echelon slices of upper crust developed along serpentinite-lubricated faults (Cann et al., 1997). These features are also associated with the unroofing of faulted footwalls in oceanic core complexes (Ranero & Reston, 1999). We suggest that the corrugations along part of the western flank of the broad depression (ie about 171°E, 28°20'S) may argue for the presence of a large detachment along the entire western edge of the Highly-Extended Zone.

We interpret a crustal-scale detachment beneath the crescent-shaped plateau (ie profile LHRNR-B ~SPs 4000-6000 from seafloor down to about 9 s TWT). This provides strong support for interpreting the entire depression as a zone of extension directed to the southeast, parallel to the Cook Fracture Zone trend. The entire stretch of elevated seafloor down the western side of the depression may be the footwall of uplifted and exposed lower crust, and possibly upper mantle, while the broad depression floor to its east represents sediment infill on a volcanic carapace overlying a footwall block of upper crust. This scenario is similar to the models of lower crust unroofing associated with volcanism in metamorphic core complexes of highly-extended terrains, as documented for the Basin and Range region of the United States (Gans, 1987). The association of these highly structured and altered complexes with extension has already been made for the D'Entrecasteaux Islands (Davies & Warren, 1988; Hill et al., 1992), to the northwest of the Norfolk Ridge – Three Kings Ridge region. There, extension results from propagation of the Woodlark Basin spreading centre. We suggest that a similar mechanism occurred down the west-southwestern spreading arm of the Minerva Triple Junction and, therefore, that the extension of the Three Kings Ridge forearc complex pre-dates Forster Basin rifting and breakup.

Cagou Trough Extension Zone

The Cagou Trough extension zone is marked on Figure 12 as a north-trending deep narrow depression lying just to the west of longitude 172°E. It defines the western boundary of the Three Kings Ridge tectonic province.

North of latitude 29°S the Cagou Trough is characterised by a prominent normal fault along the western flank facing a non-faulted and more rounded eastern flank. To the south both flanks are probably fault-controlled escarpments. The trough extends southwards to, at least, latitude 32°S.

Interpretations of AGSO deep-seismic profiles LHRNR-B and LHRNR-D indicate that the eastern edge of the trough is characterised by a deep curvilinear normal fault – reaching 9 s TWT on profile LHNNR-B. The northern extension of the Cagou Trough, abutting the Cook Fracture Zone, overprints seafloor fabric associated with the Highly-Extended Zone. Therefore, we postulate that the Cagou Trough formed in

response to extension and that this post-dates the extension event associated with the Highly-Extended Zone.

Although the west-facing forearc model for the Loyalty Ridge – Three Kings Ridge complex is favoured by the authors (see below), we do not conclude that the Cagou Trough represents the modern-day trace of a subduction zone trench. The Cagou Trough may represent the extensional re-activation of collisional shear zones or the latest-stage accommodation of rapid extension along the broad accretionary front to a relatively intact forearc basin (ie Three Kings Basin). Furthermore, the sampling of mantle-derived peridotite in the FAUST-2 dredges (see below) may provide evidence for mantle involvement along deep-seated extensional faults down the entire western flank of the Cagou Trough.

Cook Fracture Zone

The Cook Fracture Zone is a distinct west-northwest-trending feature in the north of the FAUST-2 survey area. Detailed interpretation of bathymetry shows that the Cook Fracture Zone is a complex transform system (Fig. 13).

Garfunkel (1986) describes oceanic transform zones as typically 10-30 km wide with 0.5-4 km deep valleys and a principal transform displacement zone (PTDZ) of a few hundred metres to a few kilometres width. The three-dimensional geometry is very complex, comprising strike-slip, vertical and oblique motions. Major vertical displacements along the PTDZ can create flower structures that form valleys and transverse ridges (Mauduit & Dauteuil, 1996). Strike-slip systems can develop localised extension and compression structures such as pull-apart basins and uplifted regions.

The Cook Fracture Zone displays the characteristics of an oceanic transform described by Garfunkel (1986). The visible length of the fracture is about 470 km, with a width varying from a few kilometres to about 25 km. The PTDZ is clearly defined in the western half of the Cook Fracture Zone by an escarpment and in the eastern half by a narrow valley that reaches a maximum depth of about 4350 m. The PTDZ is a series of slightly southwest-stepped faults.

The Cook Fracture Zone links the spreading ridges associated with the opening of the South Fiji Basin and Forster Basin. The spreading ridge associated with the Forster Basin is interpreted as the large ridge feature centred at about 170°51'E, 26°37'S. The ridge trends northeast and is orientated approximately perpendicular to the Cook Fracture Zone. The spreading ridge associated with the South Fiji Basin has two possible locations. A large dominant ridge that intersects the Cook Fracture Zone centred at 171°54'E, 26°45'S or a parallel set of ridges at the eastern end of the Cook Fracture Zone centred at 173°14'E, 27°13'S. Both these possible spreading ridge locations trend northeast, being oriented perpendicularly to the Cook Fracture Zone.

The eastern end of the Cook Fracture Zone is characterised by a braided fault network. A large volcanic ridge (centred at 171°53'E, 26°45'S) forms a protrusion into the fracture zone, which results in the faults converging to form a single fault trace. Seismic sections across the PTDZ valley show it is bound by steeply-dipping faults and in some areas by stepped normal faults.

To the west of the volcanic ridge the Cook Fracture Zone is characterised by several closely spaced parallel west-northwest-trending faults that diverge into a braided network of sub-parallel and northeast-trending faults between longitudes 171°36'E and 169°20'E. Seismic sections and swath bathmetry across the PTDZ indicate there is a major component of vertical displacement associated with the strike-slip system.

An elevated region south of the PTDZ valley, adjacent to the Three Kings Ridge, is distinguished by several lineaments that are orientated at a high angle to the PTDZ between longitudes 172°16'E and 172°53'E. These features may represent conjugate Reidel (antithetic) shears related to the strike-slip stress fields.

The Cook Fracture Zone displays several topographic lows, which are bound by faults (Fig. 13). These features may be the result of localised extensional stepovers forming pull-apart basins. The principal component of displacement on the bounding faults appears to be strike-slip along the west-northwest-trending faults and vertical along the northeast-trending faults.

North of the Cook Fracture Zone, within the South Fiji Basin, are several curved faults that merge with the transform domain. To the south, the branching fault system of the Cagou Trough appears to truncate at the Cook Fracture Zone.

The overall sense of movement of the Cook Fracture Zone is sinistral. This is determined by the left lateral offset of the Loyalty Ridge with respect to the Three Kings Ridge, as well as the rotation of relic spreading fabric within the South Fiji Basin from an east-northeast trend to a northeast-trend into the main fracture lineament.

FAUST-2 Dredges Petrology, Geochemistry and Dating

This section outlines the results of a geochemical study of rocks recovered from dredge sites on the eastern and northern flanks of the Three Kings Ridge. The FAUST-2 cruise recovered a total of about 600 kg of rocks from three dredge sites (see Fig. 3 for locations): 1.5 kg from dredge 1 (DR1), 200 kg from dredge 2 (DR2) and 400 kg from dredge 3 (DR3) (Mauffret & Symonds et al., 2001).

Determination of the chemistry, petrography and age of these rocks provides important constraints on the tectonic setting and history of this area, which are discussed in a later section. The data from these rocks can be compared with data from similar rocks from New Caledonia and New Zealand.

By way of comparison, and to further characterise the regional geological setting, Table 4 presents data on the dredges acquired in the wider Norfolk Ridge – Three Kings Ridge region. Further information is found in Herzer et al. (1997) and Mortimer et al. (1998).

FAUST-2 Dredge 1

DR1 was located on a major northeast-facing scarp (average slope 22°) on the western side of the Cagou Trough from approximately 3000-2200 m water depths. The few samples obtained from this site included two small (<16 cm) angular pieces of carbonate-altered peridotites and an unaltered piece of pumice (Mauffret & Symonds et al., 2001). The pumice was not coated in pelagic or benthic carbonate or manganese crust and had probably recently floated into the area and sank when it became waterlogged.

The peridotites are pervasively altered to carbonate so that only chrome spinels remain. They have multiple fracture planes suggesting brittle deformation. Sample DR1-B1 contains calcite, fine-grained recrystallised quartz or feldspar, haematite and chrome spinels. The outlines of replaced orthopyroxene crystals are visible indicating that the rock was probably harzburgite or lherzolite. Sample DR1-A1 contains a fine-grained opaque matrix of haematite and other replacement minerals and large chrome spinels. The distribution and shape of the chrome spinels indicates that these rocks are

Sample	Latitude	Longitude	Depth (m)	Age range	Lithology and Environment
U566 1-3	-35.08333	169.16666	979	?vL.Olig-lE.Mio	bioclastic, bryozoan limestone, oceanic, shoal
RE9302-5-2	-34.01083	166.95833	1270-2250	eL.Cret	Coal measures, carbonaceous mudstone, lower coastal plain
RE9302-6-1	-33.90722	167.38138	700-735	vL.Olig-E.Mio	bioclastic bryozoan limestone, bored and replaced by forminiferal limestone, bathyal (age and depth ranges common to both limestones)
RE9302-7-2	-33.56083	167.65527	650-900	vL.Olig-mE.Mio	
E-855	-33.16666	169.93333	742		sandy limestone
RE9302-2-6	-33.12638	170.91416	1875-1950	mE.Mio	micrite infilling cracks in basalt, oceanic bathyal, calm conditions
RE9302-1 1-4	-33.01111	171.70694	2500-2700	?vL.Olig-E.Mio ?lE.-?eM.Mio	calcareous volcanic sandstone, shoal, lapilli tuff, lower bathyal, rapidly deposited
G-1	-32.58333	167.38333	138	lE.Mio-?M.Mio	algal ball, shallow photic zone, sheltered
RE9302-3-6	-32.36777	170.86722	3680-4160	mM.-lM.Mio	calcareous ooze chalk, bathyal >1000m
GO350D-5	-32.36333	169.14166	1600-3400	L.Pal-M.Eo	?argillaceous limestone, cataclasite, planktonic
GO349D	-32.15833	167.47500	1000-2000		altered calcareous volcanic sandstone
GO351D-g	-31.88166	168.28666	900-2500	M.Eo	mudstone breccia, bathyal >1000m (age and depth of matrix fauna only)
U579	-31.85833	171.95999	2109	Late Paleogene? Olig?	calcareous fine sandstone, oceanic, bathyal or deeper
GO347D	-30.47500	168.09000	1840-2300		calcareous mudstone
GO348D-b	-30.12000	167.49666	900-1400	vL.Olig-vE.Mio	coquina with volcanic lithics, shallow open marine, photic zone to >100m
GO357D	-35.62000	165.77999			olivine basalt, gabbro, hyaloclastic breccia with mid-Miocene forams (from Willcox et al., 1980)
GO353D	-33.01666	167.84833	1870-1530	2.3 Ma for basalt	hyaloclastic breccia, palagonite and 'bubble' lava, pyroxene, olivine inclusions
SO-36-57KD	-31.86500	157.37833	2400-2700	Mid-Permian	granite, gabbro, undated sandstone
GO345	-30.93333	168.81666	2260-3200	E.Mio	altered olivine basalt
S565	-29.30833	169.77833	830-1350		vesicular basalt
VE209	-28.18333	173.15000	1800-2200		basalt
S573	-30.49499	172.70499	840-975		aphyric vesicular lava
S574	-30.83499	172.74000	1180-1290	E.Mio	basalt

Table 4. Summary of sample data in the Norfolk Ridge to Three Kings Ridge area (modified from Herzer et al., 1997, and Mortimer et al., 1998). Locations of the sample sites are found in Figure 3. FAUST-2 dredges are not included.

altered peridotite. Geochemical analyses of the spinels show medium to low Al_2O_3 content (Fig. 15), indicating that these rocks were probably harzburgites prior to alteration. The mineral chemistry and significance of these rocks is discussed in a subsequent section, together with that of the DR2 peridotite.

FAUST-2 Dredge 2

DR2 was located on the eastern flank of a large, flat-topped and tilted block, centred at about 172°10'E, 29°45'S, 30 km long by 15 km wide, rising approximately 1000 m above the surrounding seafloor (Fig. 5). The slope (average 11°) was dredged from 2400 to 1600 m water depths. The dredge recovered 200 kg of mafic igneous rocks, including peridotite, boninite, medium-Ti basalts, one alkaline intraplate basalt and both mafic and felsic, high-K and high-Ti igneous intrusive rocks. Sedimentary rocks were also recovered, including white pelagic limestone, manganese crust, calcareous volcaniclastic sandstone, siltstone and conglomerate.

The samples from DR2 were grouped into six separate categories based on petrography and chemistry. As we did not undertake any work on the limestone, manganese crust and fine-grained sedimentary rocks, they are not discussed here, although descriptions of hand specimens are available from the FAUST-2 survey report (Mauffret & Symonds et al., 2001). The six categories are:

1. Peridotite

Peridotites were recovered as clasts in conglomerate and as rounded cobbles up to 15 cm in diameter. Olivine has been altered to serpentine or weathered to clay, although many samples still contain unaltered orthopyroxene and clinopyroxene. Chrome spinel is fresh in all the peridotites. The rocks range in composition from dunite to harzburgite and lherzolite (Table 5).

Whole rock analyses were not undertaken due to the intense alteration. Instead, the chemistry of the unaltered orthopyroxene, clinopyroxene and spinel was examined to determine the magmatic affinities of these rocks.

Numerous studies have shown that mantle peridotite can be subdivided into three groups, based on mineralogy and chemistry (Bonatti & Michael, 1989; Parkinson et al., 1992; Seyler & Bonatti, 1994; Bizimis et al., 2000):

1. Abyssal peridotites have been dredged from transform faults and near slow-spreading ridges. Their clinopyroxenes have low Na and a small proportion of Al in 6-fold coordination (Al6) because they crystallised at relatively shallow depths and at low pressures (Seyler & Bonatti, 1994);

2. Sub-continental peridotites (dominated by lherzolite), brought to the surface as xenoliths in intraplate volcanics or exposed along major detachments at rifted margins, tend to have a higher modal abundance of clinopyroxene (Bonatti & Michael, 1989); and

3. Forearc peridotites have been dredged and drilled from the forearc of intra-oceanic island-arcs (Parkinson et al., 1992; Pearce et al., 2000). They tend to be more depleted (ie dominated by harzburgite) with less modal clinopyroxene (Bonatti & Michael, 1989). The clinopyroxene compositions are similar to those from abyssal peridotites, although they have less Al and Ti and tend to be enriched in Sr and the light rare earth elements (LREE). These rocks represent residues from more extensive degrees of partial melting than those producing abyssal peridotites. This residue is thought to be due to slab-derived fluids percolating in the mantle wedge beneath the arc and forearc, lowering the melting temperature, and promoting a greater amount of partial melting, which depletes the residual peridotite in Ti, Al and other incompatible elements. The chrome spinel compositions of forearc peridotites also tend to have less Al and more Cr than both continental and abyssal peridotites (Kamenetsky et al., 2001).

The clinopyroxene and spinels from both DR1 and DR2 are largely similar in composition to those from the forearc of intra-oceanic island-arcs (Figs 15 & 16). In Figure 17 the DR2 clinopyroxenes are similar to forearc peridotites, except in their Al_2O_3 content, which overlaps with the clinopyroxene composition from abyssal peridotites. Several analyses, particularly from DR2-A14, show higher Al_2O_3 than the forearc peridotites from the Mariana forearc of ODP Leg 125 (Parkinson et al., 1992) or the South Sandwich Arc (Pearce et al., 2000). However, TiO_2 and Na_2O in these same crystals are lower than the abyssal peridotites and similar to forearc peridotites. Rare earth element (REE) data on clinopyroxene from this sample (Fig. 17) also show characteristics that are more typical of abyssal than forearc peridotites. However, sample DR2-A14 is probably not representative of the peridotite composition on the Three Kings Ridge. Analysis of spinels from the DR2 sandstone (presumably reworked from a large number of peridotites) indicates that only two out of 35 grains analysed have spinels with similar composition to DR2-A14. The majority of spinels have the low Al_2O_3 typical of forearc-type peridotites. We encountered technical difficulties in our attempts to measure the trace element composition of clinopyroxene in other samples, but hope to be able to perform these analyses in the near future.

The spinels from the peridotites have similar Al and Ti contents to peridotites from New Caledonia (eg those from Leblanc, 1995 and Kamenetsky et al., 2001) to the north of the Three Kings Ridge (Fig. 15). Unfortunately, no comprehensive data set is available for comparison with the peridotite clinopyroxene from New Caledonia, however it is hoped some preliminary work will be undertaken on these in the near future.

The harzburgite, lherzolite and dunite from DR1 and DR2 closely resemble forearc peridotites from the Mariana and the South Sandwich island-arcs. The differences between the Three Kings Ridge and the forearc peridotites may be accounted for by the presence of a localised, less depleted mantle domain, represented by sample DR2-A14. The chrome spinels in the Three Kings Ridge peridotite are similar to those from New Caledonia to the north, supporting reconstructions that show the western side of the Three Kings Ridge as a continuation of the New Caledonian peridotites (eg Aitchison et al., 1995; Meffre, 1995).

Sample	Rock type	Serpentinised olivine	Orthopyroxene	Clinopyroxene	Al_2O_3 wt% in spinel
DR1-A1	harzburgite?	Strongly altered	Strongly altered	Strongly altered	11-29
DR1-B1	harzburgite?	Strongly altered	Strongly altered	Strongly altered	15-34
DR2-A14	Lherzolite	75%	20%	5%	42-46
DR2-I2	Lherzolite	70%	20%	10%	36-42
DR2-I3	Harzburgite	83%	15%	2%	19-24
DR2-I4	Harzburgite	76%	20%	4%	26-28
DR2-I5	Peridotite	Strongly altered	Strongly altered	Strongly altered	Not analysed
DR2-S2	Dunite	100%	0%	0%	8-9

Table 5. Visual estimate of the mineralogy of the peridotites from the Three Kings Ridge and electron microprobe analyses of Al_2O_3 content of the spinels.

Sample	K (%)	40K (ppm)	40Ar (ppm)	40Ar/total Ar	Age (Ma)
DR2 B8	0.122	0.146	0.000192	0.039	22.6 ± 1.9
DR3 E	0.338	0.403	0.000638	0.044	27.0 ± 1.4
DR3 A3	0.129	0.154	0.000417	0.043	46.0 ± 3.1

Table 6. Results of K-Ar age dating on FAUST-2 dredges.

2. High-Ca boninite and breccia

High-Ca boninites are the predominant igneous rock-type in samples from DR2. They range in composition from basalt to basaltic andesite. Their petrography varies from sparsely olivine + clinopyroxene-phyric at 11% MgO to pyroxene + plagioclase-phyric at 3% MgO. Orthopyroxene phenocrysts occur in rocks with between 3-8% MgO. The groundmass is either altered glass or a mixture of altered glass and clinopyroxene, plagioclase and magnetite microphenocrysts. One breccia (sample K3) was recovered, containing angular, clast-supported blocks of altered glassy boninitic basalt. The matrix varies over different parts of the same rock. In some places the clasts are cemented with sparry calcite, while in other areas a matrix of volcaniclastic sand fills the gaps between the clasts.

The chemistry of 10 of the 13 samples analysed has been strongly modified by seawater alteration. It has caused significant enrichment in P_2O_5, Y, CaO, the rare earth elements (REE), Th, U and Sr (Fig. 18). There is also a strong negative Ce anomaly compared to neighbouring REE, which is typical of rocks altered by seawater (Shikazono, 1999). Electron microprobe analysis suggests that high P_2O_5 zones are distributed as patches within the altered groundmass glass.

The unaltered samples can be used to correct Ca and P to their original values by subtracting CaO and P_2O_5, in the same proportions as in the mineral apatite, until

P_2O_5 is the same in both the altered and unaltered samples. This correction decreases the scatter of the magmatic trends, particularly for SiO_2, Al_2O_3 and Fe_2O_3 (Fig. 19).

Other than the seawater alteration and devitrification of the glassy groundmass, the samples show no evidence of metamorphism. Plagioclase ranges from An82 to An51, decreasing systematically with increasing fractionation. The pyroxenes are largely unaltered, although several orthopyroxenes have been altered to clay minerals. Olivine is largely altered although small, unaltered cores (Fo88) are present in the most primitive samples. Vesicles contain large (up to 1 mm) crystals of clear K-Na aluminosilicate, similar in composition to analcite, but with higher K_2O (7-11%) and less water (3-11%). These crystals occur either as radiating aggregates of needle-like clear crystals or as large single euhedral crystals with low birefringence and lamellar twinning.

These lavas are high in SiO_2 and low in TiO_2 at high MgO (Fig. 19), similar to high-Ca boninite dredged and drilled from the forearc of intra-oceanic island-arc systems (eg Arculus et al., 1992). The major element patterns and the phenocryst assemblage indicate strong initial fractionation of olivine and chrome spinel, followed by clinopyroxene and orthopyroxene after the magmas reached 7% MgO. Plagioclase fractionation began when the magmas reached 5% MgO. The late fractionation of plagioclase is typical of subduction-related magmas. The very high Al_2O_3 content of one of the rocks is due to plagioclase accumulation. Slight magnetite fractionation is required to account for the low Fe_2O_3 of the evolved samples. K_2O is variable; both altered and unaltered samples plotting into two groups with significant scatter and no clear trends. The K_2O data probably reflects alteration of the groundmass and the infilling of the vesicles rather than primary igneous concentrations.

The trace element data (Fig. 20) determined by XRF and solution ICPMS are characterised by high Rb, Ba, Sr (the large ion lithophile elements or LILE), low REE and low high field strength elements (HFSE; eg Ti, Nb and Ta) compared to typical mid-ocean ridge basalts (N-MORB). The samples also show a strong Hf and Zr enrichment, compared to elements with similar ionic radius. This type of enrichment is typical of Tertiary boninite from the western and southwestern Pacific (Jenner, 1981; Cameron, 1989; Murton et al., 1992). The composition of these rocks is transitional between depleted low-Ti island-arc tholeiite and boninite. They are just outside the boninite classification criteria of Crawford et al. (1989), although they plot within the Marianas high-Ca boninite field of Arculus et al. (1992). As these rocks resemble boninites (eg Mariana forearc boninite on Fig. 20) more than any other igneous rock type, we feel that our use of the term is justified.

A single K-Ar age determination was undertaken on plagioclase crystals separated from one of the more evolved boninites. Significant problems were encountered due to the high-K_2O minerals in the vesicles. These have similar habit and physical properties to plagioclase, but their K_2O contents are two orders of magnitude greater and even slight contamination affects the results. The K-Ar age determination was 22.6 ± 1.9 Ma, however, the K_2O content of the bulk plagioclase separate (0.147% K_2O) was significantly greater than the highest electron microprobe analysis on cores and rims of crystals (19 cores and rims with an average of 0.07% K_2O). The extra K_2O could be derived from only 0.8% contamination by the high-K_2O mineral in the vesicle, and the age could be significantly younger than the age of eruption of the

rocks. Ar-Ar dating of these samples (currently in progress), together with palaeontologic studies of the sandstones that postdate the formation of the igneous rocks will provide more information on the age of eruption.

3. Medium-Ti basalts

Basalts with medium TiO_2 content are a minor component of the DR2 rocks. They contain rare, small, partially altered olivine (Fo82-84) and clinopyroxene phenocrysts in a groundmass of altered glass, plagioclase laths (An70) and clinopyroxene microphenocrysts. They are pervasively affected by the P_2O_5 alteration described in the previous section, so their REE, P_2O_5 and Y contents are much higher than those of the unaltered precursors. High-K_2O vesicle fill is also present in these rocks and probably accounts for the high K_2O contents. The unusual decrease of K_2O and Rb with increasing fractionation and the unusual low Ba/K_2O suggest that the K_2O has been added during alteration and weathering. However, most of the less mobile elements show expected fractionation trends (eg Mg, Ti, Zr, Nb, Fe, Cr, Ni and Al) and do not seem to have been strongly remobilised.

These rocks have high MgO, medium TiO_2 and low Nb content and show many features of arc-related magmas including late crystallisation of plagioclase, indicated by the inflection in the Al_2O_3 trend at 5% MgO. Fe_2O_3 decreases with increasing fractionation, suggesting early Ti-magnetite fractionation and high water content in the primary magma. A subduction-related tectonic setting is supported by the composition of chrome spinels that plot in the arc volcanic field of Kamenetsky et al. (2001) (Fig. 15). These basalts display many chemical similarities to rocks analysed by Mortimer et al. (1998) from the central section of the Three Kings Ridge (samples S574 & S573 – see Table 4). The samples from Mortimer et al. (1998) are more evolved, but plot along similar trends for most elements with the exception of the mobile LILE (Fig. 19).

These subduction-related basalts have HFSE contents slightly higher that those for arc tholeiites (eg Tonga-Kermadec tholeiite; Ewart et al., 1977) and LILE contents (except for K_2O) too low for shoshonite. Their chemistry resembles calc-alkaline basalts such as those from the New Hebrides island-arc (eg Monzier et al., 1997).

4. Alkaline intraplate basalt

A single clast of altered aphyric basalt with strongly alkaline chemistry was analysed. The chemistry of this basalt is very different from that of the other DR2 samples, as it has very high Na_2O, HFSE and light REE, which resemble basalts dredged from seamounts in the South Norfolk Basin to the west of the Three Kings Ridge (Mortimer et al., 1998).

5. High potassium intrusive rocks

Six small pebbles of intrusive rocks were recovered from DR2. Five of these were thin sectioned (DR2-L3, -M1, a clast in conglomerate G5 and a pebble included in the manganese coating of DR2-I3), but none were large enough for whole rock analysis. Sample DR2-M3 is being studied in France by M. Seyler and C. Gorini.

These rocks are variable in their petrography and mineral chemistry. DR2-L3 is an amphibole + biotite-bearing monzonite or syenite. It contains large pink titanaugite (2-4.5% TiO_2) mantled with brown kaersutite (Ti-rich hornblende) and green amphibole. This rock also contains plagioclase, haematite with ilmenite intergrowth, partially altered biotite, abundant apatite, and igneous sphene. The clasts in conglomerate G5 contain plagioclase, K-feldspar, apatite and orthopyroxene. M1 consists of a fine-grained, felsic igneous rock intruded by veins (up to 1 cm wide) of coarse-grained felsic igneous material. The veins contain albite, quartz and haematite with ilmenite inclusions. The surrounding rock contains albite and chlorite. Small crystals (5-15 μm) of monazite (REE, Th phosphate), zircon and apatite were also noted. Sample M3 is a syenite composed of K-feldspar, aegirine (sodic pyroxene) and amphibole (M. Seyler, *pers comm* 2001). Other samples are felsic intrusive rocks consisting largely of quartz and albite with minor chlorite, epidote and haematite with ilmenite lamellae.

The tectonic setting and significance of these unusual rocks is difficult to establish. Their elevated Na_2O, Ti and K_2O content suggests that they are related to an intraplate magmatic event rather than subduction-related high-K magmas.

6. Sandstone and conglomerate

Numerous blocks of sandstone, siltstone and conglomerate were recovered from DR2, however, only one conglomerate and three of the most coarse-grained sandstones were sectioned and examined in detail. The sandstones contain various biogenic carbonate fragments (70-80% of total clasts) including benthic and planktonic foraminifera, corals, bryozoa and gastropods (Fig. 21). Monocrystalline clasts (5-10%) are also present, and include clinopyroxene, chrome spinel, plagioclase, hornblende, actinolite and orthopyroxene. Lithic clasts (10-20%) are composed of porphyritic and aphyric basalts similar to the boninites, serpentitised peridotite, felsic and mafic plutonic rocks, and metamorphic clasts with a greenschist-facies assemblage of albite, actinolite, epidote, and chlorite. Sample E6 is notable as it contains very little boninitic detritus and numerous greenschist-facies altered mafic plutonic rocks. The conglomerate (sample G5) contains no biogenic detritus, but other clast-types are similar to the sandstones.

The chemistry of the detrital chromite, clinopyroxene and hornblende were determined to assess the source of these sandstones. Compositions indicate that most of the chrome spinel, in both the sandstones and conglomerates are derived from peridotite. Most pyroxenes are derived from boninites with the exception of two crystals with higher Ti, similar to clinopyroxene from the medium-Ti basalts. Two large crystals of hornblende (0.5 mm) were also analysed. They are relatively high in TiO_2 (1%) and are probably derived from a basic igneous rock, possibly a more felsic equivalent of the medium-Ti basalts from DR2.

These results suggest that these sedimentary rocks were derived from a combination of shallow water carbonates mixed with detritus from all the igneous rocks described earlier.

Geological relationship between the rock types from dredge 2

The analyses of the FAUST-2 dredge 2 samples, together with seismic sections from the surrounding areas, provide some information about the geology of the high-standing block sampled. The seismic sections indicate that this block has had a complex history. It was initially uplifted and eroded by wave action. A flat-lying sedimentary sequence was then deposited on top of this eroded planar surface. The block was faulted by major east-dipping listric extensional faults. Sedimentary sequences were deposited on the flanks of the block above a major unconformity.

The shallow water fauna of the sandstones in DR2 indicates that these were deposited close to the time when the block was uplifted. They were probably dredged from the old tilted sedimentary unit overlying the top of the block (Fig. 11). The ratio of ultramafic, boninitic, basaltic and alkaline igneous clasts is roughly similar to that of the igneous samples recovered from DR2. Boninite-derived clasts are most abundant, followed by ultramafic, basaltic and alkaline clasts. Some of the igneous cobbles recovered from DR2 could have been clasts from a coarse conglomerate similar to sample DR2-G5. However, many of the cobbles were coated in thick manganese crust (up to 2 cm) indicating that they had existed as loose cobbles on the seafloor for an extended period of time. Some of the locations along the dredge trajectory may have had outcropping boninites. The large angular clasts in breccia DR2-K3 consist exclusively of boninitic rocks and are cemented together by sparry calcite cement growing into open spaces between the clasts. This implies that they were deposited from a nearby source area consisting entirely of boninite. This source area presumably forms part of the basement that underlies the sandstone.

The DR2 basement must therefore consist of an igneous basement comprised of boninite and peridotite overlain by shallow water sandstone and more recent sediments. The medium-Ti basalts and alkaline rocks could be sourced from further away as the clasts are always small and they form only a minor component in the sandstones.

FAUST-2 Dredge 3

Tholeiitic basalt, breccia and dolerite were dredged from the northern end of the Three Kings Ridge at dredge site 3 on the FAUST-2 survey (Fig. 3). The samples were dredged from the southern walls of the Cook Fracture Zone between 4250 m and 3500 m water depth, on a steep (~33°) north-dipping slope. The dredge recovered approximately 400 kg of pillow basalt, dolerite, pillow breccia and hyaloclastite (Mauffret & Symonds et al., 2001).

Some minerals in the basalts and dolerite are partially altered to clay. In these rocks, clay minerals and haematite form radiating aggregates replacing the groundmass and olivine crystals. In the basaltic glasses and hyaloclastite alteration is less intense. Olivine is fresh and only some of the glass has devitrified.

The basalts are generally sparsely vesicular containing equigranular plagioclase (An 70-75), clinopyroxene (Mg# 70-86) and titanomagnetite. Some of the rocks contain altered olivine and interstitial chlorite. The dolerite is ophitic textured with interlocking crystals of clinopyroxene, plagioclase and titanomagnetite. Hyaloclastite

and breccias contain basalt fragments and both fresh and altered basaltic glass. Two types of glass are present, with the more mafic glass (DR3-A) containing skeletal olivine (Fo85) with spinel inclusions (see Fig. 15 for composition). Some of this olivine is reversely zoned with older, less magnesian cores (Fo79). The more felsic glass contains smaller olivine and small tabular plagioclase crystals (An71-75).

All the igneous rocks recovered from DR3 have similar major element compositions. They are basaltic with medium TiO_2 that increases rapidly with decreasing MgO. SiO_2 is constant in all the samples analysed. Fe_2O_3 increases rapidly with increasing fractionation and K_2O remains low. These major element characteristics are typical of seafloor tholeiite formed at spreading ridges. Alteration does not seem to have had a major effect on their chemistry. Elements that are considered to be mobile during alteration (ie Ca, Ba, K_2O, Pb and Na) show expected fractionation trends with very little scatter.

Although the major elements are typical of mid-ocean ridge basalts (MORB), the incompatible elements suggest that these rocks were derived from a subduction-modified mantle. On MORB-normalised diagrams (Fig. 20) they have high LILE (ie Sr, K_2O, Ba, Rb and Cs) and a distinct Nb and Ta negative anomaly typical of subduction-related magmas. The glasses, dolerite and basalt have slightly different trace element composition. The depth of the Nb and Ta anomaly and the enrichment of the LILE are slightly less in the glasses than for the basalt and dolerite (ie they seem to have less of a subduction-related signature). Although the glasses were analysed using different techniques and instruments, these differences are unlikely to be due to analytical problems for two reasons:

- There are systematic differences in K_2O between the glasses and the crystalline rocks. These were analysed using the XRF and the electron microprobe; and

- Prior to analysing glasses using the laser-ICPMS, an attempt was made to analyse a sample using XRF. This sample proved to have too much altered glass to be useful (high water content, low MgO, high Fe_2O_3 and high Al_2O_3). However, Nb, which is not normally affected by hydrothermal alteration, is similar to the Laser-ICPMS results on the fresh glass.

The chemical differences between the glasses and the crystalline rocks may be alteration-related as they affect mostly mobile elements and involve only slight differences in Nb (maximum of 3 ppm). However, these differences could potentially be very significant as a K-Ar age determination on one of these glasses provided an age of 27.0 ± 1.4 Ma and one on a coarse-grained dolerite provided an age of 46.0 ± 3.1 Ma (Table 6). Further Ar-Ar dating to check the accuracy of these K-Ar age determinations is presently being undertaken.

The basalts, dolerite and glasses are similar to rocks erupted during the initial stages of seafloor spreading in the western Pacific back-arc basins (eg Lau Basin ODP site 834, Fig. 20) with MORB-like major elements together with a strong subduction-related trace element signature.

FAUST-2 Dredge Samples Tectonic Significance

The geochemical characteristics of the rocks from all three FAUST-2 dredge sites have major implications for tectonic reconstructions of the area. These are discussed briefly here.

Boninites are rare, restricted in their distribution to the forearc of intra-oceanic island-arcs, and are usually found within 100 km of the subduction zones (Taylor et al., 1992). They are also found in ophiolites, particularly those that are thought to have formed in the forearc of intra-oceanic island-arcs. Boninitic rocks form during hydrous partial melting of subduction-modified mantle. Melting is generally thought to occur at shallow depths and high temperatures, so that a greater amount of melt is extracted compared to that which occurs at mid-ocean ridge spreading centres (Crawford et al., 1989). Most boninites are erupted immediately after convergence is initiated (Stern & Bloomer, 1992). At this time, the arc lithosphere appears to be extending rapidly and hot mantle up-welling occurs in the shallow mantle wedge close to the subduction zone. Some high-Ca boninites are thought to form where back-arc spreading centres propagate into the arc lithosphere (eg the Hunter Zone in the southern New Hebrides Arc, or the northern section of the Lau Basin in the Tonga Kermadec Arc) (Falloon & Crawford, 1991; Sigurdsson et al., 1993).

The DR2 boninites could have formed either during the early history of the Three Kings Ridge or more recently (34-25 Ma) when the western arm of the South Fiji Basin propagated into the western part of the ridge (ie through the forearc of the Three Kings Arc), forming the Cook Fracture Zone and the Forster Basin. Both of these situations most likely promote hot mantle upwelling in the forearc. To be able to determine which of these two possibilities occurred it is necessary to accurately determine the age of the boninites and the age of seafloor spreading in the Forster Basin.

Depleted peridotites similar to those in DR2 have been dredged from the forearc of intra-oceanic island-arcs such as the Marianas and the South Sandwich arcs (eg Parkinson et al., 1992; Pearce et al., 2000). The association of high-Ca boninites and depleted peridotites in DR2 strongly suggests that these were once the forearc of an intra-oceanic island-arc.

The DR3 rocks are seafloor basalts formed in a back-arc basin (South Fiji Basin) near the Cook Fracture Zone. Their chemistry is typical of rocks produced under similar conditions to MORB, but from a mantle modified by subduction processes. The slight but significant difference in the chemistry of the basaltic glasses and the basalt and dolerite suggests more than one episode of formation.

Tectonic Evolution Model

By combining the results of the interpreted geochemistry and geophysics with data from previous studies of the Norfolk Ridge – Three Kings Ridge area, an updated tectonic model for the evolution of the Three Kings Ridge and the entire Norfolk Basin is proposed. A revised tectonic provinces map for the study area is proposed (Fig. 14). A model for the evolving geodynamic setting from the Early Tertiary was developed during this project. The latest version of the model is presented in Figure 22 (after Crawford et al., in press).

It has long been apparent that the Three Kings Ridge is an extinct intra-oceanic island-arc. However, there has been considerable debate regarding the timing and polarity of this arc (Malpas et al., 1992; Mortimer et al., 1998). Data from New Caledonia and the D'Entrecasteaux Ridge further north suggest an Eocene arc above an east-dipping subduction zone (Maillet et al., 1983; Baker et al., 1994; Aitchison et al., 1995; Auzende et al., 2000). Data further south from New Zealand suggest a Miocene arc above a west-dipping subduction zone (Brothers & Delaloye, 1982; Mortimer et al., 1998; King, 2000). The identification in this study of forearc rocks from an area to the west of the Three Kings Ridge strongly supports an east-dipping subduction model. There is no evidence for a subduction zone east of the Three Kings Ridge from seismic (Herzer et al., 2000; Mortimer & Herzer, 2000), satellite-derived gravity and bathymetric data as well as the South Fiji Basin magnetic anomalies, which is based on a new interpretation by Sdrolias (2000). In addition, analyses of AGSO Survey 177 profiles NZ-I, NZ-H, NZ-G and NZ-F (Fig. 3) show no conclusive evidence for westerly-dipping reflectors or the development of forearc-related structures. The only remaining evidence for a west-dipping subduction zone beneath the ridge is the presence of 20 Ma shoshonitic volcanics in the southern section of the Three Kings Ridge (Mortimer et al., 1998). However, the shoshonites can be explained by a magmatic event associated with the Tonga-Kermadec subduction zone further to the east during back-arc-extension (eg Pliocene calc-alkaline basalt and shoshonites in Fiji; Rodgers & Setterfield, 1994).

The proposed model involves east-dipping subduction of a probable Cretaceous basin, floored by oceanic or transitional crust. Diachronous collision of the subduction zone commenced prior to 38 Ma in northern New Caledonia and the D'Entrecasteaux Ridge, and finished at 25 Ma in New Zealand. A section of this Cretaceous basin was obducted onto northern New Zealand. Evidence for this diachronous collision includes: the collision in northern New Caledonia at, or prior to, 40 Ma (Baldwin et al. 1999); the emplacement of the ophiolite nappe in southern New Caledonia after 35 Ma (Cluzel et al. 1997; Cluzel 1998); and ophiolite obduction in New Zealand at about 25 Ma (Brothers & Delafoye, 1982; Malpas et al., 1992). This indicates a southwards propagation of the collision front of between 10-15 cm/year. It also predicts the cessation of east-dipping subduction along the Three Kings Ridge in the Oligocene between 34-25 Ma. This interaction resembles a tectonic model proposed for the area by Falvey et al. (1991), based on a review of marine geological and geophysical data.

The presence of a Cretaceous basin east of New Caledonia, the Norfolk Ridge and New Zealand is now well established (Eissen et al., 1998; Nicholson et al., 2000; Ali

& Aitchison, 2000). Seismic interpretation of the survey area indicates that sections of the North and South Norfolk basins were probably formed at this time. In the model postulated there is a narrow continental fragment stranded in the Cretaceous North and South Norfolk basins prior to collision from the east (see Fig. 12 for location). This fragment is required to the east of the preserved Cretaceous basins and is supported by some morphological evidence (eg the seafloor scarp along FAUST-2 profile 13 may be the preserved western margin to this basin; ie see Fig. 12 at around 169°10'E, 29°S). The continental fragment may have blocked the collision of the combined Three Kings-Loyalty arc with the Norfolk Ridge. In addition, the presence of a continental fragment also explains the large volume of high-standing crust presently located to the east of the North Norfolk Basin, later rifted by the Forster Basin opening event. It could also account for the erosion and uplift in the central section of the Three Kings forearc (around DR2), but absent in the southern and northern sections of the Three Kings Ridge. Collision of the Three Kings Arc with this continental fragment probably caused localised thickening of the crust in the middle of the ridge followed by uplift above wave base with consequent erosion.

The proposed model at 34-25 Ma implies that the modern west-dipping Tonga-Kermadec system was initiated gradually during arc reversal, following the collision zone moving southwards at 10 cm/year. In the model the Three Kings Ridge curves towards the southeast into the Northland Plateau and the Lau Ridge. This can be inferred from the shape of the southern termination of the Three Kings Ridge in the Northland Plateau area, as seen on both the gravity and magnetic images (eg see Sdrolias, 2000 and Smith, 2000; Fig. 14).

Some of the differences between the geochemistry and structure of the New Zealand and New Caledonian obductions (eg Nicholson et al., 2000) can be explained by slight differences in the geometry of the margins and composition of the obducted crust. In New Caledonia, slices of both the Cretaceous eastwards down-going plate (the Poya Terrane), and the overlying forearc peridotites were obducted to the west. In New Zealand most of the obducted ophiolitic material consists of seafloor created during the Cretaceous rifting of Gondwana, probably in a marginal basin environment. This terrane has only subtly different chemistry to the Poya Terrane in New Caledonia (ie more of a subduction influence; Nicholson et al., 2000). The geochemical differences are similar to the chemical variations in the modern Lau Basin where the subduction signature of the seafloor basalts has decreased both with increasing basin width and with time (Hawkins & Allan, 1994).

In New Zealand equivalents of the New Caledonian peridotite nappes are not present or have been eroded. However, the presence of minor serpentinites (Brothers & Delaloye, 1982; Malpas et al., 1992; Nicholson et al., 2000) suggests that at least small sections of forearc peridotites were also involved.

In the proposed model, extension in the northeastern section of the North Norfolk Basin (ie the Forster Basin) and movement along the Cook Fracture Zone would occur immediately after cessation of subduction, when the western arm of the South Fiji spreading centre propagated into the Three Kings Ridge – Loyalty Ridge forearc and collisional orogen. The high standing blocks in the the North Norfolk Basin would probably contain extended parts of the forearc (peridotite and boninite), sections of old Cretaceous downgoing oceanic or transitional crust, and continental fragments

from the Norfolk Ridge in the Cretaceous. These were then rifted in the Oligocene and probably overlain and intruded by the rift-related Oligocene volcanics. True seafloor spreading is believed to have only occurred in the Forster Basin just south of the Cook Fracture Zone.

The FAUST-2 data constrain the tectonic reconstruction. However, it only represents part of the region's complete evolution. A large amount of mostly unpublished data has been collected over the last few years from areas to the south of New Caledonia and north of New Zealand. In the future, when these data becomes available, the tectonic models for the evolution of this area will be further refined.

Resource Potential

The Norfolk Ridge – Three Kings Ridge region is unexplored for subsea resources. Nevertheless, the presence of a substantial sedimentary pile and widespread aerial and subsea volcanism suggests that the area has potential.

Hydrocarbons

The hydrocarbon prospectivity of the wider Norfolk Ridge – Three Kings Ridge region is limited to the New Caledonia Basin (Uruski & Wood, 1991; Herzer et al., 1999; Stagg et al., in press), the Reinga Basin (Herzer et al., 1997; Herzer et al., 1999; Stagg et al., in press) and the West Norfolk Ridge (Herzer et al., 1999; Stagg et al., in press). In addition, some mention is made of the South Norfolk Basin and Three Kings Ridge setting in Herzer et al. (1999).

The southern New Caledonia Basin contains up to 4000 m of sedimentary sequences with the basal 1500 m being of probable Cretaceous age (Stagg et al., in press). Extrapolated above average heat-flow values reported on the Lord Howe Rise (Grim, 1969), with more average values recorded in DSDP 206 (Von Herzen, 1973), indicate that much of this Cretaceous sequence is thermally mature for oil generation. Several tectono-stratigraphic markers suggest that the North Norfolk Basin is of Cretaceous age (see discussion above). However, seismic data shows a substantially thinner sedimentary pile for the North Norfolk Basin implying that the potential for commercial quantities of hydrocarbons is reduced. In addition, the restricted size of the basin, and the probable compromise of trap integrity by Eocene-Oligocene tectonism, downgrade the potential for hydrocarbon plays.

Estimates of southern New Caledonia Basin age and petroleum potential may also apply to the interpreted Cretaceous South Norfolk Basin. The dredging of Late Cretaceous organic matter in marine shales from near the junction of the Reinga Ridge and Norfolk Ridge (Herzer et al., 1999) may be significant for hydrocarbon potential in the adjoining Norfolk Ridge and South Norfolk Basin. The South Norfolk Basin setting is favoured by the shedding of large quantities of sediment off the active Vening-Meinesz Fracture Zone scarp and elevated Norfolk Ridge. However, seismic data indicates that sediment thickness is considerably less for the South Norfolk Basin than for the New Caledonia Basin and the Reinga Basin, thereby limiting the generation of similar quantities of hydrocarbons. Later faulting associated with the

Eocene-Oligocene tectonism, as well as continual movement along the Vening-Meinesz Fracture Zone, may have fractured any developing plays.

The Cagou Trough has a substantial thickness of sediment, but is small in overall area. The trough is a recent extension event and is largely filled with sediment shed from its steep flanks. This results in a restricted basin that is heavily faulted and unlikely to contain source rocks. Therefore, organic-derived hydrocarbon generation is unlikely to have occurred.

Although seismic data, as well as gravity for the northern half of the Three Kings Basin (see Fig. 6a), show the presence of a thick sedimentary pile, no dredges or wells have sampled the sequences. However, shale dredged at the junction of the Norfolk Ridge and Reinga Ridge has been proposed as a potential source rock for the Three Kings Ridge (Herzer et al., 1999). Based on the tectonic setting it is expected that the sediments are those found in a volcanic island-arc environment with little potential for the input of organic matter. It must be considered that the island-arc is underlain by rifted continental crust resulting from eastern Gondwana fragmentation, which may, therefore, host source rocks.

Exon et al. (1998) reports the presence of a bottom-simulating reflector (BSR) on the adjoining respective flanks of the northern Lord Howe Rise and New Caledonia Basin. This reflector has also been mapped further south in the Monawai Basin (Stagg et al., in press). These areas are considerably distant from the Norfolk Ridge – Three Kings Ridge setting. The investigations of the seismic data reveal no shallow reflector sub-parallel to the water bottom. Therefore, we suggest that the area is not thermally conducive either for the generation of methane hydrates or for the establishment of a frozen methane hydrate interface.

Minerals

Mineral resources for the Norfolk Ridge – Three Kings Ridge region essentially refers to extractable mineral deposits on the seafloor. At the present, very little is known about the economic potential of the region.

The three dredges on the FAUST-2 survey reveal large amounts of manganese crusting and iron coating (Mauffret & Symonds et al., 2001). Although the dredges were taken from relatively steep environments, this encrustation indicates widespread manganese precipitation. There is a possibility of the presence of Mn/Fe nodule fields in the areas of low slope at least within the overall area circumscribed by these dredge sites (compare Figs 3 & 7).

Conclusions

This study confirms that the geological framework of the southwest Pacific, and in particular the Norfolk Ridge – Three Kings Ridge setting, is complex. In this initial analysis of the FAUST-2 data, along with other existing data and ideas in the wider region, we have attempted to unravel some of this complexity.

A detailed morphological analysis using, largely, swath bathymetry reveals, most importantly, that:

- the Three Kings Ridge Province has similar physiographic characteristics to the Loyalty arc system to the north;
- the narrow north-trending Cagou Trough with a stepped arcuate and steep western margins indicates extensional tectonics;
- a central region of undulating plateaus with crenulated surfaces and shallow basins reflects the rifted history of the Forster Rift Zone and extension in the adjoining Highly-Extended Zone;
- the Nepean Saddle is dominated by east-west and west-northwest-trending lenticular seamounts, which may be aligned along a major structural feature (?Norfolk Fracture Zone);
- the west-northwest-trending Cook Fracture Zone is an oceanic transform fault separating the South Fiji Basin to the north from the Forster Basin to the south; and
- the Forster Basin, south of the Cook Fracture Zone, has distinctly deeper bathymetry relative to the adjacent North Norfolk Basin.

A detailed analysis of tectono-stratigraphy in the high-resolution FAUST-2 seismic data reveals, most importantly, that:

- the seismic sequences within the southern North Norfolk Basin can be correlated with those in the New Caledonia Basin;
- the basement underlying the southern North Norfolk Basin is probably of at least Late Cretaceous age or older; and
- the basement underlying the Three Kings Ridge is probably of at least Late Cretaceous age or older.

A detailed structural analysis using deep and high-resolution seismic data reveals, most importantly that:

- the presence of rift zones at opposing ends of the Loyalty Ridge and Three Kings Ridge complexes suggests that the Cook Fracture Zone began as north-south oriented rifting within the combined island-arc system;

- the widespread presence of rift zones south of the Forster Basin indicates that rifting and breakup associated with its formation propagated southwards into the South Norfolk Basin; and

- the presence of a broad zone of depressed seafloor trending north-northeast from the South Norfolk Basin to the Cook Fracture Zone, which may be the expression of extension in line with the Cook Fracture Zone along crustal-scale detachments.

A detailed petrological and geochemical analysis shows that:

- the presence of forearc peridotites on the western side of the Cagou Trough (DR1), on the margin with the Highly-Extended Zone, indicates that the Cagou Trough is not a fossil subduction zone but a later extensional feature;

- depleted forearc peridotites and high-Ca boninites are present on the western flanks of the Three Kings Ridge (DR2). These are the southward extension of the forearc peridotites in New Caledonia;

- medium-Ti island-arc basalt, alkaline intrusive rocks and alkaline basalts are present along the western side of the Three Kings Ridge (DR2);

- the erosion and the incorporation of sediments derived from the FAUST-2 Dredge 2 rocks into shallow marine sandstones indicates that the central section of the Three Kings Ridge collided with a ridge or another large seafloor feature such as a continental plateau; and

- back-arc basin basalts and dolerite are present along the northern flanks of the Three Kings Ridge (DR3), possibly ranging in age from the Eocene to the Late Oligocene.

Based on the FAUST-2 dredge samples the resource potential for the region is currently limited to manganese. The overall restricted sedimentary thicknesses between the Norfolk Ridge and Three Kings Ridge, as well as the active tectonic setting, are unlikely to have promoted the development of hydrocarbon deposits since the Late Cretaceous.

A tectonic evolution model is proposed that combines the Loyalty Ridge – Three Kings Ridge arc and Tonga-Kermadec arc, which represent opposing limbs of a curved island-arc system advancing towards the south. This expanding front consumed east Gondwana crust to its west and Pacific crust to its east until it collided with the Norfolk Ridge and New Caledonia system to the east and Northland, New Zealand to the south.

Acknowledgments

The authors would like to thank Barry Willcox and Tony Stephenson of Geoscience Australia, Dr. Tony Crawford of the University of Tasmania and both Dr. Dietmar Müller and Maria Sdrolias of the University of Sydney for their reviews of this report.

References

Abell, R.S. & Taylor, F.J., 1981. Hydrogeological and geophysical investigations on Norfolk Island. *Bureau of Mineral Resources Record*, 1981/078.

Aitchison, J.C., Clarke, G.L., Cluzel, D. & Meffre, S., 1995. Eocene arc-continent collision in New Caledonia and implications for regional SW Pacific tectonic evolution. *Geology*, 23, 161-164.

Ali, J.R. & Aitchison, J.C., 2000. Significance of palaeomagnetic data from the oceanic Poya Terrane, New Caledonia, for SW Pacific tectonic models. *Earth and Planetary Science Letters*, 177, 153-161.

Andrews, J.E., Packham, G., Eade, J.V., Holdsworth, B.K., Jones, D.L., Klein, G.D., Kroenke, L.W., Saito, T., Shafik, S., Stoeser, D.B. & Van der Lingen, G.J., 1975. Site 285. *In* Andrews, J.E., Packham, G. et al., *Initial Reports of the Deep Sea Drilling Project*, 30, Washington (U.S. Government Printing Office), 27-67.

Arculus, R.J., Pearce, J.A., Murton, B.J. & van der Laan, S.R., 1992. Igneous stratigraphy and major element geochemistry of Holes 786A and 786B. *In* Fryer, P., Pearce, J.A., Stokking, L.B. et al., *Proceedings of the Ocean Drilling Program, Scientific Results*, 125: College Station, TX (Ocean Drilling Program), 143-169.

Auzende, J-M., Van de Beuque, S., Régnier, M., Lafoy, Y. & Symonds, P., 2000. Origin of the New Caledonia ophiolites based on a French-Australian seismic transect. *Marine Geology*, 162, 225-236.

Auzende, J-M., Lafoy, Y. & Marsset, B., 1988. Recent geodynamic evolution of the north Fiji Basin (southwest Pacific). *Geology*, 16, 925-929.

Aziz-ur-Rahman & McDougall, I., 1973. Paleomagnetism and paleosecular variation on lavas from Norfolk and Philip Islands, Southwest Pacific Ocean. *Geophysical Journal of the Royal Astronomical Society*, 33 (2), 141-155.

Baker, P.E., Coltorti, M., Briqueu, L., Hasenaka, T., Condliffe, E. & Crawford, A.J., 1994. Petrology and composition of the volcanic basement of Bougainville Guyot, Site 831. *In* Greene, H.G., Collot, J.-Y., Stokking, L.B. et al., *Proceedings of the Ocean Drilling Program, Scientific Results*, 134: College Station, TX (Ocean Drilling Program), 363-373.

Baldwin, S.L., Rawlings, T. & Fitzgerald, P.G., 1999. Thermochronology of the northern high P/T terrane of New Caledonia: implications for mid-Tertiary plate boundary processes in the SW Pacific. *In* Baldwin, S.L. & Lister, G.S. (eds), *Mid-Cretaceous to Recent Plate Boundary Processes in the Southwest Pacific, a Penrose Conference*, Arthur's Pass, New Zealand, 13-14.

Ballance, P.F., Ablaev, A.G., Pushchin, I.K., Pletnev, S.P., Birylina, M.G., Itaya, T., Follas, H.A. & Gibson, G.W., 1999. Morphology and history of the Kermadec Trench-arc-backarc basin-remnant arc system at 30 to 32 degrees S; geophysical profile, microfossil and K-Ar data. *Marine Geology*, 159, 35-62.

Barberi, F. & Varet, J., 1977. Volcanism of Afar: Small-scale plate tectonics implications. *Geological Society of America Bulletin*, 88, 1251-1266.

Bernardel, G., Lafoy, Y., Van de Beuque, S., Missegue, F. & Nercessian, A., 1999. Preliminary results from AGSO Law of the Sea Cruise 206: an Australian/French collaborative deep-seismic marine survey in the Lord Howe Rise / New Caledonia region. *Australian Geological Survey Organisation Record*, 1999/14.

Bizimis, M., Salters, V.J.M. & Bonatti, E., 2000. Trace and REE content of clinopyroxenes from supra-subduction zone peridotites. Implications for melting and enrichment processes in island arcs. *Chemical Geology*, 165, 67-85.

Black, P., 1996. Mesozoic evolution of the Norfolk Ridge system : Evidence from New Caledonia and northern New Zealand. *Geological Society of Australia Extended Abstracts*, 43, 90-92.

Bloomer, S.H., Ewart, A., Hergt, U.M. & Bryan, W.B., 1994. Geochemistry and origin of igneous rocks from the outer Tonga forearc (Site 841). *In* Hawkins, J., Parson, L., Allan, J. et al., *Proceedings of the Ocean Drilling Program Scientific Results*, 135: College Station, TX (Ocean Drilling Program), 625-646.

Bonatti, E. & Michael, P.J., 1989. Mantle peridotites from continental rifts to ocean basins to subduction zones. *Earth and Planetary Science Letters*, 91, 297-311.

Brothers, R.N. & Delaloye, M., 1982. Obducted ophiolites of North Island, New Zealand: origin, age, emplacement and tectonic implications from Tertiary and Quaternary volcanicity. *New Zealand Journal of Geology and Geophysics*, 25, 257-274.

Brothers, R.N. & Lillie, A.R., 1988. Regional geology of New Caledonia. *In* Nairn, A.E.M., Stehli, F.G. & Uyeda, S. (eds), *The Ocean Basins and Margins, 7B: The Pacific Ocean*, Plenum Press, New York, 325-374.

Burns, R.E, Andrews, J.E., Van der Lingen, G.J., Churkin, M., Galehouse, J.S., Packham, G.H., Davies, T.A., Kennett, J.P., Dumitrica, P., Edwards, A.R. & Von Herzen, R.P., 1973. Site 205. *In* Burns, R.E., Andrews, J.E. et al., *Initial Reports of the Deep Sea Drilling Project*, 21, Washington (U.S. Government Printing Office), 57-82.

Cameron, W.E., 1989. Contrasting boninite-tholeiite associations from New Caledonia. *In* Crawford, A.J. (ed), *Boninites*, London, Unwin Hyman, 314-336.

Cann, J.R., Blackman, D.K., Smith, D.K., McAllister, E., Janssen, B., Mello, S., Avgerinos, E., Pascoe, A.R. & Escartin, J., 1997. Corrugated slip surfaces formed at ridge-transform intersections on the Mid-Atlantic Ridge. *Nature*, 385, 329-332.

Cluzel, D., 1998. Le « flysch post-obduction » de Népoui, un bassin transporté ? Conséquences sur l'âge et les modalités de l'obduction tertiaire en Nouvelle-Calédonie (Pacifique sud-ouest). *Sciences de la terre et des planetes*, 327, 419-424.

Cluzel, D., Picard, C., Aitchison, J.C., Laporte, C., Meffre, S. & Parat, F., 1997. La nappe the Poya (ex-formation des Basaltes) de Nouvelle-Calédonie (Pacifique Sud-Ouest): un plateau océanique Campanien-Paléocène superieur obducté à l'Eocène: *Compte Rendu de l'Academie des Science*, Serie II, 324, 443-451.

Crawford, A.J., Meffre, S. & Symonds, P.A., *in press*. Tectonic Evolution of the SW Pacific 0-100 Ma, and analogous evolution of the 600-240 Ma Lachlan Fold Belt, Eastern Australia. *In* Muller R.D. & Hillis, R. (eds), *The Australian Plate*, Geological Society of America & Geological Society of Australia.

Crawford, A.J., Falloon, T.J. & Green, D.H., 1989. Classification, petrogenesis and tectonics setting of boninites. *In* Crawford, A.J. (ed), *Boninites*, London, Unwin Hyman, 1-49.

Davey, F.J., 1982. The Structure of the South Fiji Basin, *Tectonophysics*, 87, 185-241.

Davies, H.L. & Warren, R.G., 1988. Origin of eclogite-bearing, domed, layered metamorphic complexes (« core complexes ») in the D'Entrecasteaux Islands, Papua New Guinea. *Tectonics*, 7 (1), 1-21.

Dubois, J., Ravenne, C., Aubertin, A., Louis, J., Guillaume, R., Launay, J. & Montadert, L., 1974. Continental margins near New Caledonia. *In* Burk, C.A. & Drake, C.L. (eds), *The Geology of Continental Margins*, Springer-Verlag, New York, 521-535.

Duncan, R.R., Vallier, T.L. & Falvey, D.A., 1985. Volcanic episodes at 'Eua, Tonga Islands. *In* Scholl, D.W. & Vallier, T.L., (eds) *Geology and Offshore Resources of the Pacific Islands Arcs – Tonga Region*, Circum-Pacific Council for Energy and Mineral Resources Earth Science Series 2, 281-290.

Dupont, J., 1988. The Tonga and Kermadec Ridges. *In* Nairn, A.E.M., Stehli, F.G. & Uyeda, S. (eds), *The Ocean Basins and Margins, 7B: The Pacific Ocean*, Plenum Press, New York, 375-409.

Eade, J.V., 1988. The Norfolk Ridge system and its margins. *In* Nairn, A.E.M., Stehli, F.G. & Uyeda, S. (eds), *The Ocean Basins and Margins, 7B: The Pacific Ocean*, Plenum Press, New York, 303-324.

Eissen, J-P., Crawford, A.J., Cotton, J., Meffre, S., Bellon, H. & Delaune, M., 1998. Geochemistry and tectonic significance of basalts in the Poya Terrane, New Caledonia. *Tectonophysics*, 284, 203-219.

Ewart, A., Bryan, W.B., Chappell, B.W. & Rudnick, R.L., 1994. Regional geochemistry of the Lau-Tonga arc and backarc systems. *In* Hawkins, J., Parson, L., Allan, J. et al., *Proceedings of the Ocean Drilling Program Scientific Results*, 135: College Station, TX (Ocean Drilling Program), 385-425.

Ewart, A., Brothers, R.N. & Mateen, A., 1977. An outline of the geology and geochemistry & the possible petrogenetic evolution of the volcanic rocks of the Tonga-Kermadec arc. *Journal of Volcanology and Geothermal Research*, 2, 205-250.

Exon, N.F., Dickens, G.R., Auzende, J-M., Lafoy, Y., Symonds, P.A. & Van de Beuque, S., 1998. Gas hydrates and free gas on the Lord Howe Rise. *PESA Journal*, 26, 148-158.

Falloon, T.J. & Crawford, A.J., 1991. The petrogenesis of high-calcium boninite lavas dredged from the northern Tonga ridge. *Earth and Planetary Science Letters*, 102, 375-394.

Falvey, D.A., Colwell, J.B., Coleman, P.J., Greene, H.G., Vedder, J.G. & Burns, T.R., 1991. Petroleum prospectivity of Pacific island arcs: Solomon Islands and Vanuatu. *APEA Journal*, 31, 191-205.

Fujiwara, T., Yamazaki, T., Joshima, M., 2001. Bathymetry and magnetic anomalies in the Havre Trough and southern Lau Basin : from rifting to spreading in back-arc basins. *Earth and Planetary Science Letters*, 185, 253-264.

Gaina, C., Müller, R.D., Royer, J.-Y., Stock, J., Hardebeck, J. & Symonds, P., 1998. The tectonic history of the Tasman Sea: a puzzle with 13 pieces. *Journal of Geophysical Research*, 103, 12413-12433.

Gans, P.B., 1987. An open-system, two-layer crustal stretching model for the eastern Great Basin. *Tectonics*, 6 (1), 1-12.

Garfunkel, Z., 1986. Review of oceanic transform activity and development. *Journal of the Geological Society London*, 143, 775-784.

Greene, G.H., Collot, J-Y., Fisher, M.A. & Crawford, A.J., 1994. Neogene tectonic evolution of the New Hebrides Island Arc : a review incorporating ODP drilling results. *In* Greene, H.G., Collot, J.-Y., Stokking, L.B. et al., *Proceedings of the Ocean Drilling Program, Scientific Results*, 134: College Station, TX (Ocean Drilling Program), 19-46.

Grim, P.J., 1969. Heatflow measurements in the Tasman Sea. *Journal of Geophysical Research*, 74, 3933-3934.

Hawkins, J.W. & Alan, J.F., 1994. Petrologic evolution of Lau Basin Sites 834 through 839. *In* Hawkins, J.W., Parson, L.M. & Allan, J.F. (eds), *Proceedings of the Ocean Drilling Program*, 135, 427-470.

Herzer, R.H., 1995. Seismic Stratigraphy of a Buried Volcanic Arc, Northland, New Zealand, and Implications for Neogene Subduction. *Marine and Petroleum Geology*, 12, 511-531.

Herzer, R.H. & Mascle, J., 1996. Anatomy of a continent-backarc transform - the Vening Meinesz Fracture Zone northwest of New Zealand. *Marine Geophysical Researches,* 18, 401-427.

Herzer, R., Mascle, J., Davy, B., Ruellan, E., Mortimer, N., Laporte, C. & Duxfield, A., 2000. New constraints on the New Zealand-South Fiji Basin continent-back-arc margin. *Comptes Rendus de l'Academie des Sciences,* Serie II, 330, 701-708.

Herzer, R.H., Sykes, R., Killops, S.D., Funnell, R.H., Burggraf, D.R., Townend, J., Raine, J.I. & Wilson, G.J., 1999. Cretaceous carbonaceous rocks from the Norfolk Ridge system, Southwest Pacific : implications for regional petroleum potential. *New Zealand Journal of Geology and Geophysics,* 42, 57-73.

Herzer, R.H., Chaproniere, G.C.H., Edwards, A.R., Hollis, C.J., Pelletier, B., Raine, J.I., Scott, G.H., Stagpoole, V., Strong, C.P., Symonds, P., Wilson, G.J. & Zhu, H., 1997. Seismic stratigraphy and structural history of the Reinga Basin and its margins, southern Norfolk Ridge system. *New Zealand Journal of Geology and Geophysics,* 40, 425-451.

Hill, P.J., 1993. N/O *L'Atalante* swath-bathymetry and geophysical survey of the Norfolk Ridge and Vening-Meinesz Fracture Zone, October 1993. *Australian Geological Survey Organisation Record,* 1993/85.

Hill, E.J., Baldwin, S.L. & Lister, G.S., 1992. Unroofing of active metamorphic core complexes in the D'Entrecasteaux Islands, Papua New Guinea. *Geology,* 20, 907-910.

Ishii, T., Robinson, P.T., Maekawa, H. & Fiske, R., 1992. Petrological studies of peridotites from diapiric serpentinite seamounts in the Izu-Ogasawara-Mariana forearc, Leg 125. *In* Fryer, P., Pearce, J.A., Stokking, L.B. et al., *Proceedings of the Ocean Drilling Program, Scientific Results,* 125: College Station, TX (Ocean Drilling Program), 445-486.

Jenner, G.A., 1981. Geochemistry of high-Mg andesites from Cape Vogel, Papua New Guinea. *Chemical Geology,* 33, 307-332.

Jones, J.G. & McDougall, I., 1973. Geological history of Norfolk and Philip Islands, southwest Pacific Ocean. *Journal Geological Society Australia,* 20, 239-254.

Johnson, K.T., Dick, H.J.B. & Shimizu, N., 1990. Melting in the oceanic upper mantle: an ion microprobe study of diopsides in abyssal peridotites. *Journal of Geophysical Research,* 95, 2661-2678.

Kamenetsky, V.S., Crawford, A.J. & Meffre, S., 2001. Factors controlling chemistry of magmatic spinel: An empirical study of associated olivine, Cr-spinel and melt inclusions from primitive rocks. *Journal of Petrology,* 42, 655-671.

Karig, D.E., 1970. Ridges and basins of the Tonga-Kermadec island arc system. *Journal of Geophysical Research,* 75 (2), 239-254.

King, P.R., 2000. Tectonic reconstructions of New Zealand: 40 Ma to the present [Review]. *New Zealand Journal of Geology & Geophysics*, 43, 611-638.

Kroenke, L.W., 1984. Cenozoic tectonic development of the southwest Pacific. *United Nations Economic and Social Commission for Asia and the Pacific, Committee for Co-ordination of Joint Prospecting for Mineral Resources in the South Pacific Offshore areas, Technical Bulletin*, 6, 122 pp.

Kroenke, L.W. & Dupont, J., 1982. Subduction-obduction: a possible north-south transition along the west flank of the Three Kings Ridge. *Geo-Marine Letters*, 2, 11-16.

Kroenke, L.W. & Eade, J.V., 1982. Three Kings Ridge: a west-facing arc. *Geo-Marine Letters*, 2, 5-10.

Lafoy, Y., Van de Beuque, S., Missegue, F., Nercessian, A. & Bernardel, G., 1998. Campagne de sismique multitraces entre la marge est Australienne et le sud de l'arc des Nouvelles-Hebrides: rapport de la campagne Rig Seismic 206 (21 avril - 24 mai 1998), *Programme FAUST (French-Australian Seismic Transect) Rapport ZoNéCo*, 40 pp.

Lapouille, A., 1978. Southern New Hebrides Basin and Western South Fiji Basin as a Single Marginal Basin. *In* Coleman, P.J. (ed), *Second Southwest Pacific Earth Science Symposium and I.G.C.P. Project Meeting, Australian Society of Exploration Geophysicists Bulletin*, 9, 131-133.

Lapouille, A., 1977. Magnetic Surveys Over the Rises and Basins in the South-West Pacific. *In International Symposium of Geodynanics in Southwest Pacific, Noumea (New Caledonia) 27 August-2 September 1976 Editions Technip. Paris*, 15-28.

Lapouille, A. & Dugas, F., 1975. Geological evolution of New Hebrides and Loyalty areas. *Australian Society of Exploration Geophysicists Bulletin*, 6 (2/3), 52.

Launay, J., Dupont, J. & Lapouille, A., 1982. The Three Kings Ridge and the Norfolk Basin (Southwest Pacific): an attempt at structural interpretation. *South Pacific Marine Geological Notes*, 2 (8), 121-130.

Leblanc, M., 1995. Chromitite and ultramafic rock compositional zoning through a paleotransform fault, Poum, New Caledonia. *Economic Geology*, 90, 2028-2039.

Maillet, P., Monzier, M., Selo, M. & Storzer, D., 1983. The D'Entrecasteaux Zone (southwest Pacific). A petrological and geochronological reappraisal. *Marine Geology*, 53, 179-197.

Malpas, J., Spörli, K.B., Black, P.M. & Smith, I.E.M., 1992. Northland ophiolite, New Zealand, and implications for plate-tectonic evolution of the southwest Pacific. *Geology*, 20, 149-152.

Mauduit, T. & Dauteuil, O., 1996. Small-scale models of oceanic transform zones. *Journal of Geophysical Research*, 101(B9), 20195-20209.

Mauffret, A., Symonds, P., Benkhelil, J., Bernardel, G., Buchanan, C., D'Acremont, E., Gorini, C., Lafoy, Y., Nercessian, A., Ryan, J., Smith, N. & Van de Beuque, S., 2001. Collaborative Australia/France Multibeam Seafloor Mapping Survey – Norfolk Ridge to Three Kings Ridge Region: FAUST-2, Preliminary Results. *Australian Geological Survey Organisation Record,* 2001/27.

Meffre, S., 1995. The development of island arc-related ophiolites and sedimentary sequences in New Caledonia. *PhD Thesis*, University of Sydney, 236 pp.

Meffre, S., Aitchison, J.C. & Cluzel, D., 1993. New constraints on the Permian to Eocene tectonics of the SW Pacific: Evidence from New Caledonia. *In* STAR meeting at 22nd SOPAC annual session, Suva, Fiji, 2-5 October 1993, *STAR 1993 Abstracts*, http://www.sidenet.org/pacific/sopac/star/star5af.htm

Monzier, M., Robin, C., Eissen, J.-P. & Cotten, J., 1997. Geochemistry vs. seismotectonics along the volcanic New Hebrides island arc chain (southwest Pacific). *Journal of Volcanology and Geothermal Research*, 78, 1-29.

Mortimer, N. & Herzer, R.H., 2000. Diverse SW Pacific Miocene Volcanotectonic Architecture: New seismic and petrologic data favour simple model. *Eos 81*, 48, F1088.

Mortimer, N., Herzer, R.H., Gans, P.B., Parkinson, D.L. & Seward, D., 1998. Basement geology from Three Kings Ridge to West Norfolk Ridge, southwest Pacific Ocean : evidence from petrology, geochemistry and isotopic dating of dredge samples. *Marine Geology*, 148, 135-162.

Müller, R.D., Gaina, C., Tikka, A., Mihut, D., Cande, S. & Stock, J.M., 2000. Mesozoic/Cenozoic tectonic events around Australia. *American Geophysical Union*, Monograph 121, 161-188.

Murton, B.J., Peate, D.W., Arculus, R.J., Pearce, J.A. & Van der Laan, S., 1992. Trace-element geochemistry of volcanic rocks from site 786: the Izu Bonin forearc. *In* Fryer, P., Pearce, J.A., Stokking, L.B. et al., *Proceedings of the Ocean Drilling Program, Scientific Results*, 125: College Station, TX (Ocean Drilling Program), 211-236.

Nicholson, K.N., Picard, C. & Black, P.M., 2000. A comparative study of Late Cretaceous ophiolitic basalts from New Zealand and New Caledonia. *Tectonophysics*, 327, 157-171.

Norman, M.D., Griffin, W.L., Pearson, N.J., Garcia, M.O. & Oreilly, S.Y., 1998. Quantitative Analysis of Trace Element Abundances in Glasses and Minerals - a Comparison of Laser Ablation Inductively Coupled Plasma Mass Spectrometry, Solution Inductively Coupled Plasma Mass Spectrometry, Proton Microprobe and Electron Microprobe Data. *Journal of Analytical Atomic Spectrometry*, 13, 477-482.

Norman, M.D., Pearson, N.J., Sharma, A. & Griffin, W.L., 1996. Quantitative Analysis of Trace Elements in Geological Materials by Laser Ablation Icpms - Instrumental Operating Conditions and Calibration Values of Nist Glasses. *Geostandards Newsletter*, 20, 247-261.

Packham, G.H. & Falvey, D.A., 1971. A hypothesis for the formation of marginal seas in the western Pacific. *Tectonophysics*, 11, 79-109.

Packham, G.H. & Terrill, A., 1975. Submarine geology of the South Fiji Basin. *In* Andrews, J.E., Packham, G. et al., *Initial Reports of the Deep Sea Drilling Project*, 30, Washington (U.S. Government Printing Office), 617-645.

Paris, J.P., 1981. Géologie de la Nouvelle Calédonie: Un essai de synthèse. *Bureau de Recherches Géologiques et Minières, Orléans, France, Memoire*, 113, 277 pp.

Parkinson, I.J., Pearce, J.A., Thirlwall, M.F., Johnson, K.T.M. & Ingram, G., 1992. Trace element geochemistry of peridotites from the Izu-Bonin-Mariana forearc, Leg 125. *In* Fryer, P., Pearce, J.A., Stokking, L.B. et al., *Proceedings of the Ocean Drilling Program, Scientific Results*, 125: College Station, TX (Ocean Drilling Program), 487-506.

Parson, L.M. & Hawkins, J.W., 1994. Two-stage ridge propagation and the geological history of Lau back-arc basin. *In* Hawkins, J., Parson, L., Allan, J. et al., *Proceedings of the Ocean Drilling Program Scientific Results*, 135: College Station, TX (Ocean Drilling Program), 819-828.

Pearce, J.A., Barker, P.F., Edwards, S.J., Parkinson, I.J. & Leat, P.T., 2000. Geochemistry and tectonic significance of peridotites from the South Sandwich arc-basin system, South Atlantic. *Contributions to Mineralogy and Petrology*, 139, 36-53.

Ramsay, D.C., Herzer, R.H. & Barnes, P.M., 1997. Continental shelf definition in the Lord Howe Rise and Norfolk Ridge regions: Law of the Sea Survey 177, part 1 - preliminary results. *Australian Geological Survey Organisation Record*, 1997/54.

Ranero, C.R. & Reston, T.J., 1999. Detachment faulting at ocean core complexes. *Geology*, 27 (11), 983-986.

Rigolot, P., 1989. *Origine et évolution du "système" Ride de Nouvelle-Calédonie/Norfolk (Sud-Ouest Pacifique): synthèse des données de géologie et de géophysique marine, étude des marges et bassins associés.* Brest, 319 pp.

Robinson, P., Townsend, A.T., Yu, Z.S. & Munker, C., 1999. Determination of scandium, yttrium and rare earth elements in rocks by high resolution inductively coupled plasma-mass spectrometry. *Geostandards Newsletter*, 23, 31-46.

Rodgers, N.W. & Setterfield, T.N., 1994. Potassium and incompatible-element enrichment in shoshonitic lavas from the Tavua volcano, Fiji. *Chemical Geology*, 118, 43-62.

Sandwell, D.T. & Smith, W.H.F., 2000. Satellite gravity for the world. *Ftp topex.ucsd.edu/pub/global_grav_2min.*

Sandwell, D.T. & Smith, W.H.F., 1997. Marine gravity anomaly from Geosat and ERS-1 satellite altimetry. *Journal of Geophysical Research*, Vol. 102 (B5), 10039-10054.

Sdrolias, M., 2000. Tectonic history of southwest Pacific back-arc basins. *Honours Thesis*, University of Sydney, 101 pp.

Severinghaus, J.P. & Macdonald, K.C., 1988. High Inside Corners at Ridge-Transform Intersections. *Marine Geophysical Researches*, 9, 353-367.

Seyler, M. & Bonatti, E., 1994. Na, Al(IV) and Al(VI) in Clinopyroxenes of Subcontinental and Suboceanic Ridge Peridotites - a Clue to Different Melting Processes in the Mantle. *Earth and Planetary Science Letters*, 122, 281-289.

Shaw, R.D., 1978. Seafloor spreading in the Tasman Sea : a Lord Howe Rise – eastern Australia reconstruction. *Australian Society of Exploration Geophysicists*, 9 (3), 75-81.

Shikazono, N., 1999. Rare earth element geochemistry of Kuroko ores and hydrothermally altered rocks: Implication for evolution of submarine hydrothermal system at back arc basin. *Resource Geology*, special issue 20, 23-30.

Shor, G.G., Kirk, H.K. & Menard, G.L., 1971. Crustal structure of the Melanesian arc. *Journal of Geophysical Research*, 76, 2562-2586.

Sigurdsson, I.A., Kamenetsky, V.S., Crawford, A.J., Eggins, S.M. & Zlobin, S.K., 1993. Primitive island arc and oceanic lavas from the Hunter Ridge-Hunter Fracture Zone. Evidence from glass, olivine and spinel compositions. *Mineralogy and Petrology*, 47, 149-169.

Smith, N., 2000. A revised theory for the origin and tectonic evolution of the Norfolk Ridge-Three Kings ridge area in the South-west Pacific. *Honours Thesis*, University of Sydney, 90 pp.

Smith, W.H.F. & Sandwell, D.T., 1997. Global Sea Floor Topography from Satellite Altimetry and Ship Depth Soundings. *Science*, 277, 1956-1962.

Smith, W.H.F., Sandwell, D.T. & Small, C., 1997. Predicted bathymetry and GTOPO30 for the world. *Ftp topex.ucsd.edu/pub/global_topo_2min.*

Souriot, T. & Brun, J.-P., 1992. Faulting and block rotation in the Afar triangle, East Africa : The Danakil « crank-arm » model. *Geology*, 20, 911-914.

Spörli, K.B. & Kear, D., 1989 (eds). Geology of Northland : accretion, allochthons and arcs at the edge of the New Zealand micro-continent. *Royal Society of New Zealand Bulletin*, 26.

Stagg, H.M.J., Alcock, M.B., Borissova, I., Moore, A.M.G. & Symonds, P.A., *in press.* Geological framework of the southern Lord Howe Rise and adjacent ocean basins. *Australian Geological Survey Organisation Record.*

Stern, R.J. & Bloomer, S.H., 1992. Subduction zone infancy: Example from the Eocene Izu-Bonin-Mariana and Jurassic California arcs. *Geological Society of America*, 104, 1621-1636.

Symonds, P.A., Stagg, H.M.J. & Borissova, I., 1999. The transition from rifting and break-up to convergence in the Lord Howe Rise – Norfolk Ridge region. *In Mid-Cretaceous to Recent plate boundary processes in the Southwest Pacific, Penrose Conference, New Zealand, 1999, Abstract Volume*, 94-95.

Symonds, P.A., Colwell, J.B., Struckmeyer, H.I.M., Willcox, J.B. & Hill, P.J., 1996. Mesozoic rift basin development off eastern Australia. *Geological Society of Australia Extended Abstracts*, 43, 528-542.

Tajima, F. & Okal, E.A., 1995. The 1977 Three Kings Ridge earthquake (M_s = 6.7): broad-band aspect of the source rupture. *Physics of the Earth and Planetary Interiors*, 89, 109-125.

Taylor, R.N., Murton, B.J. & Nesbit, R.W., 1992. Chemical transects across intra-oceanic island arcs: implications for the tectonic settings of ophiolites. *In* Parson, L.M., Murton, B.J. & Browning, P. (eds), *Ophiolites and their Modern Analogues*, Volume 60: Geological Society of London Special Publication, 117-132.

Tucholke, B.E. & Lin, J., 1994. A geological model for the structure of ridge segments in slow spreading ocean crust. *Journal of Geophysical Research*, 99 (B6), 11937-11958.

Uruski, C. & Wood, R., 1991. A new look at the New Caledonia Basin, an extension of the Taranaki Basin, offshore North Island, New Zealand. *Marine and Petroleum Geology*, 8, 379-391.

van der Linden, W.J.M., 1967. Structural Relationships in the Tasman Sea and South-west Pacific Ocean. *New Zealand Journal of Geology and Geophysics*, 10, 1280-1301.

Veevers, J.J., 2000. Change of tectono-stratigraphic regime in the Australian plate during the 99 Ma (mid-Cretaceous) and 43 Ma (mid-Eocene) swerves of the Pacific. *Geology*, 28, 47-50.

Von Herzen, R.P., 1973. Geothermal measurements, Leg 21. *In* Burns, R.E., Andrews, J.E. et al., *Initial Reports of the Deep Sea Drilling Project*, 21, Washington (U.S. Government Printing Office), 443-457.

Weissel, J.K. & Hayes, D.E., 1977. Evolution of the Tasman Sea reappraised. *Earth and Planetary Science Letters*, 36, 77-84.

Willcox, J.B., Baillie, P., Exon, N.F., Lee, C.S. & Thomas, B., 1989. The geology of western Tasmania and its continental margin – with particular reference to petroleum potential. *Bureau of Mineral Resources Record*, 1989/13.

Williams, J.W. & Murray, A.S., 1985. Gravity measurements at Sydney, Lord Howe and Norfolk Islands. *Bureau of Mineral Resources Record*, 1985/001.

Yan C.-Y. & Kroenke, L.W., 1993. A plate tectonic reconstruction of the southwest Pacific, 0-100 Ma. *In* Berger, W.H., Kroenke, L.W., Mayer, L.A., et al., *Proceedings of the Ocean Drilling Program, Scientific Results*, 130 : College Station, TX (Ocean Drilling Program), 697-709.

Yu, Z.S., Robinson, P., Townsend, A.T., Munker, C. & Crawford, A.J., 2000. Determination of high field strength elements, Rb, Sr, Mo, Sb, Cs, Tl and Bi at ng g(-1) levels in geological reference materials by magnetic sector ICP-MS after HF/HClO4 high pressure digestion. *Geostandards Newsletter*, 24, 39-50.

Zhu, H. & Symonds, P.A., 1994. Seismic Interpretation, Gravity Modelling and Petroleum Potential of the Southern Lord Howe Rise Region. *1994 New Zealand Petroleum Conference Proceedings, Energy Resources Division, Ministry of Commerce, New Zealand*, 223-230.

Appendices

Appendix 1: Proposed naming of seafloor/tectonic features

Proposal for naming of seafloor/tectonic features

Bates Plateau	Named after Mt Bates on Norfolk Island. The Bates Plateau is the triangular zone of elevated seafloor centred at about 171°20'E, 29°30'S.
Blackbourne Seamount	Named after Point Blackbourne on Norfolk Island. The lenticular seamount is centred at 169°10'E, 29°50'S.
Cagou Trough	Named after the Cagou bird, which is the emblem of New Caledonia. The Cagou Trough is a narrow north-south trending trough to the east of Bates Plateau.
Faust Guyot	Named after the FAUST-2 (French AUstralian Seismic Transect) survey. The large lenticular guyot is centred at 170°04'E, 29°44'S
Highly-Extended Zone	North-northeast-trending zone of crust stretching from the South Norfolk Basin to the Cook Fracture Zone representing a zone of 'highly-extended' crust. Its bathymetric expression is given by the Philip Trough.
Kingston Plateau	Named after the city of Kingston on Norfolk Island. The Kingston Plateau region is east of the North Norfolk Basin.
Nepean Saddle	Named after Nepean Island, south of Norfolk Island. The Nepean Saddle is the spur-like protrusion of the Norfolk Ridge east of Norfolk Island.
Philip Trough	Named after Philip Island, south of Norfolk Island. The Philip Trough is the northeast-trending broad trough between the Bates and Kingston Plateaus.
Forster Basin	Formerly known as part of the North Norfolk Basin, named after John Reinhold Forster, a naturalist aboard Cook's second voyage. The Forster Basin is that part of the formerly named North Norfolk Basin resulting from seafloor spreading propagating down a South Fiji Basin spreading arm.
Forster Rift Zone	North-south-trending zone of rifted crust that extends south from the Forster Basin and its flanks into the South Norfolk Basin.
Three Kings Basin	Sedimentary basin underneath the Three Kings Terrace west of the main volcanic chain surmounting the Three Kings Ridge.
Three Kings Terrace	Bathymetric feature above the Three Kings Basin.
'Transitional' SFB	Strip of seafloor to the east of the Loyalty Ridge and the Three Kings Ridge leading into the South Fiji Basin.

Appendix 2: Southwest Pacific tectonic events table from the Late Cretaceous to the present

Time scale	Epoch	Plate Motion	Compression/ Extension	Basin Spreading	Magnetic Anomalies			Volcanism	Chrono-Stratigraphy Lord Howe Rise	Seismic Sequences Lord Howe Rise
1.8			~3-1.5 Ma initial impact of d'Entrecasteaux Zone with the New Hebrides Island Arc (Epi Island) (26)		Lau Basin: 2-3 anomalies (28)	North Fiji Basin: 2'-J anomalies (3-0.9 Ma) (18)				
4	Pliocene			Post 5.4 Ma opening of the Harve Trough (1)				3.05-2.32 Ma Norfolk & Philip Islands subaerial intraplate volcanism (2)		
5								5.8-5.3 Ma New Hebrides Island arc (central belt) oldest volcanism (3, 26)		
6	Miocene			6-5.6 Ma opening of the Lau Basin (1,5)				5.4-15 Ma Lau-Colville arc volcanism (1); 10 Ma South Solomon arc volcanism begins (21); 9-11 Ma Loyalty Ridge intraplate volcanism (9, 25); 12 Ma Lord Howe volcanism (15); Early to Late Miocene New Hebrides Island arc (eastern belt) volcanism (26)		
8			8-10 Ma Solomon Island Arc collides with Ontong Java Plateau, and Vitiaz subduction ceased. 10-12 Ma separation of the New Hebrides Island Arc and counter-clockwise rotation from Vitiaz Trench (26); 12 Ma South Solomon subduction initiated (21)							
10				12-10 Ma opening of the North Fiji Basin (26)						
12		12 Ma change in the Indo-Australia Plate motion to a northward direction (21)							**Mid -Tertiary to Late Miocene (~7.7 Ma) volcanics:** Lord Howe Island & nearby Ball's Pyramid, three major periods of oceanic island volcanics; **Mid-Miocene or younger volcanics:** Southern Lord Howe Rise (24)	
14										Post-Oligocene (post-olig = GB1-3): foraminiferal-nannofossil ooze (24)
16										
18								18 Ma South Norfolk Basin intraplate volcanism (4)		
20								22/26 -16 Ma Northland, New Zealand arc-related volcanism (4, 19); 19-22 Ma Three Kings Ridge (4)		
22			~23/25 Ma subduction along the Melanesian trench ceased after the docking of the Ontong Java Plateau (5,21); 25-22 Ma obduction of Northland Allochton from the northeast onto Northland, New Zealand (7,16)							
24		27-23 Ma change in the Indo-Australia Plate to roughly a northwestward direction, Pacific Plate motion is to the northwest (1,7,21)						26-25 Ma Norfolk Ridge volcanism (4); 28-24 Ma inception of Tonga-Kermadec arc (1); Late Oligocene to early Miocene New Hebrides Island Arc (western belt) earliest volcanism (26)		
26	Oligocene			26/25.5 Ma South Fiji Basin finishes opening (1,8)		South Fiji Basin: 7N-13 anomalies (33.1-24.5 Ma) (11)				
28										
30			?27-28/40Ma onset of subduction along the proto-Tonga-Kermadec Trench (21, 1, 29)							
32									**Late Eocene to Oligocene regional unconformity**: New Caledonia Basin Site 206, 33-43Ma; Lord Howe Rise Site 592, Late Eocene to Oligocene; Site 207, 46-13 Ma; Site 208, Upper Eocene to mid-Oligocene (24)	
34				33/35.5 Ma South Fiji Basin starts opening (1,8)				37-36 Ma Southern Lord Howe Rise and Challenger Plateau basaltic volcanics related to regional extension (24)		Lower Eocene-Oligocene Post-rift sequence 2 (eocl-olig = GB4): foraminiferal-nannofossil ooze and chert (24)
36	Eocene									
38			Commencement of convergence along the eastern margin of east Australia Plate from New Guinea, through New Caledonia to New Zealand (10); 42-36 Ma obduction of ophiolites from the northeast onto New Caledonia (9,20)					~38 Ma Loyalty Ridge volcanism ceased (9)		
40								~40 Ma Melanesian arc volcanism commences (21)		
42		43 Ma change in the Pacific Plate to a northwestward motion (17); major change in Indo-Australia Plate motion to a northwestward direction (21)		42 Ma North Loyalty Basin finishes opening (12,14)						
44			43 Ma southward subduction began along Manus-North Solomon-Vitiaz Trench (21)							
46								Eocene rhyolite, early stage of arc volcanism in the Tonga region (27)		
48							North Loyalty Basin: 28-21 anomalies (58.1-45.6 Ma) (11,10)			
50			50 Ma end of Gondwana break up and rifting (6)							
52			55-40 Ma northward subduction beneath the Rennell-New Caledonia and Norfolk arcs. Convergence was accommodated along transform faults along South Rennell-d'Entrecasteaux fracture zones and the western side of Norfolk Ridge (21)	52 Ma cessation of spreading in the Coral Sea (11)					**Early Eocene regional unconformity:** Southern & northern Lord Howe Rise DSDP 207 & 206 sites, New Caledonia Basin DSDP 206 (24)	
54		~55 Ma major change in the Indo-Australia plate motion to roughly a northeastward direction, Pacific Plate motion is northward (21)		54/52 Ma cessation of spreading in the Tasman Sea (10,13)	Coral Sea: 27-24 anomalies (54 Ma) (10)					Campanian-Lower Eocene post-rift sequence 1 (camp-maas-eocl = GB5-6): shallow marine silty claystone (24)
55				55 Ma North Loyalty Basin starts opening (12,14)						
56	Palaeocene			56 Ma cessation of spreading in the New Caledonia Basin (9)		Tasman Basin: 33-24 anomalies (75-55 Ma) (10,23)				
58										
60										
62				61 Ma Coral Sea starts opening (11)						
64										
65		~74-65 Ma change in the Pacific Plate motion to a northwest direction, Australia-Antarctica continue to slowly separate, while counterclockwise rotating (21)								
66	Late Cretaceous									
70										
74		~85-74 Ma Pacific Plate is moving northward direction. ~85 Ma major change in Australia-Antarctica Plate motion to a northward direction. Challenger Plateau, Lord Howe Rise, Norfolk Ridge, North Island, NZ slowly separates from Australia, moving towards the northeast (21)		72 Ma rifting ceased in the Lord Howe & Middleton Basins (14)						Cenomanian - Campanian syn-rift fill (cen-camp = GB7-10): continental to paralic clastics (24)
78				75 Ma New Caledonia Basin starts opening (9)	Norfolk Basin: 33o-34 anomalies (85-75 Ma) (22)					
82			Preceding 80 Ma subduction of the Pacific-Phoenix ridge east of New Zealand (5)	82/84 Ma Tasman Sea starts opening (10,13,14)						
86			~84 Ma extension of Lord Howe Rise & Dampier Ridge (14)	~84 Ma Lord Howe & Middleton Basins began to form (14)						
90		100-85 Ma change in the Pacific Plate motion to northwards, Australia is roughly moving in a northeastward direction with the Antarctica Plate (21)	90 Ma break up and rifting of Gondwana (6)					94 Ma Southern Lord Howe Rise subaerial to very shallow rhyolites and tuffs, DSDP site 207 (24)		
94										
98				96 Ma slow spreading between Australia and Antarctica (21)						

References:

(1) Ballance et al., 1999; (2) Jones & McDougall, 1973; (3) Lapouille & Dugas, 1975; (4) Mortimer et al., 1998; (5) Müller et al., 2000; (6) Hill, 1993; (7) Malpas et al., 1992; (8) Davey, 1982; (9) Eissen et al., 1998; (10) Symonds, et al., 1996; (11) Sdrolias, 2000; (12) Meffre, 1995; (13) Weissel & Haynes, 1977; (14) Mauffret & Symonds et al., 2001; (15) Symonds et al., 1999; (16) Mortimer & Herzer, 2000; (17) Veevers, 2000; (18) Auzende, et al., 1988; (19) Herzer, 1995; (20) Aitchison, et al., 1995; (21) Yan & Kroenke, 1993; (22) Launay et al., 1982; (23) Shaw, 1978; (24) Stagg et al., in press; (25) Kroenke, 1984; (26) Greene, et al., 1994; (27) Bloomer et al., 1994; (28) Parson & Hawkins, 1994; (29) Crawford et al., in press.

Appendix 3: Analytical methods used on the FAUST-2 dredge samples

Dating

The K-Ar dating was performed at Geochron Laboratories, Cambridge, Massachussets, USA by Richard Reesman. K was measured by flame spectrometry and Ar by mass spectrometry. Between 1 and 2 g of samples were prepared by Sébastien Meffre at the University of Tasmania. Samples were crushed in mortar and pestle and sieved to 200-600 µm. The least magnetic fractions were separated using a *Franz magnetic separator* and the final concentrates were picked by hand.

Whole rock geochemistry

The samples were coarsely crushed in a jaw to a grainsize smaller than 5 mm. Approximately 20 g of the rock, free of vesicles and manganese crust, was picked for analysis and washed in distilled water. The material was then dried and crushed to a powder in an agate mill. For major element determinations 0.77 g of samples were fused at 1100°C with *Norrish Flux* in Au/Pt crucibles and quenched to glass discs in platinum moulds. For trace element determination the powdered 10 gm samples were pressed into pills (3.5 ton/cm^2 pressure). Analysis was undertaken on the discs and pellets using a *Philips PW1480 X-Ray Spectrometer* calibrated with pure element oxide mixes in pure silica, along with international and Tasmanian standard rocks.
Low level trace elements were determined by dissolving the powders in triple distilled hydrofluoric and nitric acids. Analysis was performed on a *Hewlett Packard HP4500* ICPMS using the method of Robinson et al. (1999) and Yu et al. (2000). International standards were run with the samples with results generally within 1% of the recommended values on BHVO (maximum difference 5%).

Major elements in mineral and glasses

Major element analyses were undertaken using a *Cameca SX50* electron microprobe with 4 wave length dispersive spectrometers calibrated using natural standard minerals and operated at an accelerating voltage of 15kV, a beam current of 25 nA and a beam size of approximately 3 µm.

Trace elements in minerals and glasses

Trace elements in pyroxene and the DR3 glasses were determined using a *Hewlett Packard HP4500* ICPMS equipped with a *Merchantek Nd-YAG* laser using a method similar to Norman et al. (1998). The pyroxenes were analysed with a laser beam size of 100 µm at 4 Hz and 1.1 mJ. The glasses were analysed with a 50 µm laser beam at 10 Hz and 0.5 mJ. Analysis was performed in line mode so that the beam was moved along a line 260 µm long during the analysis. Matrix effects were corrected for by normalising data to Ca values determined by ion microprobe. Mass bias and fractionation effects using natural glass standard BCR-2G (values from Norman et al. 1998). To check the accuracy of the analyses the natural glasses BHVO and BIR were analysed both before and after the DR3 glasses. The clinopyroxene analyses were checked using standard clinopyroxene BB-2 and BP1 (see Norman et al. 1996 for values). The values for these were generally close to the recommended values for the standards down to approximately 20 ppb.

Appendix 4: Whole rock analyses for FAUST-2 dredge 1

Note that sample identifiers are those given in Mauffret & Symonds et al. (2001).

Ident	B3	B4	B8	H5	A28	H3	B12	K3	H7	B21	G5-1	A9	H8	A27	A29	A34	A4	Q1	P1
SiO_2	46.64	46.8	48.1	46.6	52.59	50.2	39.5	44.3	43.9	38.9	52.13	48.89	57.69	42	36.9	34.7	40.5	44.7	38.9
TiO_2	0.23	0.28	0.36	0.25	0.28	0.28	0.21	0.38	0.26	0.37	0.26	0.27	0.32	0.77	0.88	1.03	0.96	2.3	0.79
Al_2O_3	14.49	21.3	19.2	15.7	16.15	15.8	13.6	17.4	14.7	14.6	18.39	18.42	17.61	16	15.5	14.9	17	13.8	14.7
Fe_2O_3	9.3	7.62	7.1	7.82	6.12	7.25	8.07	5.33	5.96	5.63	6.98	7.18	5.4	8.83	10.3	10.3	10.2	10.6	11
MnO	0.1	0.05	0.07	0.08	0.14	0.07	0.66	0.05	0.49	0.29	0.14	0.23	0.1	0.11	0.28	0.56	0.17	0.32	0.15
MgO	8.42	3.26	4.77	10	4.16	3.79	6.24	4.16	3.05	3.35	3.47	3.13	2.97	3.85	5.11	4.21	4.69	1.54	7.73
CaO	9.13	9.42	7.65	7.56	9.31	10.3	14.9	12.6	15.6	17.7	6.28	11.37	7.19	14.3	11.4	13.7	10.4	8.08	7.98
Na_2O	2.01	2.74	3.54	1.66	3.82	3.95	2.09	3.61	3.64	3.24	4.39	3.62	5.78	2.47	2.02	2.09	2.32	6.09	1.88
K_2O	0.74	0.68	0.7	1.78	1.75	2.24	0.73	0.66	1.33	0.73	2.40	1.77	1.50	1.63	2.44	2.11	1.83	2.87	2.56
P_2O_5	0.33	0.17	0.18	0.08	2.04	2.55	4.76	3.88	5.68	7.15	0.49	2.05	0.16	4.15	4.62	5.84	2.81	4.86	2.92
LOI	8.18	7.5	8.38	8.18	3.52	3.62	8.88	7.34	4.95	7.24	5.11	3.24	1.66	5.82	10.3	10.1	8.93	4.51	11.3
Total	99.57	99.7	100	99.8	99.88	100	99.6	99.8	99.6	99.1	100.0	100.1	100.3	99.8	99.6	99.5	99.78	99.64	99.90
S	0.02	0.02	0.02	0.01	0.06	0.06	0.12	0.09	0.13	0.16	0.02	0.04	0.01	0.09	0.11	0.14	0.07	0.1	0.07
Ba	17	30	50	36	145	151	94	49	132	74	147	87	113	29	49	67	34	56	292
Be	1.35	0.99	0.96	1.08															
Ce	2.40	2.93	8.42	1.54	12	10	6	21	13	21	15	11	15	13	8	11	8	12	114
Co	43.1	10.3	20.9	31.2															
Cr	1254	66	195	999	217	236	836	182	197	165	139	127	125	152	210	203	206	310	8
Cs	0.19	0.33	0.18	0.40															
Dy	1.01	0.85	1.17	0.70															
Er	0.70	0.56	0.73	0.48															
Eu	0.25	0.30	0.43	0.16															
Ga	12.7	16.6	15.5	12.2															
Gd	0.89	0.79	1.21	0.52															
Hf	0.85	1.84	2.61	0.71															
Ho	0.23	0.19	0.25	0.16															
La	2.29	1.72	4.10	1.14	18	22	9	7	13	8	11	49	14	34	39	38	26	24	82
Li	39.4	30.3	57.4	89.5															
Lu	0.11	0.09	0.11	0.08															
Mo	0.96	0.38	0.33	0.41															
Nb	1.03	1.79	2.06	0.99	1.7	2	2.2	1.9	3.1	2.6	2.9	3.2	2.6	2.6	2.5	2.6	1.9	1.8	85.6
Nd	2.59	2.21	3.83	1.25	8	14		10	10	10	11	31	15	22	24	24	18	16	70
Ni	343	76	122	218	172	99	369	126	191	148	180	187	85	86	364	509	262	409	143
Pb	2.71	7.05	4.08	3.02	3	3	4	3	4	2	4	7	2	6	9	14	5	7	10
Pr	0.59	0.48	0.87	0.28															
Rb	7.83	8.57	6.46	15.7	32	42	7	10	22	10	29	72	13	17	21	20	20	25	54
Sb	2.91	2.35	1.78	1.07															
Sc	44	36	29	48	29	32	45	21	32	22	22	33	19	40	40	40	41	36	14
Sm	0.68	0.65	1.08	0.37															
Sn	0.39	0.48	0.97	0.25															
Sr	121	298	432	79	331	353	339	705	490	736	287	295	384	309	303	380	234	216	419
Ta	0.08	0.12	0.15	0.07															
Tb	0.15	0.13	0.19	0.10															
Th	0.41	0.88	1.06	0.31					2	2									5
U	3.90	1.00	1.03	0.63		2	6	2	2	3	2			2	3	4	3	3	3
V	199	201	138	224	175	189	172	106	144	112	174	231	191	249	232	261	243	234	231
Y	6.8	4.7	6.5	3.8	34	37	17	7	27	7	23	101	20	67	84	96	68	53	87
Yb	0.70	0.58	0.70	0.52															
Zn	138	114	99	150							62	79	41	131	202	216	178	245	145
Zr	45	72	90	34	70	75	33	95	61	87	86	73	83	55	67	68	64	51	332

Appendix 5: Whole rock and glass analyses for FAUST-2 dredge 3

Note that sample identifiers are those given in Mauffret & Symonds et al. (2001).

Ident	A	A1	A2	A3	B1	B2	D3	glass B	glass E	Glass A
SiO_2	44.77	47.31	47.37	47.51	47.95	47.86	47.25	48.13	47.91	47.61
TiO_2	1.47	1.17	1.26	1.26	1.65	1.35	1.36	1.70	1.70	1.38
Al_2O_3	18.59	16.75	16.37	16.41	15.89	16.56	16.18	16.36	16.40	16.69
Fe_2O_3	12.16	9.42	9.36	9.94	11.32	10.02	10.18	11.50	11.48	10.80
MnO	0.13	0.19	0.12	0.19	0.17	0.14	0.15	0.21	0.18	0.21
MgO	3.23	6.89	7.57	6.92	5.95	6.48	7.22	6.77	6.63	7.29
CaO	10.59	11.24	10.66	10.84	11.42	11.27	10.52	10.64	10.49	11.53
Na_2O	3.07	2.97	3.12	3.05	3.41	3.31	3.19	3.12	3.12	2.72
K_2O	0.59	0.43	0.35	0.49	0.37	0.35	0.36	0.32	0.31	0.21
P_2O_5	0.42	0.19	0.2	0.23	0.25	0.21	0.22	0.32	0.27	0.15
LOI	5	3.49	3.77	3.43	1.99	2.64	3.37			
Total	100.02	100.05	100.15	100.27	100.37	100.19	100	99.07	98.49	98.59
S	0.02	0.01	0.01	0.01	0.01	0.01	0.01			
Ba	85	155	80	177	110	88	88	128.71	124.82	89.45
Be			0.60	0.59	0.69					
Ce	18	15	12.78	14.28	16.09	12	16	21.06	20.12	13.01
Co			36.8	35.0	36.8			40.04	41.20	42.12
Cr	293	156	192	133	128	186	170			
Cs			0.36	1.09	0.55			0.08	0.11	0.05
Dy			4.26	4.39	5.34			5.05	5.43	4.13
Er			2.51	2.60	3.21			2.70	3.01	2.33
Eu			1.27	1.33	1.57			1.54	1.58	1.22
Ga			15.8	16.5	17.9					
Gd			4.05	4.17	5.06			4.88	5.47	3.79
Hf			2.08	1.89	2.58			2.36	2.61	1.94
Ho			0.89	0.91	1.13			1.03	1.16	0.86
La	12	4	4.74	5.53	5.56	5	5	7.91	8.27	5.00
Li			54.9	44.8	26.2					
Lu			0.32	0.34	0.42			0.38	0.41	0.34
Mo			0.15	0.43	0.30					
Nb	4.8	2.6	1.83	2.80	2.38	1.2	1.4	6.44	6.42	3.49
Nd	18	10	11.39	12.06	14.25	13	13	15.23	15.40	10.23
Ni	78	73	89	69	46	74	74	77.89	83.97	91.21
Pb	2		0.83	1.08	1.27			1.45	1.56	0.95
Pr			2.19	2.35	2.77			2.86	2.80	1.86
Rb	9	10	5.85	10.78	8.92	7	8	3.95	4.04	2.72
Sb			0.22	0.40	0.48					
Sc	50	34	29	31	30	31	31	31.87	35.23	35.98
Sm			3.41	3.56	4.30			4.48	4.79	3.32
Sn			1.13	1.04	1.35					
Sr	344	262	227	257	251	245	231	318.45	323.57	286.64
Ta			0.14	0.19	0.17			0.41	0.43	0.25
Tb			0.69	0.71	0.86					
Th			0.22	0.41	0.29			0.50	0.56	0.39
U			0.15	0.48	0.35			0.15	0.17	0.10
V	303	247	235	234	304	256	258	287.23	287.40	259.75
Y	40	20	22.8	24.3	29.7	24	24	27.22	30.29	23.04
Yb			2.20	2.32	2.85			2.63	2.89	2.26
Zn			103	121	111					
Zr	93	63	83	75	103	88	92	107.40	118.53	84.47

Appendix 6: Selected mineral analyses for FAUST-2 dredge samples

Note that sample identifiers are those given in Mauffret & Symonds et al. (2001).

Pyroxenes

	DR2 A14	DR2 A14	DR2 B4	DR2 B8	DR2 B21	DR2 I3	DR2 I3	DR2 I2	DR2 I2	DR2 B12	DR2 B12	DR2 H5	DR2 I4	DR2 I4	DR2 A28	DR2 A28	DR2 G5-2	DR2 L3	DR3 A2
SiO_2	51.80	55.61	55.20	54.08	54.86	56.33	54.32	56.74	53.38	57.66	53.44	53.43	53.06	56.62	58.09	54.14	53.73	43.50	50.55
TiO_2	0.07	0.04	0.05	0.03	0.05	0.01	0.04	0.04	0.08	0.02	0.10	0.06	0.06	0.03	0.01	0.09	0.14	4.32	0.73
Al_2O_3	4.19	4.12	0.51	0.66	0.68	1.54	1.36	3.02	3.25	0.64	2.10	1.98	2.35	2.13	0.42	1.37	1.62	8.62	4.77
Cr_2O_3	1.02	0.77	0.16	0.61	0.38	0.56	0.56	0.79	0.93	0.31	0.83	1.11	0.98	0.61	0.31	0.34	0.01	0.00	0.68
FeO	2.33	6.18	3.45	3.11	4.28	5.27	1.98	6.15	2.12	7.26	4.66	4.11	2.00	5.99	6.12	4.34	19.81	8.60	5.78
MnO	0.10	0.13	0.08	0.11	0.20	0.16	0.04	0.15	0.08	0.21	0.17	0.07	0.04	0.21	0.20	0.14	0.54	0.14	0.12
MgO	16.34	32.89	18.68	18.81	18.36	33.58	17.76	33.66	16.85	32.62	18.18	18.56	16.49	33.33	33.42	17.65	19.99	11.24	15.16
CaO	24.04	1.28	22.30	20.59	22.31	0.88	25.23	0.49	24.48	1.98	21.06	19.88	24.10	0.69	1.70	22.03	0.99	22.73	21.59
Na_2O	0.11	0.00	0.18	0.16	0.18	0.00	0.13	0.00	0.11	0.01	0.14	0.12	0.21	0.01	0.01	0.15	0.09	0.53	0.27
K_2O	0.01	0.00	0.00	0.00	0.00	0.01	0.00	0.01	0.00	0.01	0.00	0.00	0.00	0.00	0.01	0.00	0.08	0.00	0.00
Sum Ox%	100.0	101.0	100.6	98.16	101.3	98.34	101.4	101.0	101.2	100.7	100.6	99.32	99.29	99.62	100.2	100.2	97.00	99.68	99.65

Spinel

Label	DR1 A1	DR1 B1	DR2 A14	DR2 S2	DR2 I3	DR2 I2	DR2 B12	DR2 I4	DR2 H5	DR2 A34	DR3 glass A
SiO_2	0.00	0.02	0.05	0.03	0.00	0.02	0.12	0.00	0.10	0.04	0.08
TiO_2	0.20	0.02	0.05	0.09	0.05	0.04	0.16	0.04	0.20	0.87	0.81
Al_2O_3	13.84	26.47	42.49	9.08	21.76	36.64	9.54	27.79	13.71	17.04	32.97
Cr_2O_3	52.01	42.39	25.45	58.93	46.83	31.40	53.47	39.39	51.43	41.47	26.51
Fe_2O_3	3.81	1.91	3.04	2.60	2.30	1.66	5.23	2.20	4.58	10.76	9.07
FeO	21.48	16.62	13.71	18.48	17.06	14.38	16.87	16.63	16.73	18.83	15.46
V_2O_3	0.13	0.07	0.13	0.12	0.25	0.15	0.17	0.28	0.25	0.20	0.12
CaO	0.04	0.12	0.00	0.02	0.00	0.02	0.06	0.09	0.42	0.05	0.07
MnO	0.33	0.18	0.15	0.23	0.24	0.05	0.19	0.19	0.14	0.19	0.16
MgO	8.08	12.54	16.57	9.50	11.87	15.05	10.08	12.45	10.70	10.74	14.53
ZnO	0.19	0.29	0.12	0.20	0.25	0.33	0.13	0.27	0.15	0.00	0.03
NiO	0.09	0.13	0.25	0.05	0.07	0.06	0.07	0.05	0.17	0.06	0.24
	100.2	100.8	102.0	99.3	100.7	99.8	96.1	99.4	98.6	100.3	100.1

Feldspar

Label	DR2 B4	DR2 B8	DR2 B21	DR2 A2	DR2 D3	DR2 G5-2	DR2 G5-2	DR3 Glass E
SiO_2	47.77	51.89	52.55	49.86	48.94	58.29	65.57	50.81
TiO_2	0.00	0.02	0.03	0.05	0.04	0.01	0.01	0.10
Al_2O_3	33.52	30.66	30.18	32.15	32.19	27.13	19.14	31.21
Fe_2O_3	0.74	0.61	0.85	0.64	0.63	0.16	0.02	0.76
MnO	0.00	0.04	0.01	0.01	0.02	0.01	0.00	0.00
MgO	0.06	0.10	0.07	0.21	0.21	0.02	0.01	0.16
CaO	16.84	13.47	13.37	15.46	15.79	8.49	0.08	14.54
Na_2O	1.98	3.75	3.99	2.74	2.69	6.51	0.11	3.24
K_2O	0.13	0.06	0.09	0.03	0.02	0.15	16.82	0.05
Sum Ox%	101.0	100.6	101.1	101.2	100.5	100.8	101.8	100.9

Olivine

Label	DR2 A34	DR2 H5	DR3 glass A	DR3 glass A	DR3 glass E
SiO2	39.92	40.41	40.48	39.38	40.39
TiO2	0.01	0.00	0.03	0.01	0.02
Al2O3	0.03	0.02	0.06	0.04	0.08
Cr2O3	0.01	0.02	0.10	0.08	0.07
FeO	14.44	11.44	14.33	19.06	13.97
MnO	0.29	0.13	0.22	0.32	0.23
MgO	45.06	47.71	45.74	41.20	44.44
CaO	0.20	0.22	0.30	0.26	0.31
NiO	0.24	0.20	0.20	0.08	0.14
Sum Ox%	100.2	100.2	101.5	100.5	99.6

List of Figures

shown across the top with two-way seismic time in seconds. No structural interpretation is shown.

12. Hill-shaded view of Norfolk Ridge to Three Kings Ridge terrain with structural interpretation. Black crosses on seismic lines represent shotpoint multiples of 500. Shaded dashed polygon outline represents inferred continental fragment – see text for discussion.

13. (a) Hill-shaded view of terrain for the Cook Fracture Zone province with structural interpretation; and (b) 3D perspective view from the southeastern end of the fracture looking towards the northwest.

14. Tectonic province outlines of the Norfolk Ridge to Three Kings Ridge region of the southwest Pacific. Province names in bold are already established. Top map is hill-shaded image of merged bathymetry (see Fig. 3) and lower map pseudo-colour image of satellite gravity (cf. Fig. 2).

15. Chrome spinel compositions for the rocks from FAUST-2 dredges 1 (DR1), 2 (DR2) and 3 (DR3). Fields based on Kamenetsky et al. (2001).

16. Major element composition of clinopyroxene from FAUST-2 dredge 2 (DR2) compared to clinopyroxene from peridotites worldwide. Abyssal and subcontinental peridotite from Seyler and Bonatti (1994), Mariana forearc peridotite from Parkinson et al. (1992) and Ishii et al. (1992) and South Sandwich peridotite from Pearce et al. (2000). Note: no Na_2O or paired spinel-clinopyroxene data available for the Mariana forearc peridotite.

17. Chondrite-normalised REE diagram showing the composition of clinopyroxene from lherzolite in FAUST-2 dredge 2 sample A14 (DR2A14) compared with those from the forearc of the Mariana arc (Parkinson et al., 1992) and abyssal peridotite (Johnson et al., 1990).

18. Plot showing alteration in the boninite. The thick line is a slightly altered boninite (0.4% P_2O_5 at 9.3% MgO) and the thin line is a strongly altered boninite (6% P_2O_5 at 3.7% MgO). The values are normalised to an unaltered boninite (0.09% P_2O_5 at 10.9% MgO).

19. Various plots showing the fractionation trends of the FAUST-2 dredge rocks. Values are recalculated for loss on ignition and P_2O_5-alteration.

20. MORB and chondrite-normalised diagrams for FAUST-2 rocks dredged from the Three Kings Ridge (DR2 and DR3). A Lau Basin backarc basalt (Ewart et al., 1994, sample 834B 8R-2 12-18 cm) and a Mariana forearc boninite (Murton et al., 1992, sample 786B 21R-2 103-107 cm) are shown for comparison.

21. Photomicrograph of sandstone sample from FAUST-2 dredge 2 (DR2E2). Field of-view is 2 mm with plane-polarised light.

22. Tectonic reconstructions for the southwest Pacific in the Norfolk Ridge to Three Kings Ridge region from 70 Ma to the present (after Crawford et al., in press, as modified from earlier versions constructed in this report).

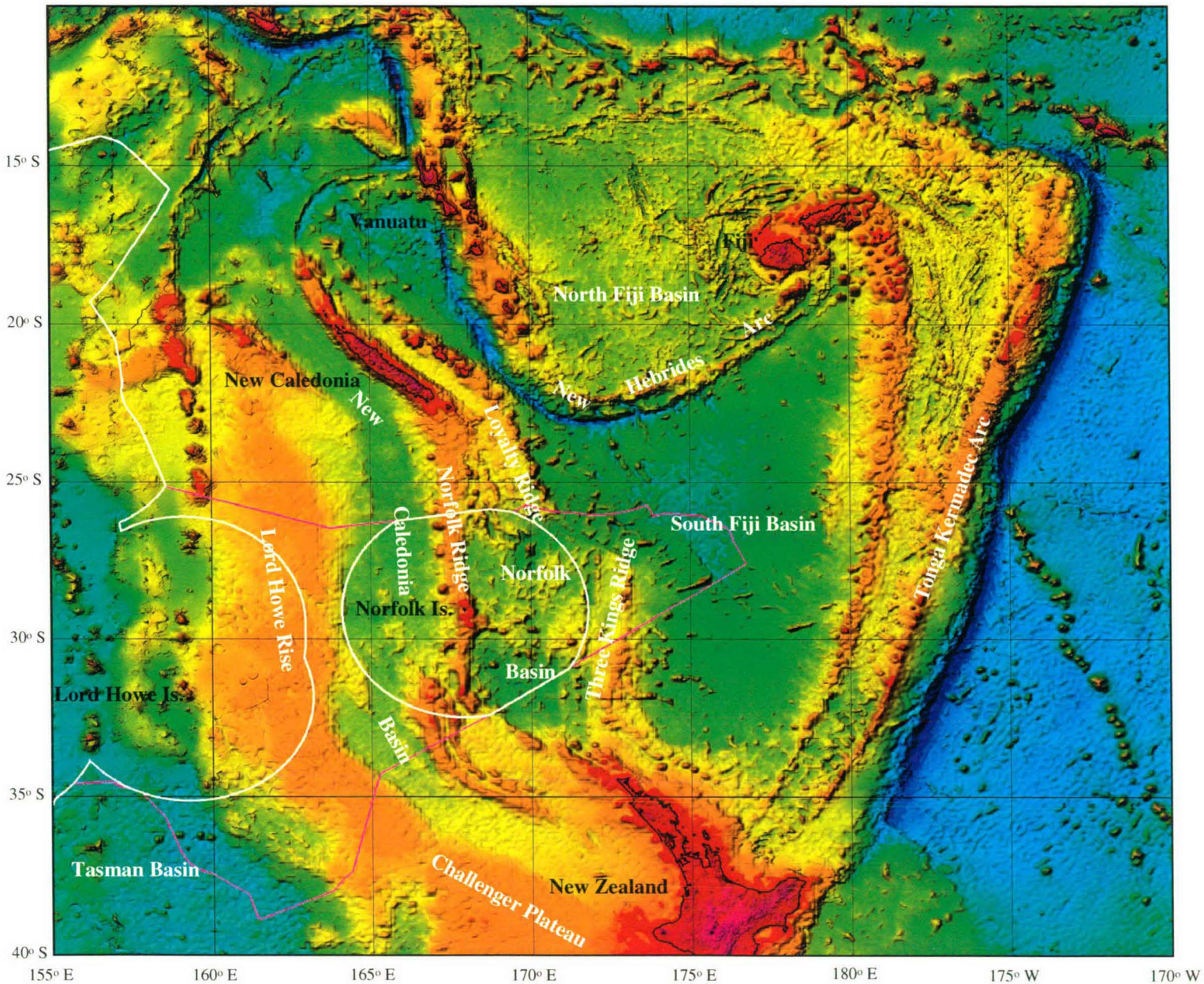

Figure 1. Hill-shaded view of terrain for the southwest Pacific region. Large-scale tectonic elements are marked along with Australia's Exclusive Economic Zone (white line) and claim for extended Continental Shelf (magenta line). Terrain data derived from Smith et al. (1997) and projection is Geodetic.

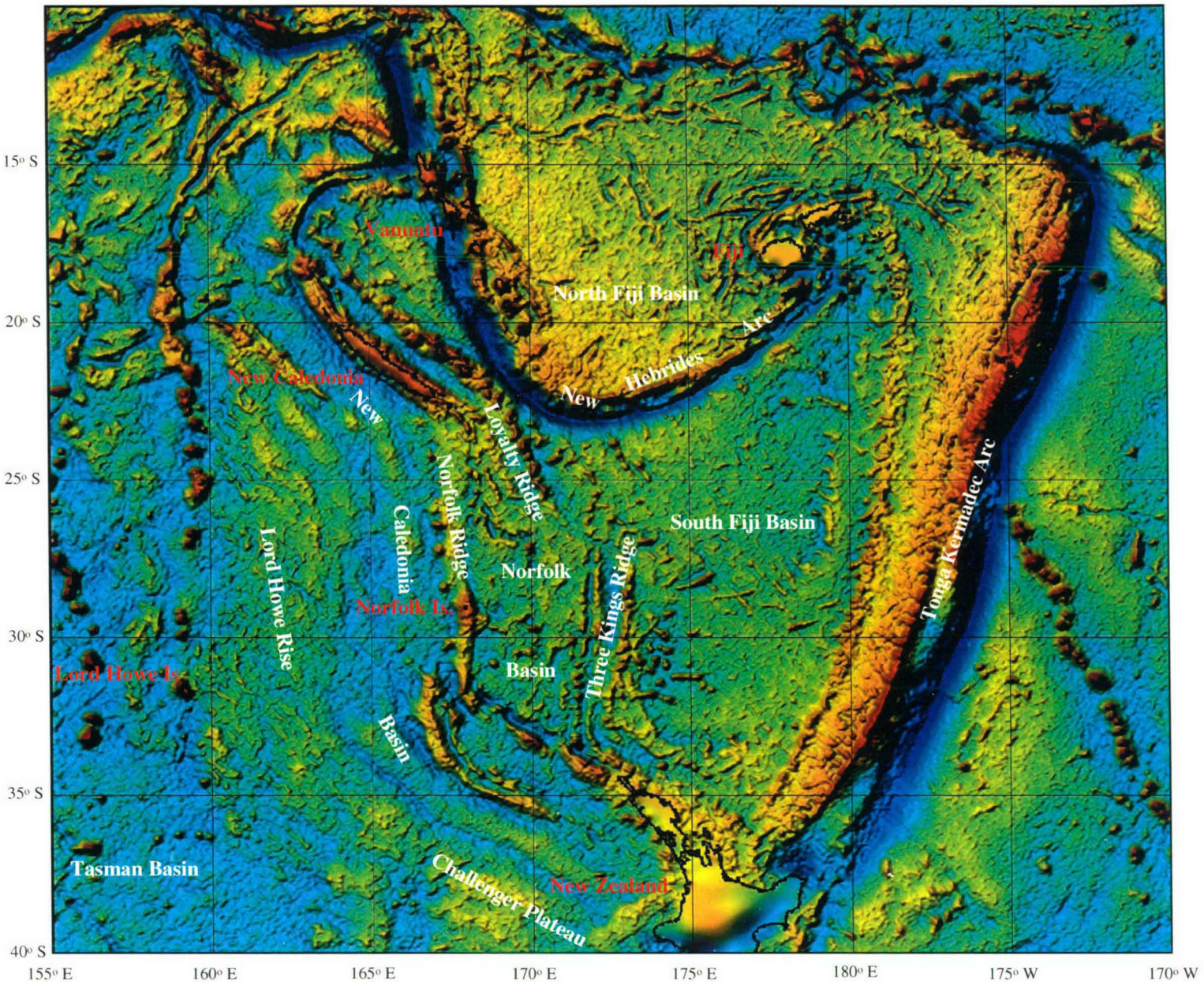

Figure 2. Hill-shaded view of satellite-derived gravity for the southwest Pacific region. Large-scale tectonic elements are marked. Data are from Sandwell and Smith (2000) and projection is Geodetic.

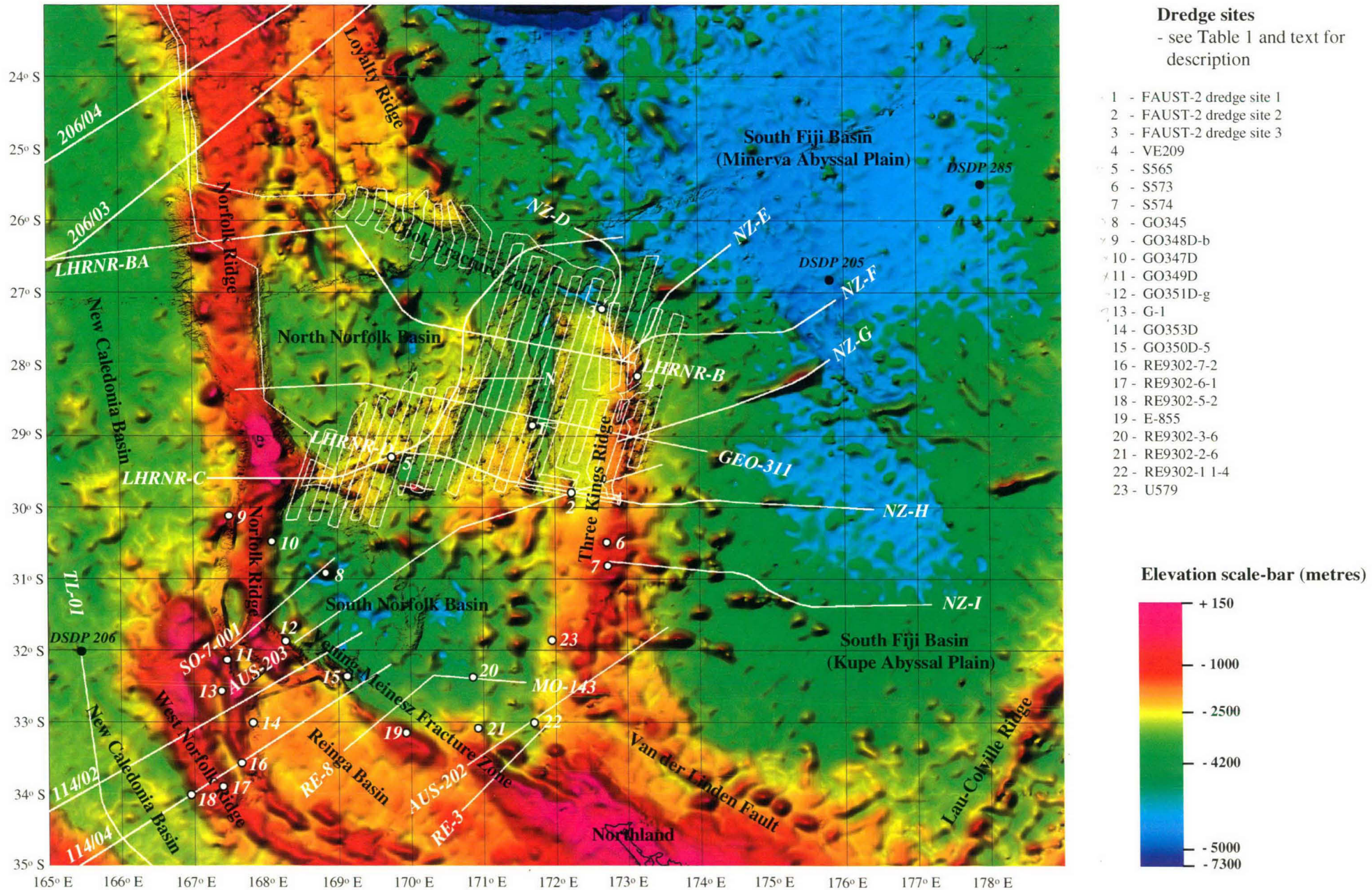

Figure 3. Hill-shaded view of Norfolk Ridge to Three Kings Ridge region with dredge sites (white circles), DSDP sites (black circles) and seismic lines marked. Non-annotated lines are FAUST-2 survey tracks. Seafloor feature names shown are those commonly used prior to this study.

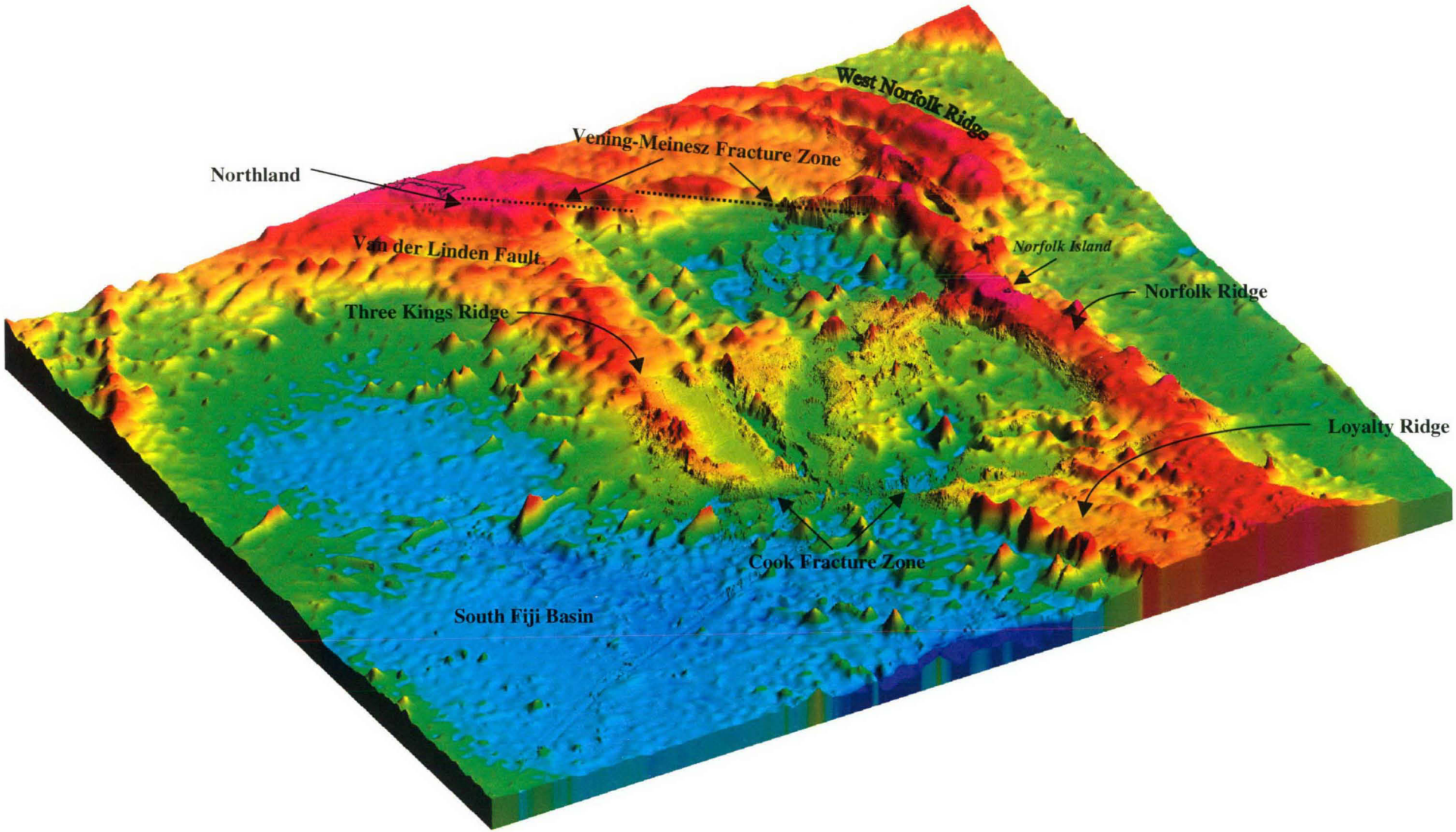

Figure 4. 3D perspective view from the northeast of the wider Norfolk Ridge to Three Kings Ridge region. Both area and terrain-to-colour mapping is the same as presented in Figure 3.

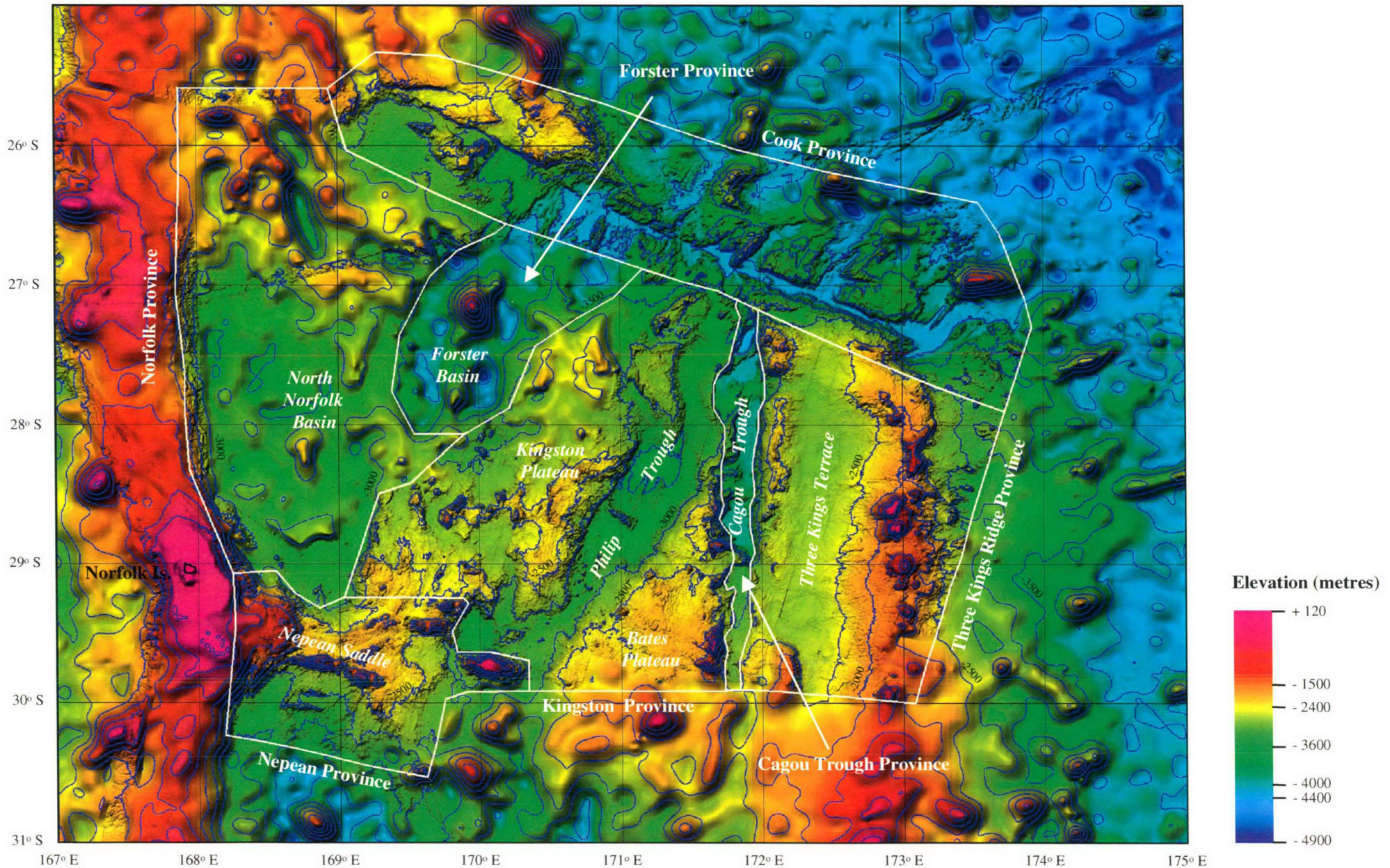

Figure 5. Hill-shaded view of the recently-mapped seafloor (Mauffret & Symonds et al., 2001) between the Norfolk Ridge and Three Kings Ridge. Contours are shown for every 500 m. White polygons refer to physiographic provinces discussed in the text. Italicised names are suggested naming of bathymetric features.

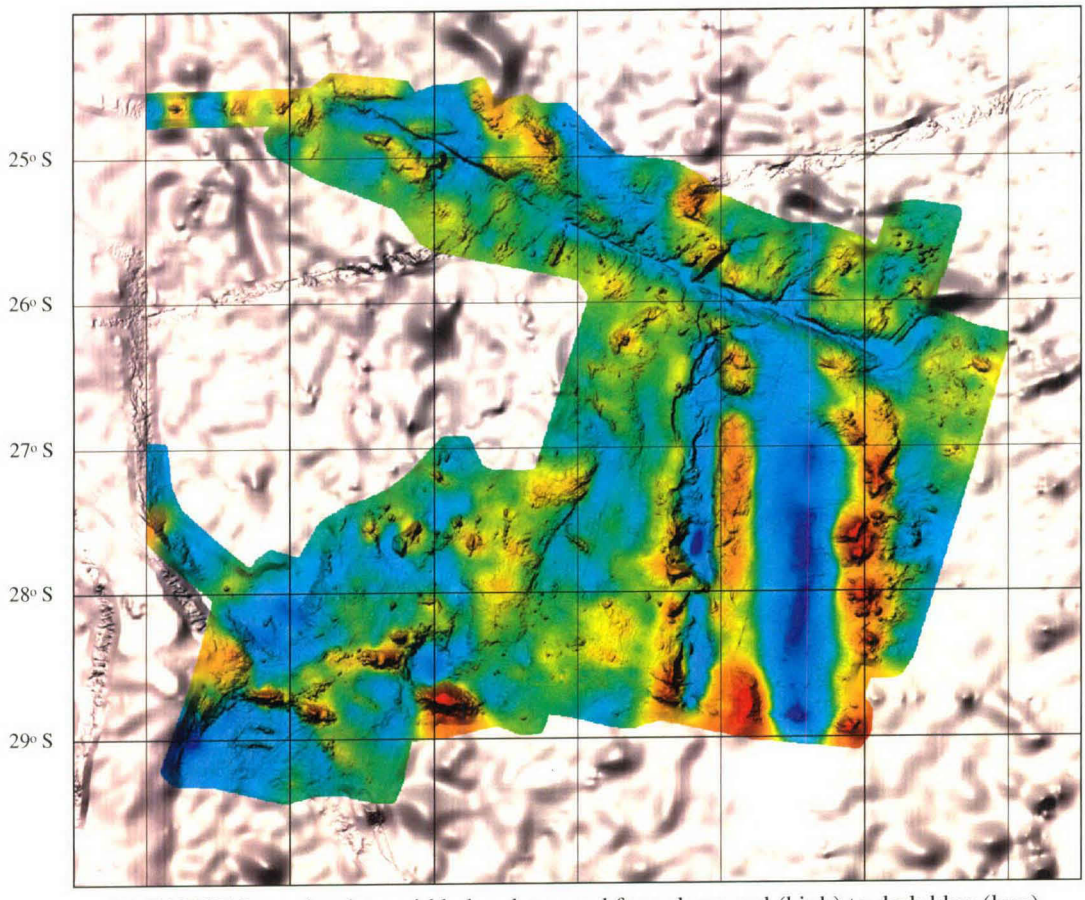

(a) FAUST-2 gravity data gridded and mapped for colours red (high) to dark blue (low).

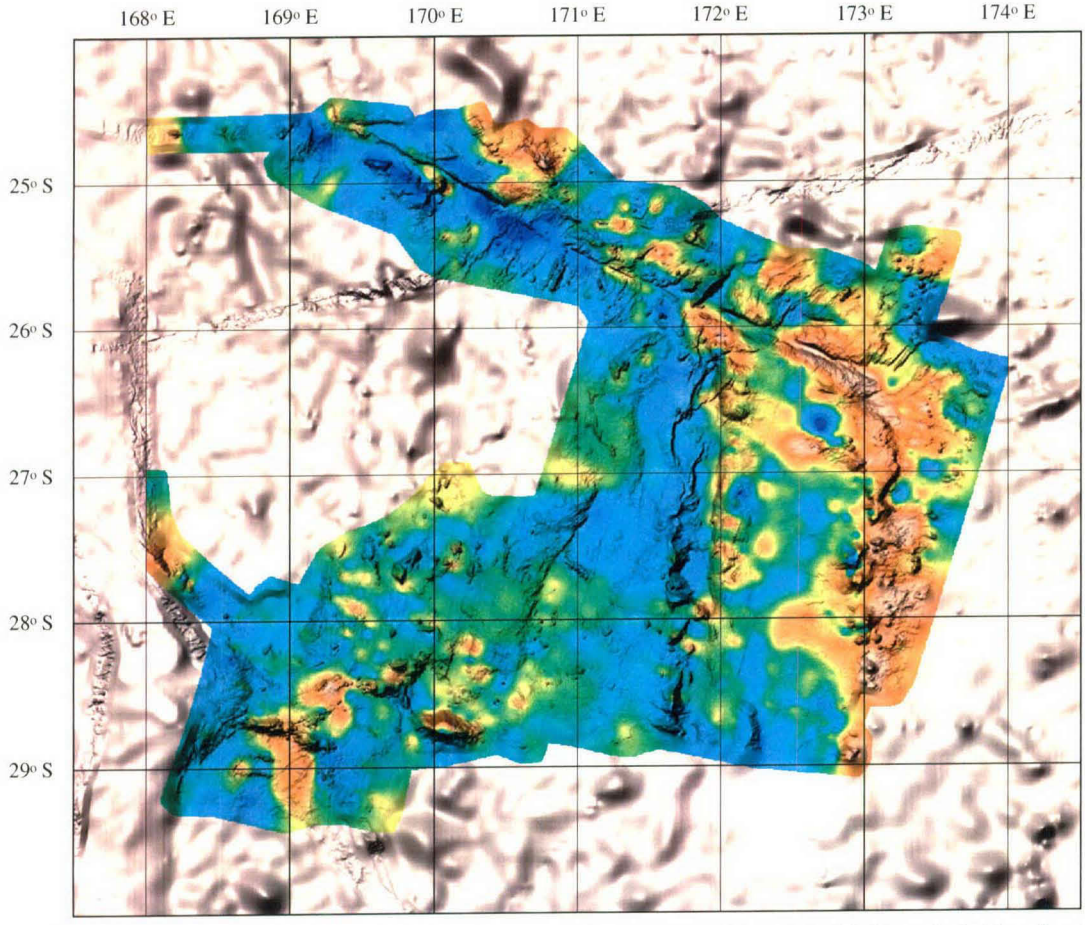

(b) FAUST-2 magnetic data gridded and mapped for colours white-pink (high) to dark blue (low).

Figure 6. Drape of grided FAUST-2 gravity (a) and magnetic (b) ship track data over hill-shaded gray-scale terrain grid.

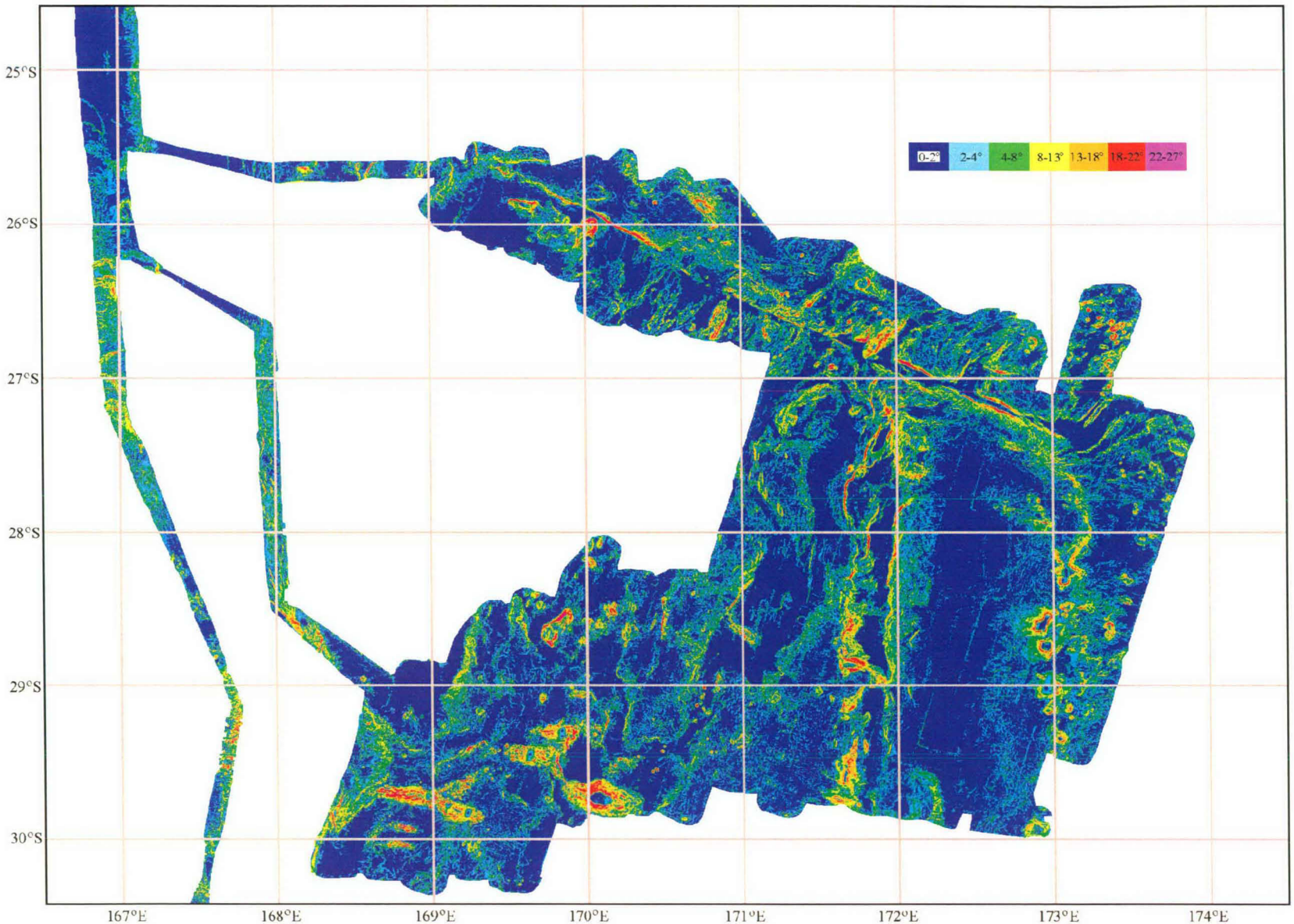

Figure 7. Terrain slope image of the seafloor in the FAUST-2 survey area. Slope ranges are: dark blue - 0-2°; light blue - 2-4°; green - 4-8°; yellow - 8-13°; orange - 13-18°; red - 18-22°; and purple - 22-27°, as indicated on the colour bar.

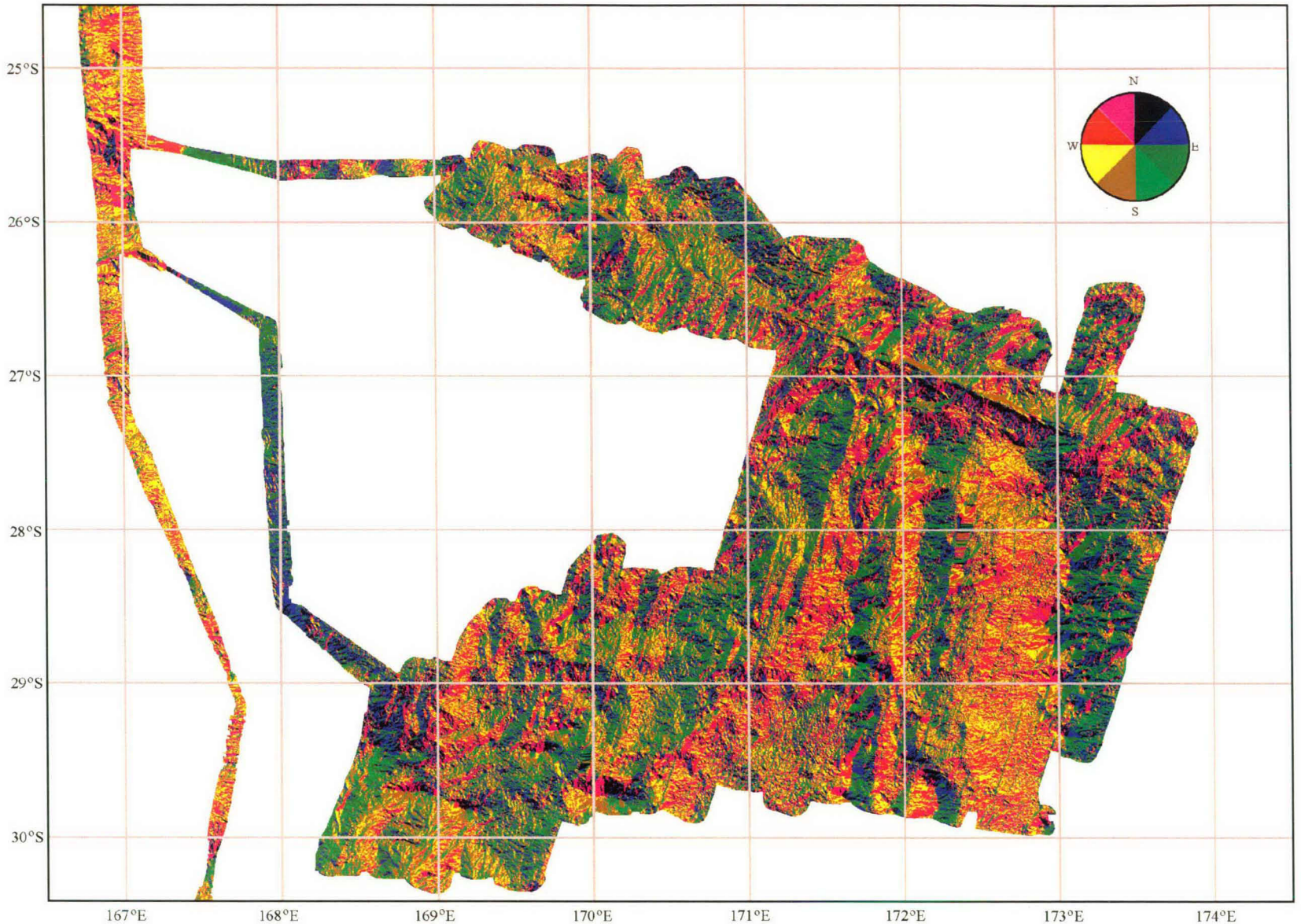

Figure 8. Terrain aspect image of the seafloor in the FAUST-2 survey area. Aspect azimuths are divided into 45° sectors as indicated on the colour wheel.

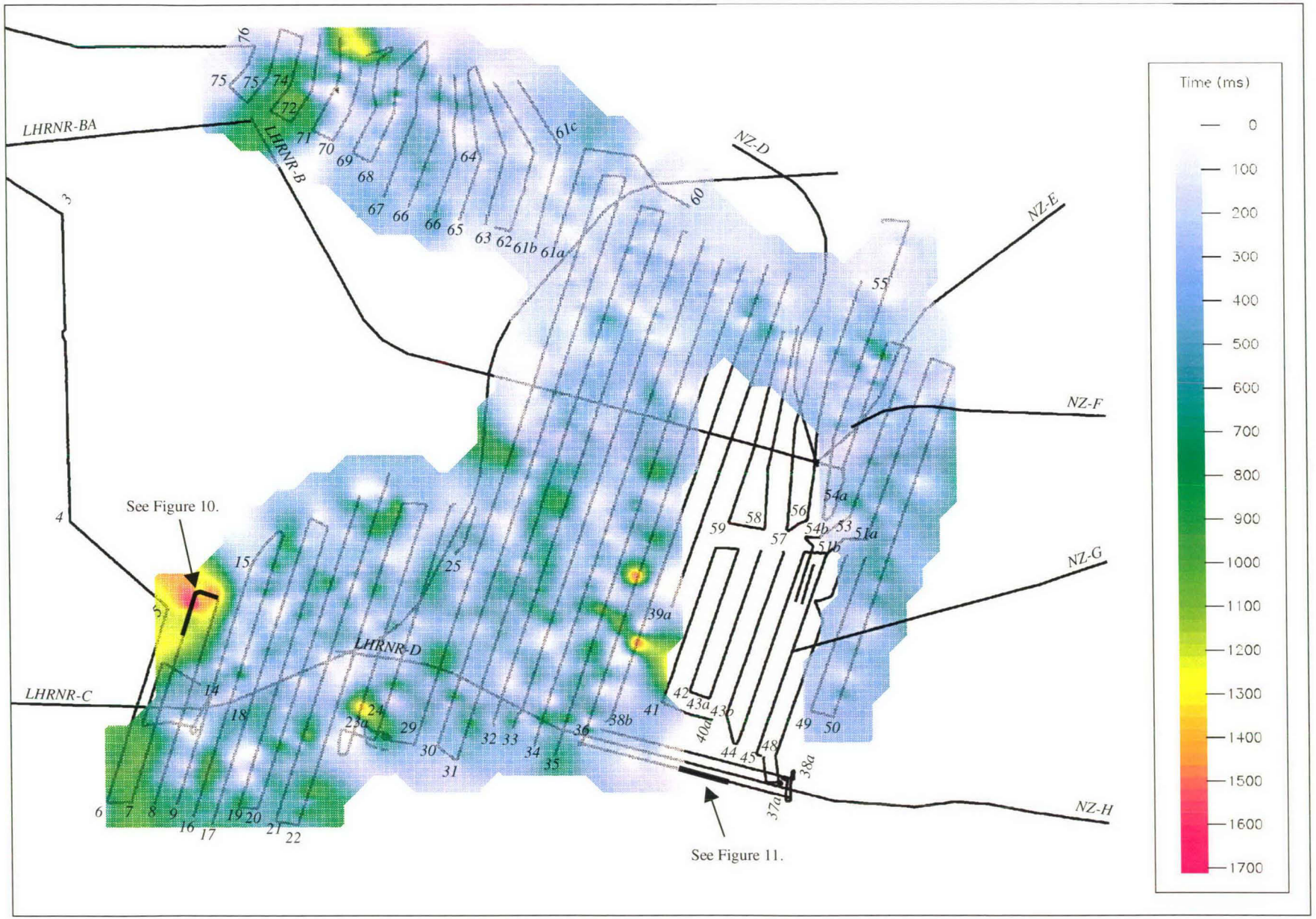

Figure 9. Isochron map of interpretable sedimentary sequences over basement for the FAUST-2 data. Note: Three Kings Basin was not mapped because of the difficulty in identifying the base of sedimentary sequences. Numbered lines are processed FAUST-2 seismic profiles. For tectonic elements compare with Figure 3.

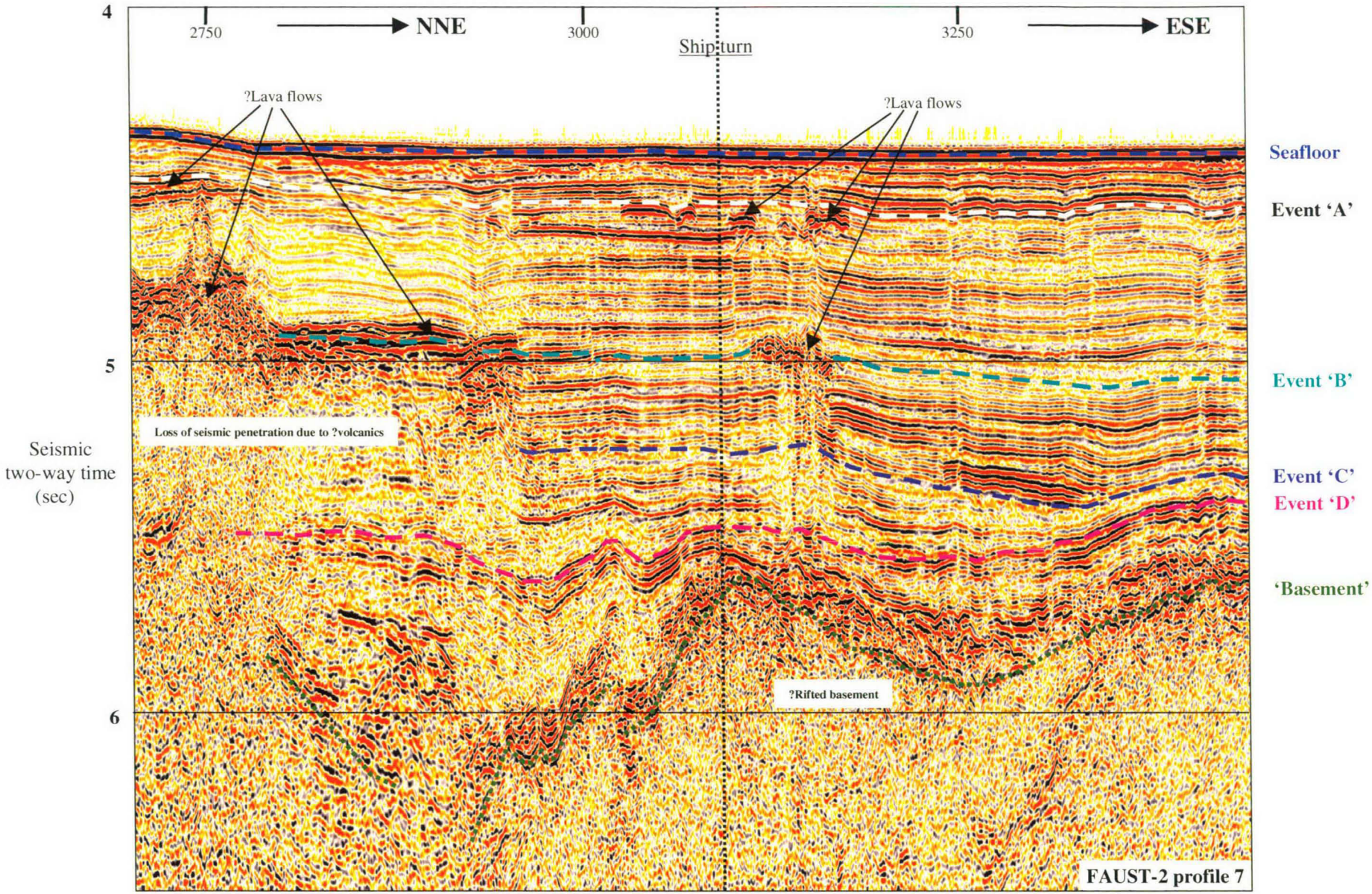

Figure 10. Sequence boundary definitions for part of FAUST-2 seismic profile 7 in the southern North Norfolk Basin (see Figure 9). Shotpoints are shown across the top with two-way seismic time in seconds. Note that this portion of the profile was shot around a 90° bend from north-northeast to east-southeast. No structural interpretation is shown.

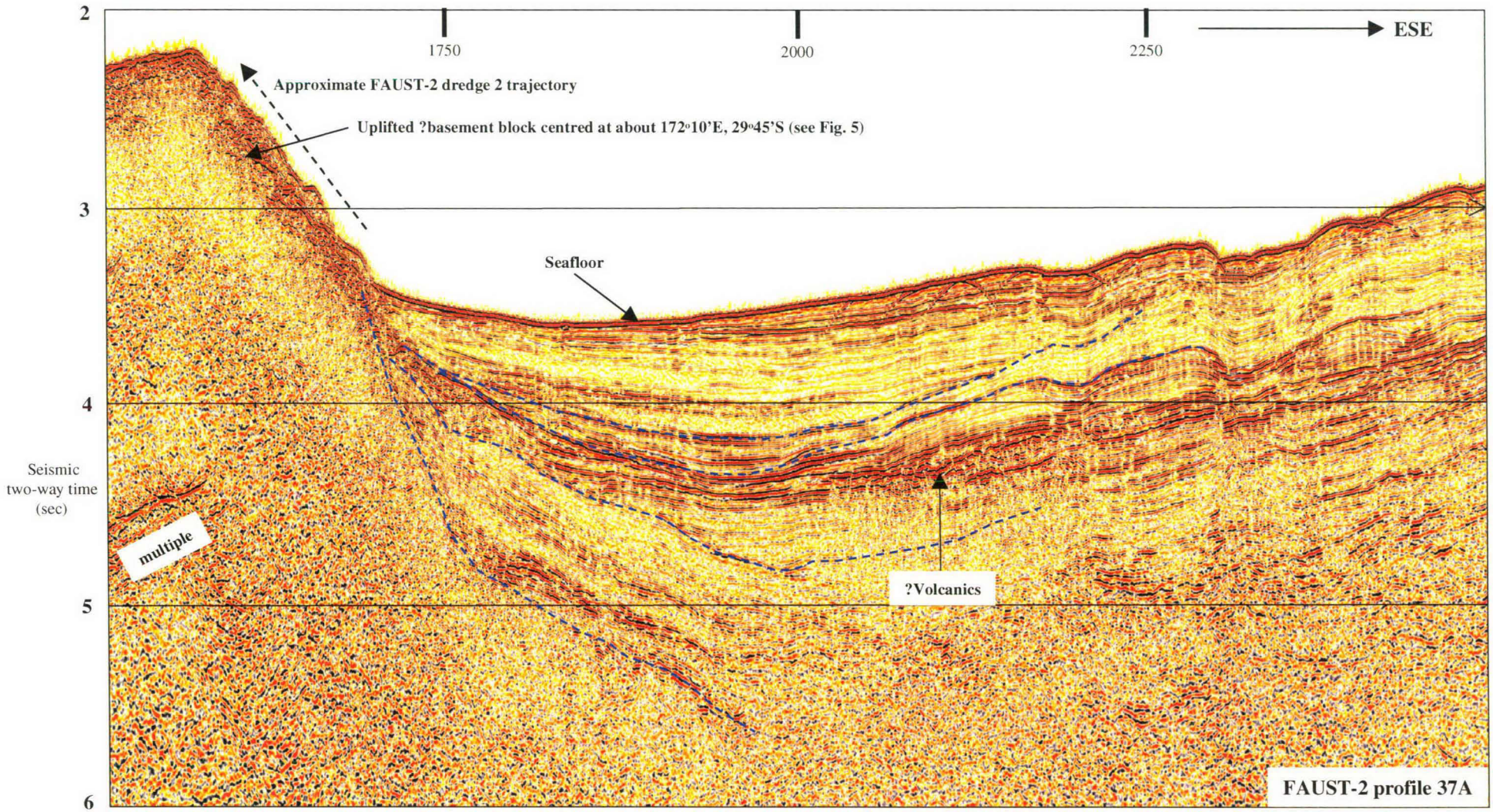

Figure 11. Interpretation of four major sequences (dashed blue lines) within the Three Kings Basin onlapping a large 'basement' block to the west (see Figure 9). Shotpoints are shown across the top with two-way seismic time in seconds. No structural interpretation is shown

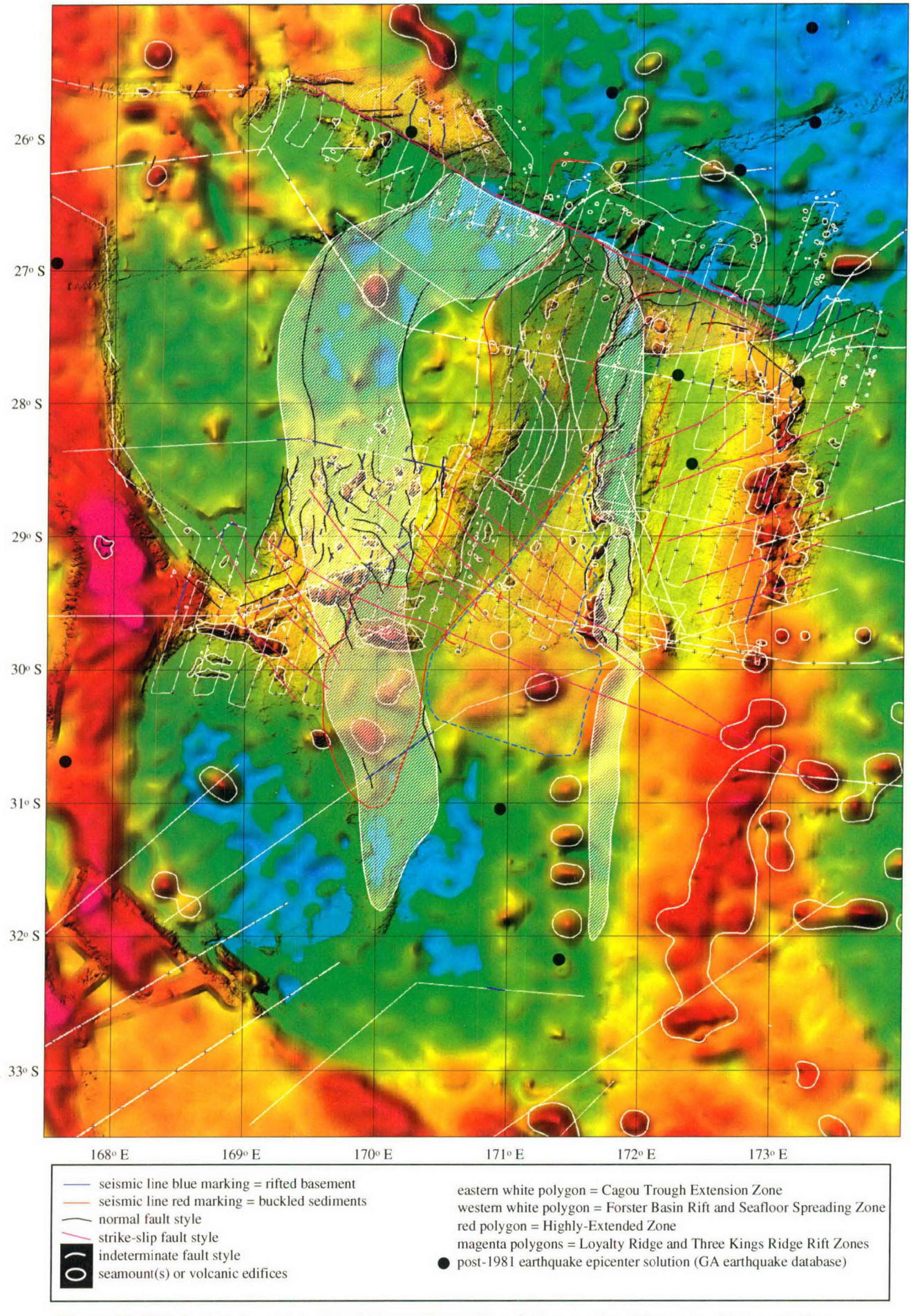

Figure 12. Hill-shaded view of Norfolk Ridge to Three Kings Ridge terrain with structural interpretation. Black crosses on seismic lines represent shotpoint multiples of 500. Shaded dashed polygon outline represents inferred continental fragment - see text for discussion.

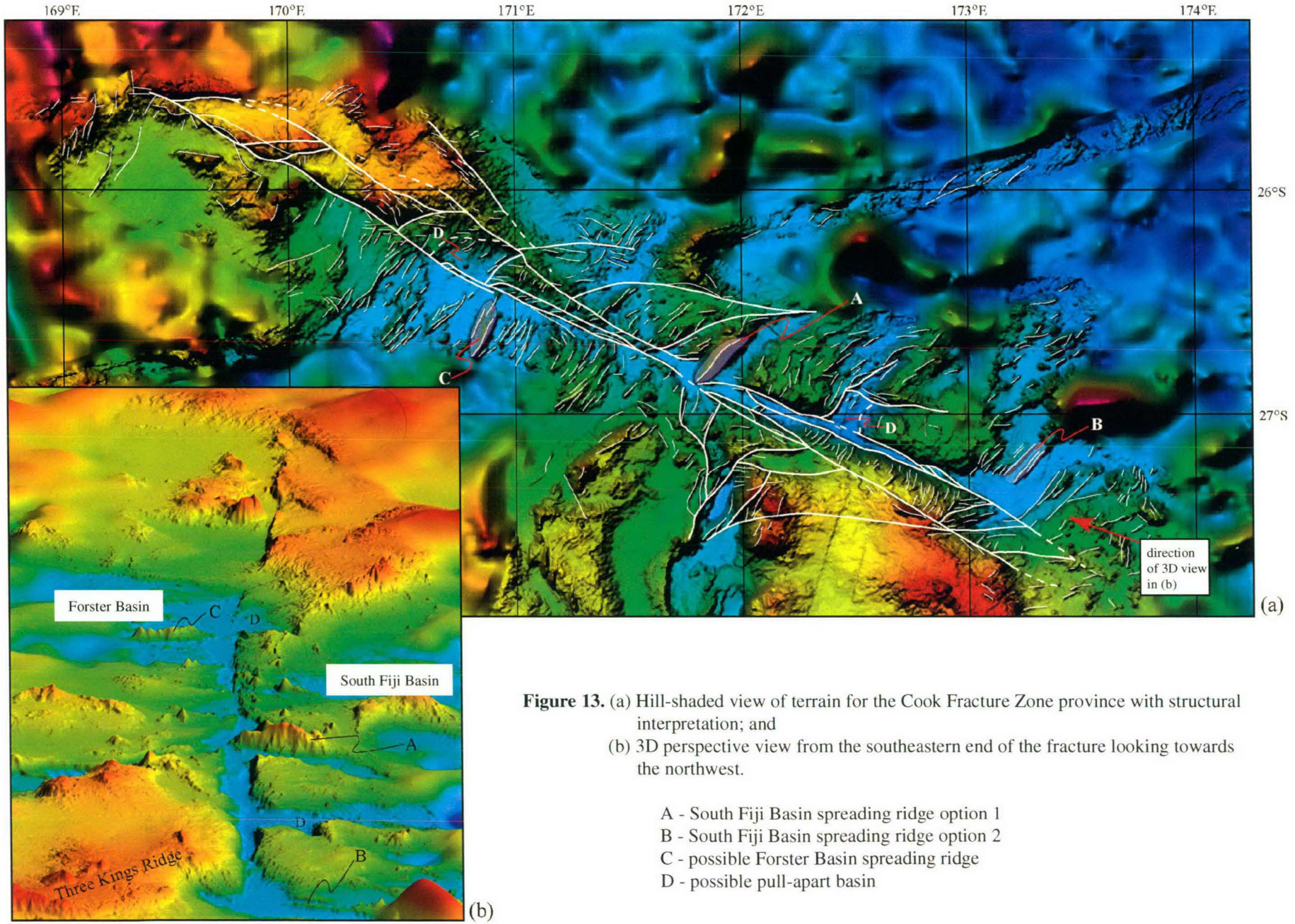

Figure 13. (a) Hill-shaded view of terrain for the Cook Fracture Zone province with structural interpretation; and
(b) 3D perspective view from the southeastern end of the fracture looking towards the northwest.

A - South Fiji Basin spreading ridge option 1
B - South Fiji Basin spreading ridge option 2
C - possible Forster Basin spreading ridge
D - possible pull-apart basin

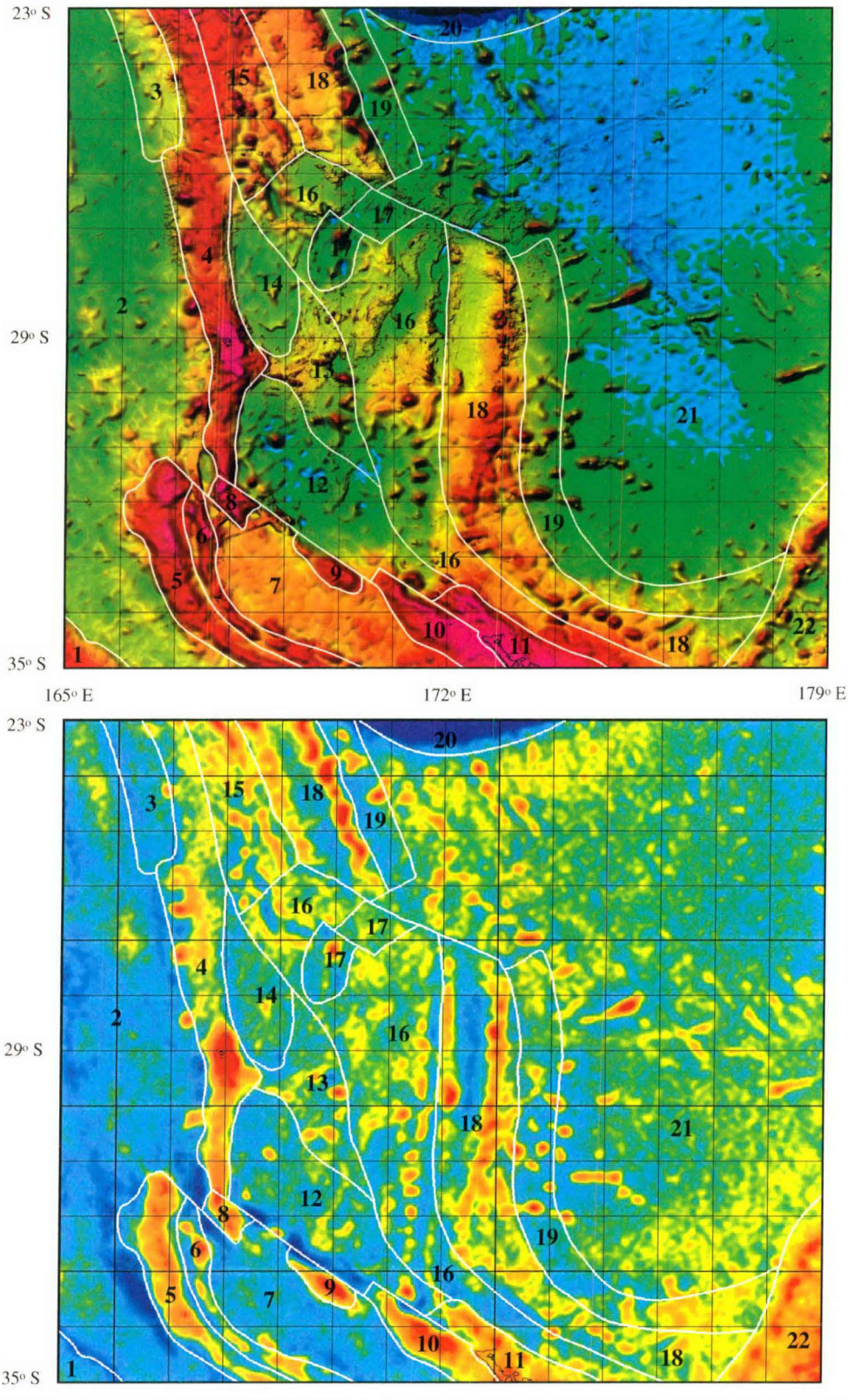

1. **Lord Howe Rise**
2. **New Caledonia Basin**
3. **West New Caledonia Basin**
4. **Norfolk Ridge**
5. **West Norfolk Ridge**
6. **Wanganella Ridge**
7. **Reinga Basin**
8. **Taranui Block**
9. **Reinga Ridge**
10. **South Maria Block**
11. **Northland**
12. **South Norfolk Basin**
13. 'transitional' Norfolk Basin crust
14. **North Norfolk Basin**
15. Eastern Norfolk Ridge collision complex
16. Three Kings Ridge 'extended' forearc collision front
17. Forster Basin
18. **Three Kings Ridge + Loyalty Ridge** complex
19. 'transitional' South Fiji Basin
20. **New Hebrides Trench**
21. **South Fiji Basin**
22. **Lau-Colville Ridge**

Figure 14. Tectonic province outlines of the Norfolk Ridge to Three Kings Ridge region of the southwest Pacific. Province names in bold are already established. Top map is hill-shaded image of merged bathymetry (see Fig. 3) and lower map pseudo-colour image of satellite gravity (cf. Fig. 2).

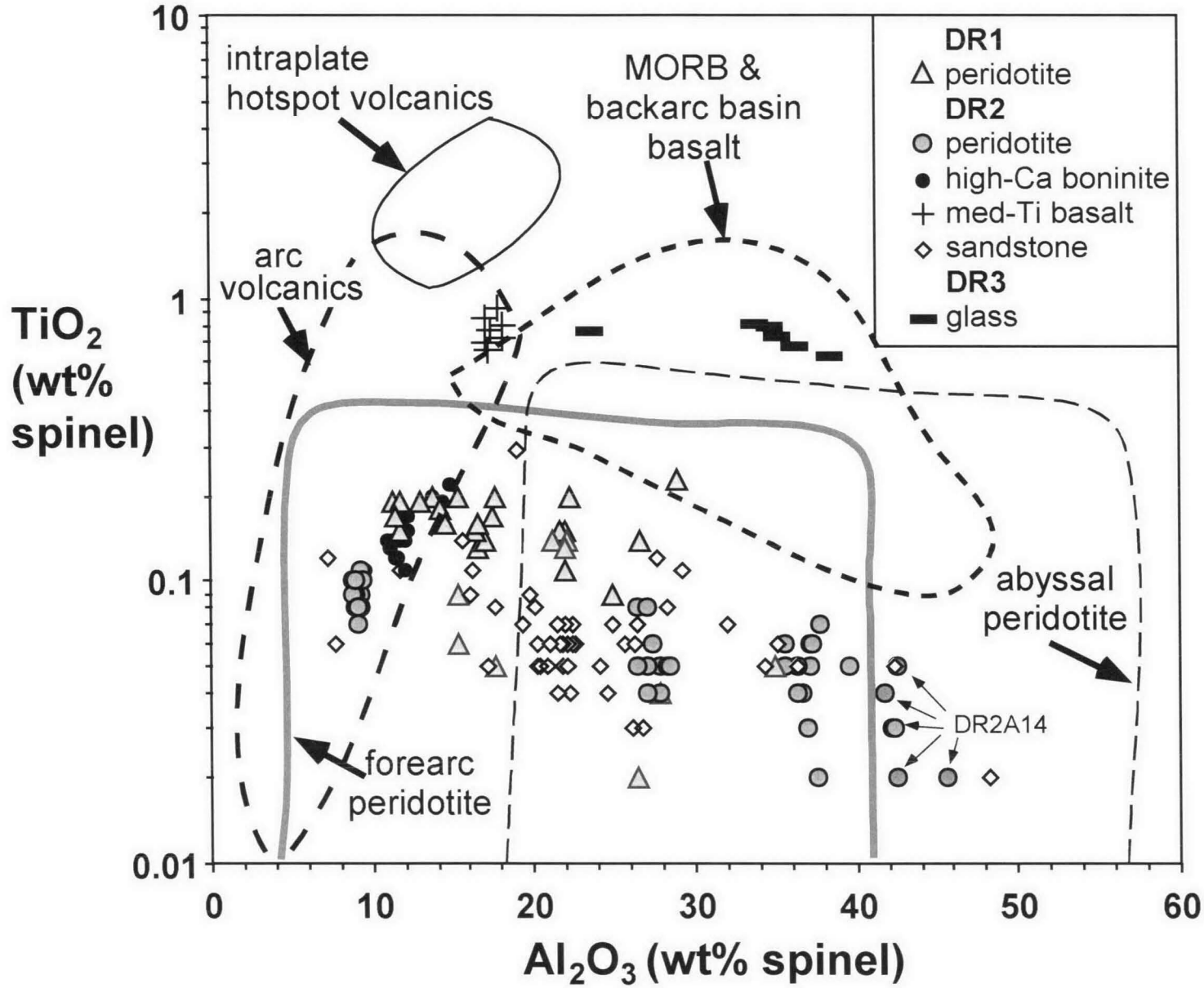

Figure 15. Chrome spinel compositions for the rocks from FAUST-2 dredges 1 (DR1), 2 (DR2) and 3 (DR3). Fields based on Kamenetsky et al. (2001).

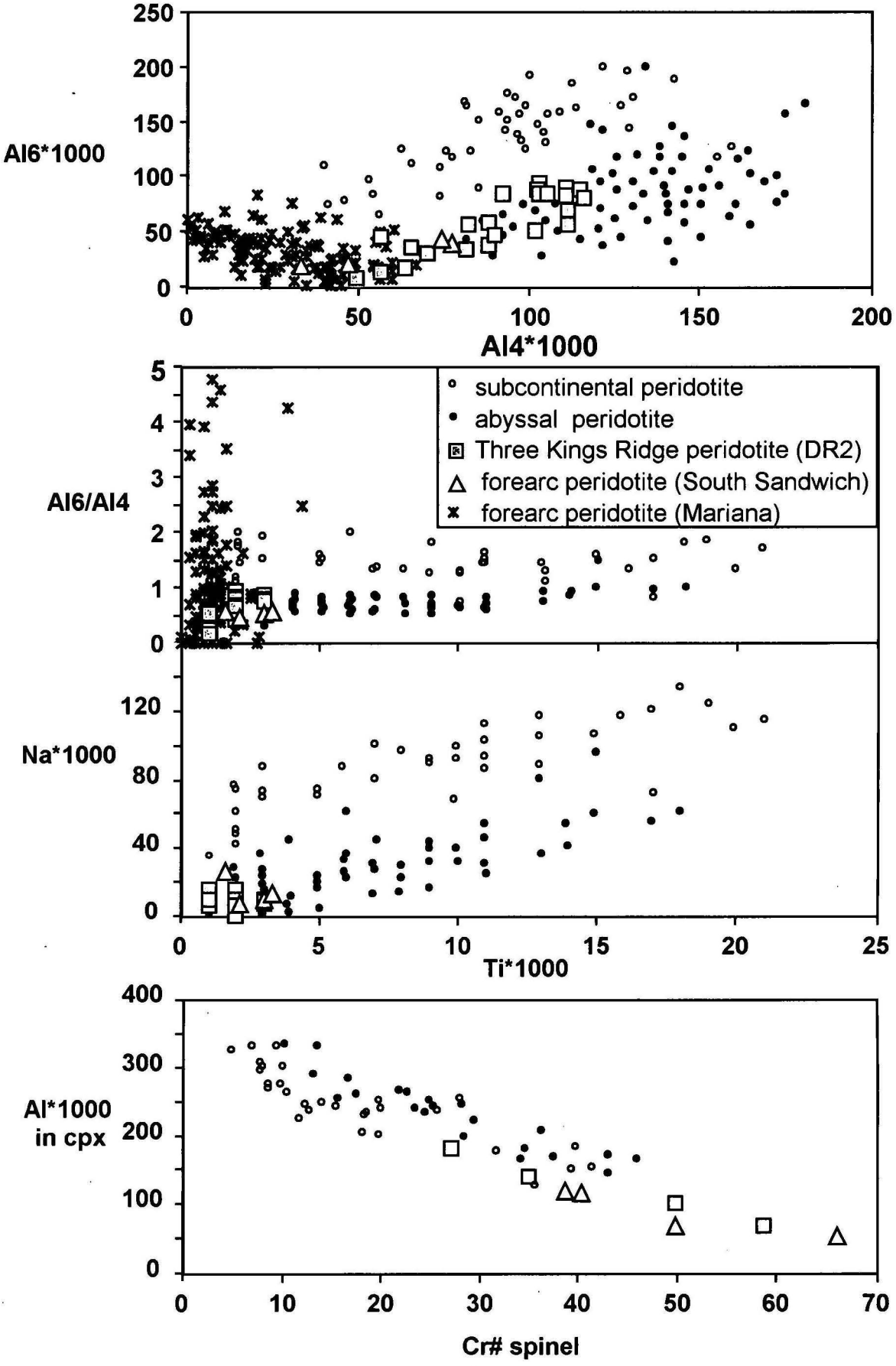

Figure 16. Major element composition of clinopyroxene from FAUST-2 dredge 2 (DR2) compared to clinopyroxene from peridotites worldwide. Abyssal and subcontinental peridotite from Seyler and Bonatti (1994), Mariana forearc peridotite from Parkinson et al. (1992) and Ishii et al. (1992) and South Sandwich peridotite from Pearce et al. (2000). Note: no Na_2O or paired spinel-clinopyroxene data available for the Mariana forearc peridotite.

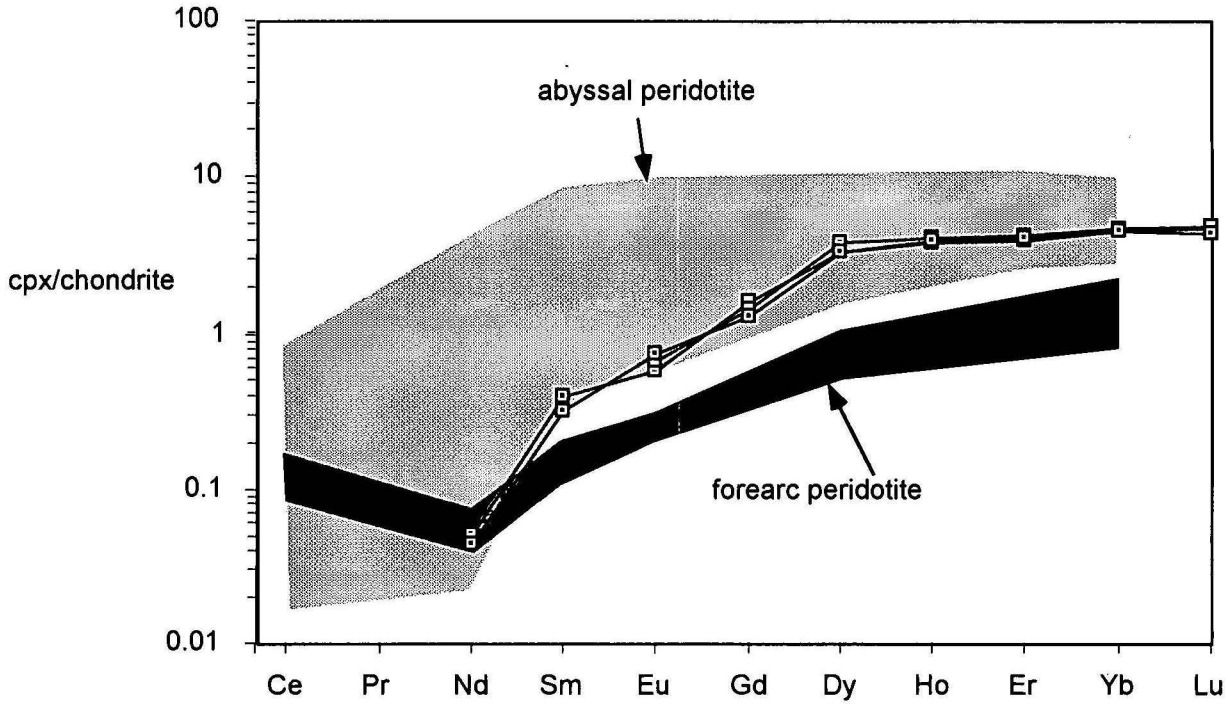

Figure 17. Chondrite-normalised REE diagram showing the composition of clinopyroxene from lherzolite in FAUST-2 dredge 2 sample A14 (DR2A14) compared with those from the forearc of the Mariana arc (Parkinson et al., 1992) and abyssal peridotite (Johnson et al., 1990).

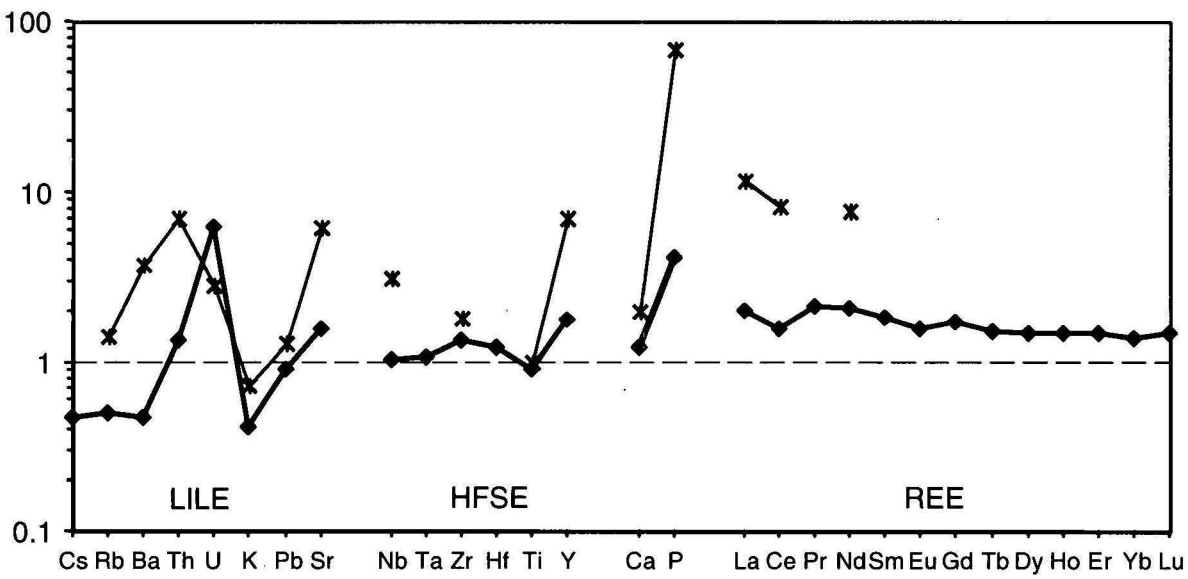

Figure 18. Plot showing alteration in the boninite. The thick line is a slightly altered boninite (0.4% P_2O_5 at 9.3% MgO) and the thin line is a strongly altered boninite (6% P_2O_5 at 3.7% MgO). The values are normalised to an unaltered boninite (0.09% P_2O_5 at 10.9% MgO).

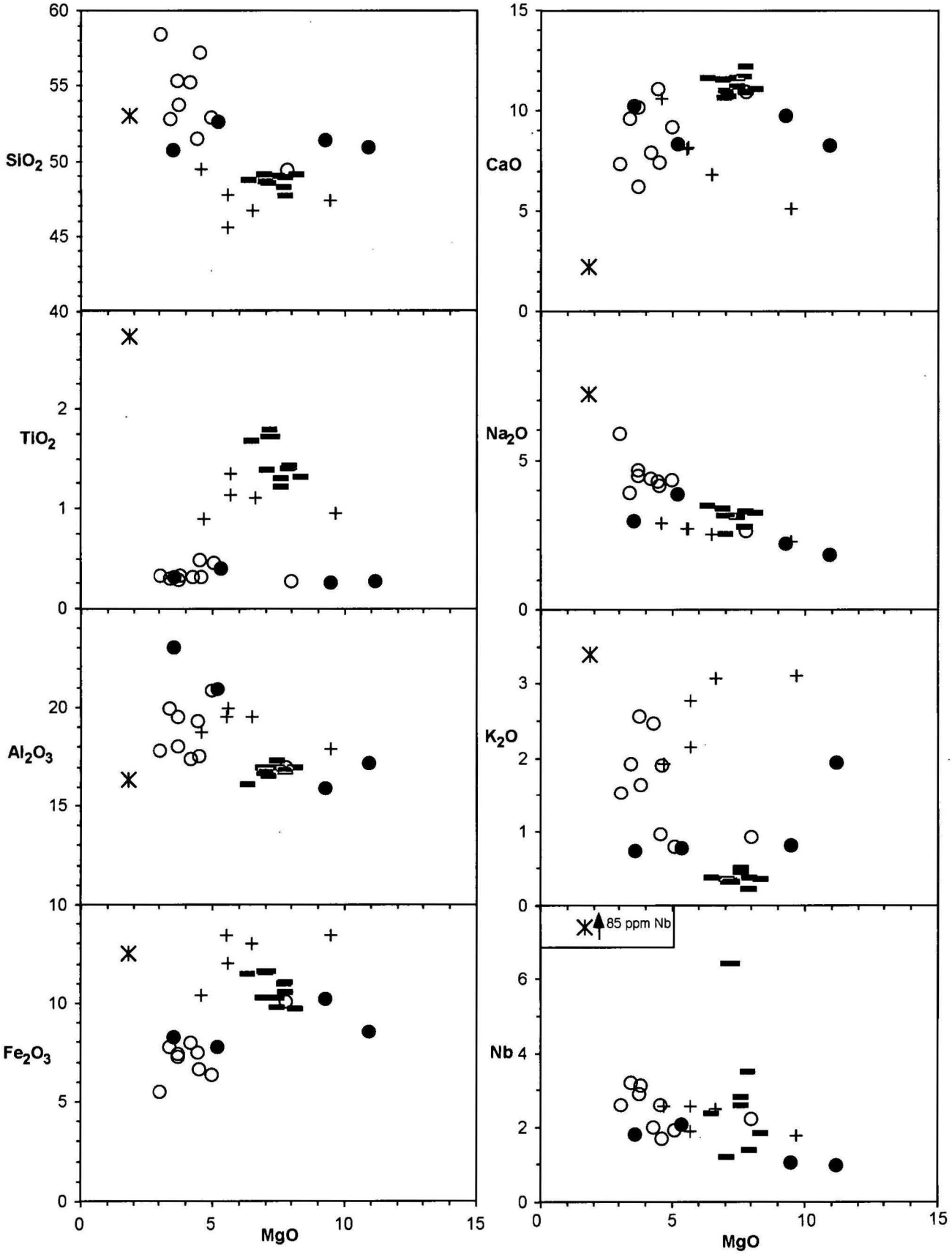

Figure 19. Various plots showing the fractionation trends of the FAUST-2 dredge rocks. Values are recalculated for loss on ignition and P_2O_5-alteration.

● DR2 high-Ca boninite
○ DR2 altered high-Ca boninite
▬ DR3 basaltic glass
▬ DR3 dolerite
✱ DR2 alkalic basalt
+ DR2 medium titanium basalt

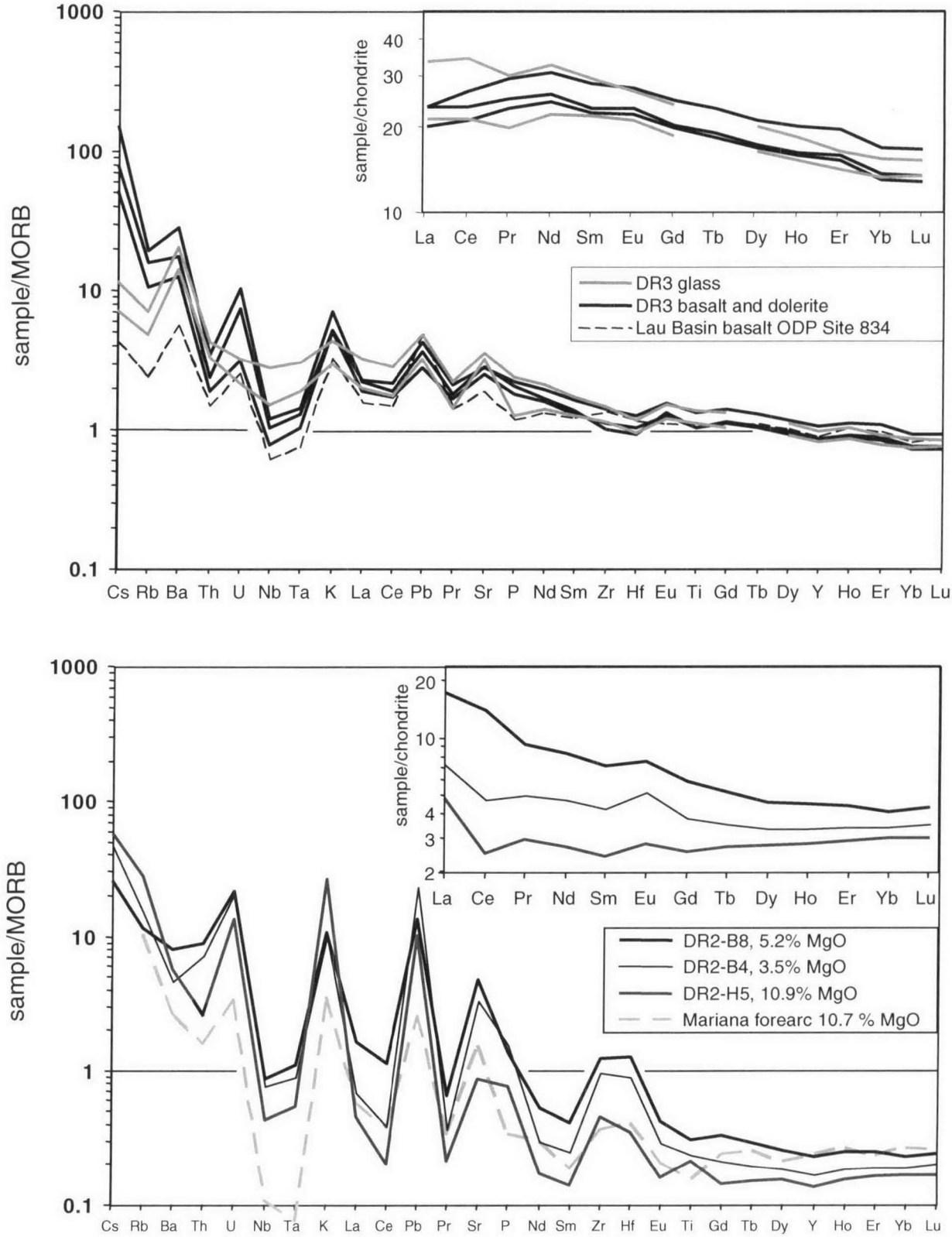

Figure 20. MORB and chondrite-normalised diagrams for FAUST-2 rocks dredged from the Three Kings Ridge (DR2 and DR3). A Lau Basin backarc basalt (Ewart et al., 1994, sample 834B 8R-2 12-18 cm) and a Mariana forearc boninite (Murton et al., 1992, sample 786B 21R-2 103-107 cm) are shown for comparison.

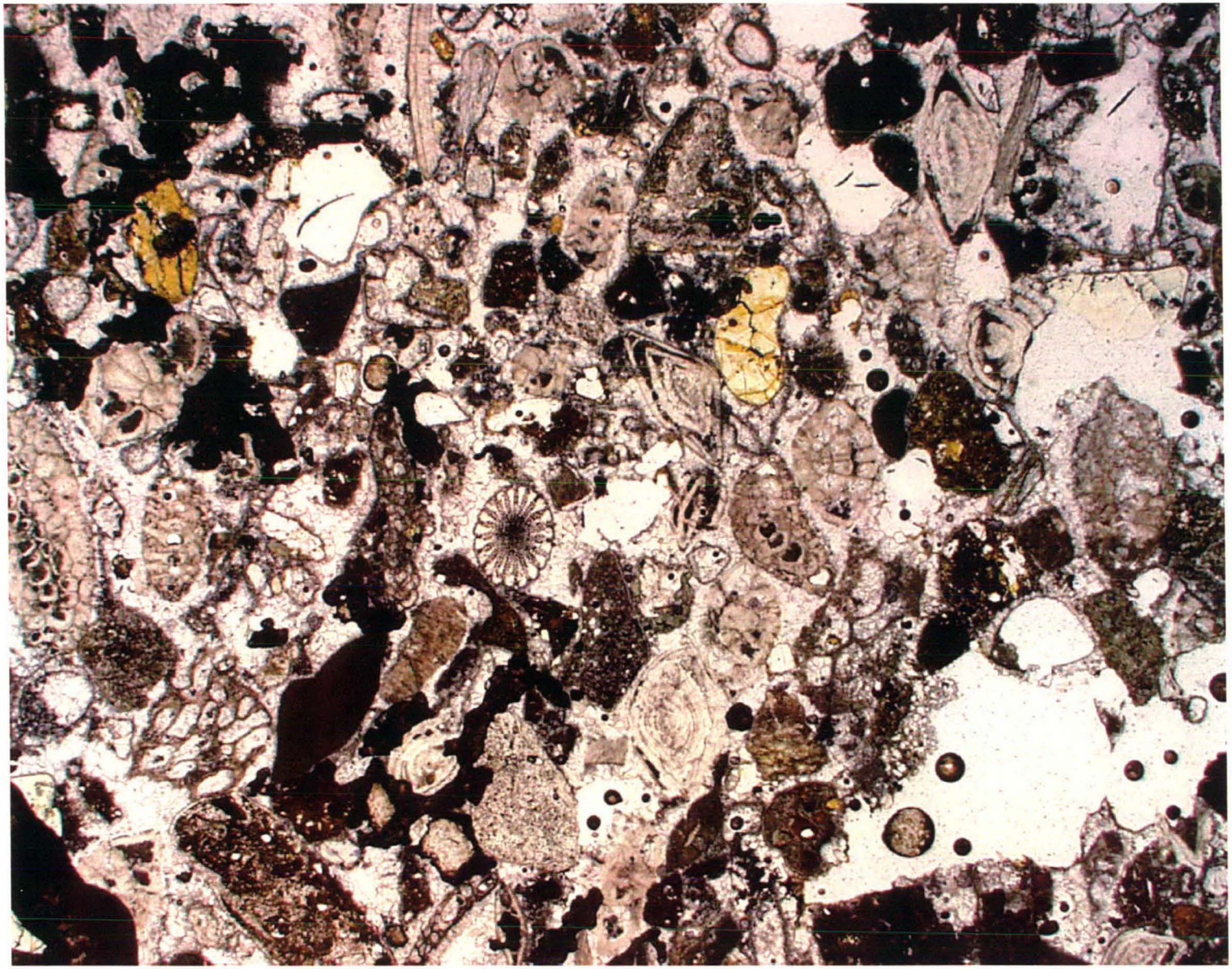

Figure 21. Photomicrograph of sandstone sample from FAUST-2 dredge 2 (DR2E2). Field-of-view is 2 mm with plane-polarised light.

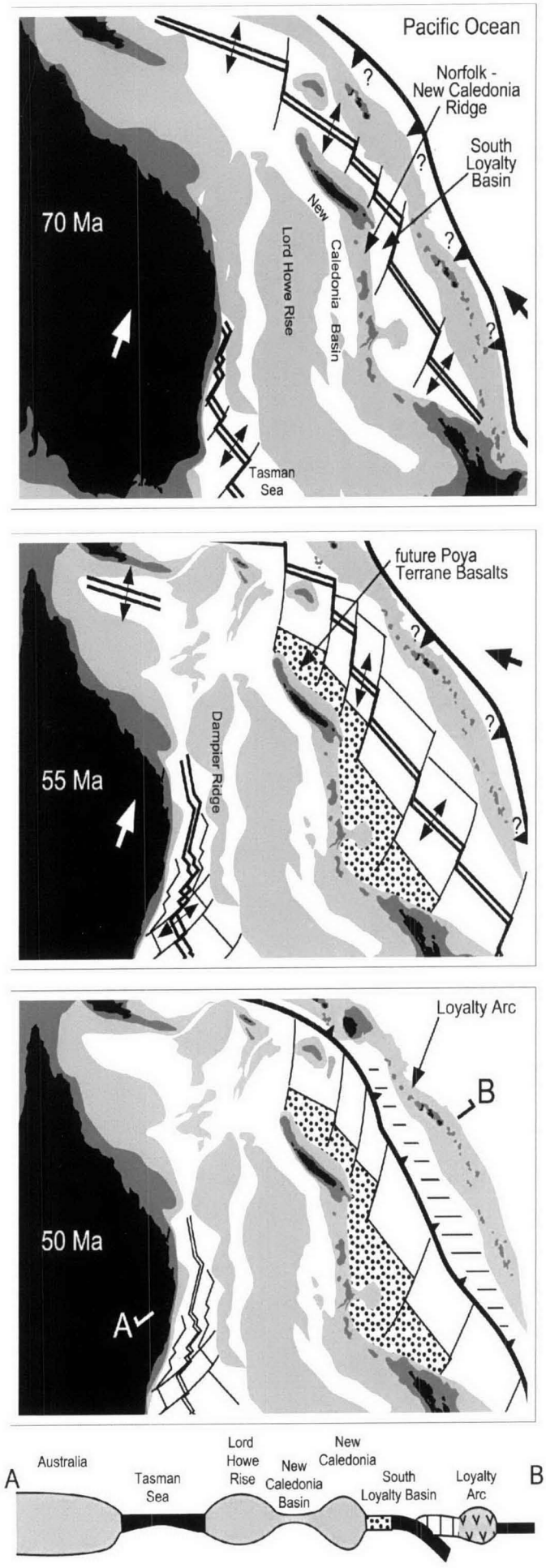

Figure 22. Tectonic reconstructions for the southwest Pacific in the Norfolk Ridge to Three Kings Ridge region from 70 Ma to the present (after Crawford et al., in press, as modified from earlier versions constructed in this report).

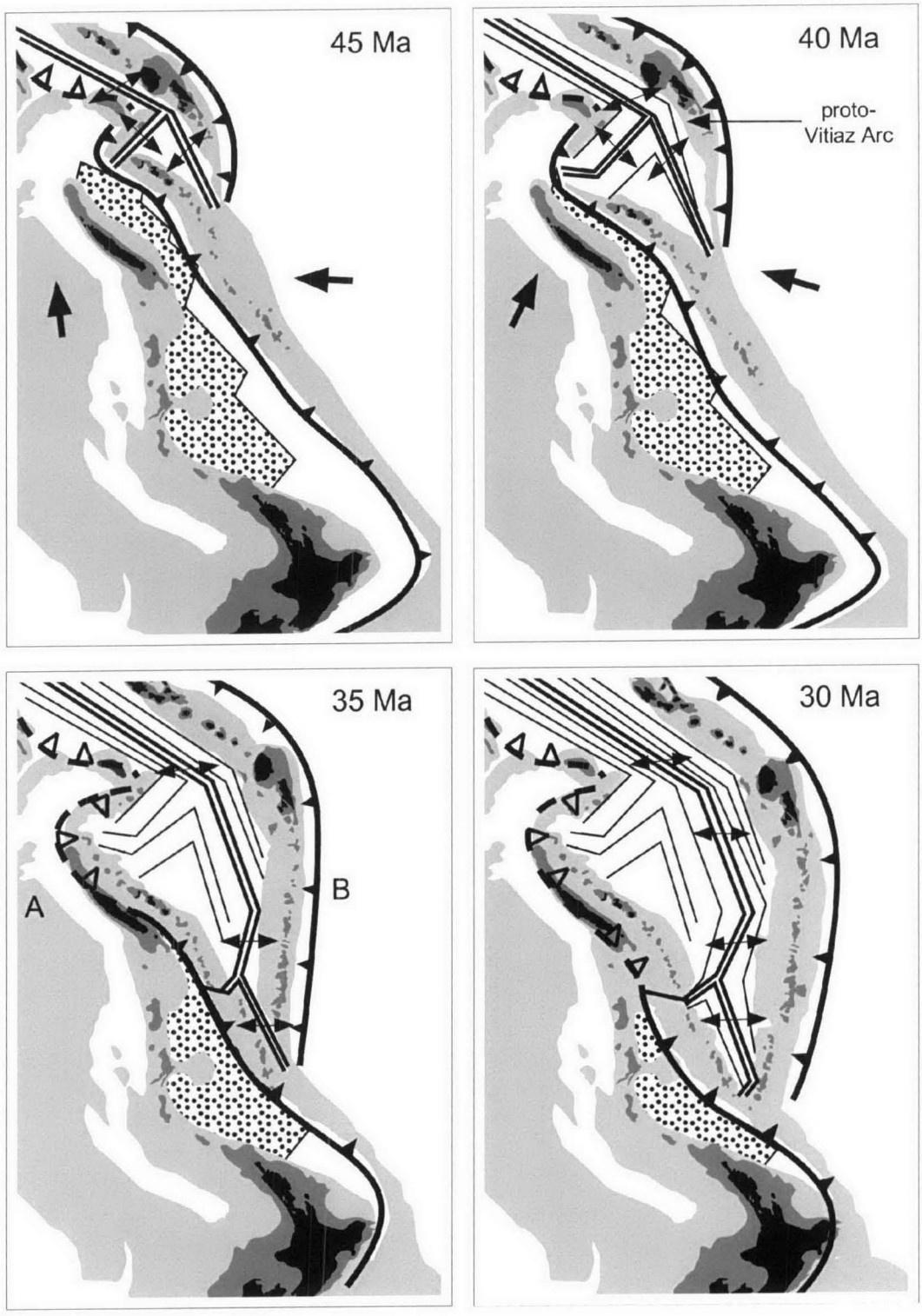

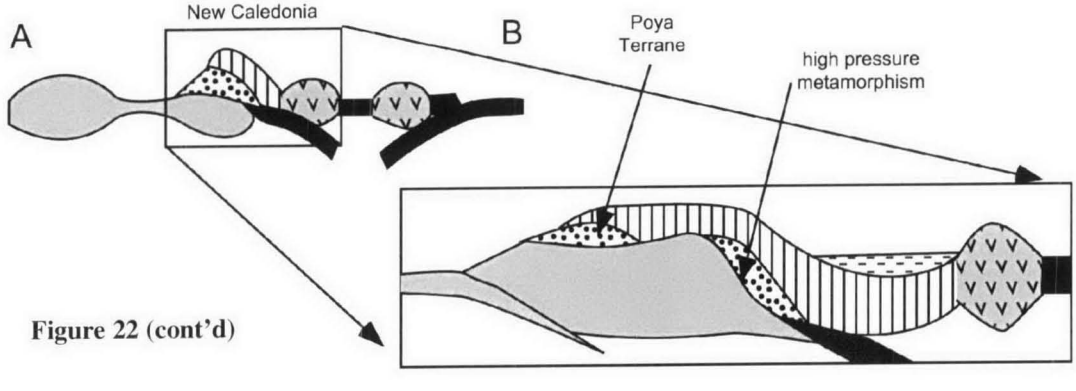

Figure 22 (cont'd)

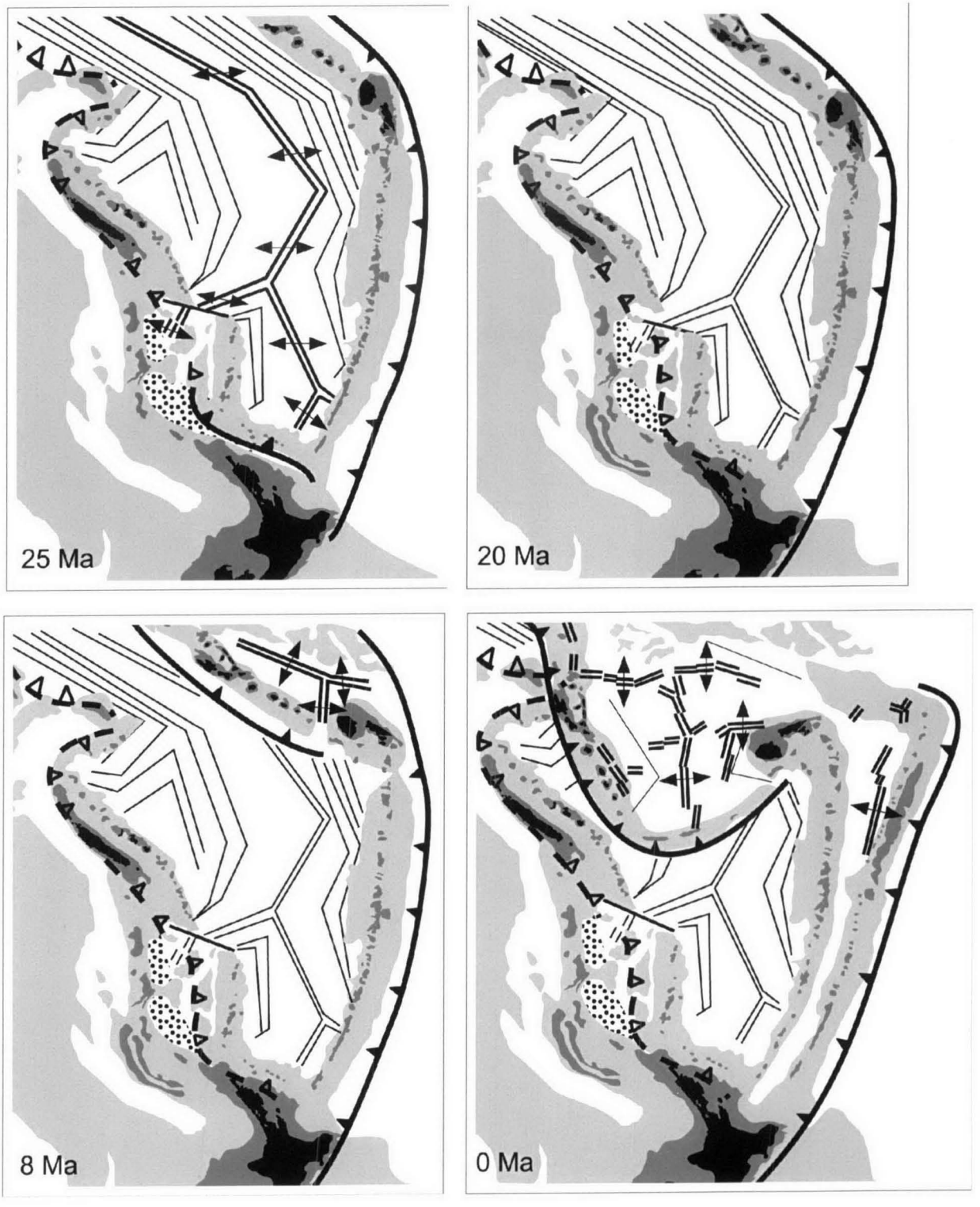

Figure 22 (cont'd)

Three Kings Ridge $^{40}Ar/^{39}Ar$ Report

Geoff Fraser: Geoscience Australia

January 2002

This report presents the results of $^{40}Ar/^{39}Ar$ analyses of several samples dredged from the sea-floor in the region of the Three Kings Ridge, north of New Zealand and east of the Norfolk Basin. Petrology, sample selection and mineral separation were done by Sebastien Meffre at the University of Tasmania. Argon analyses were carried out by Geoff Fraser at the Research School of Earth Sciences, ANU, between November 2001 and January 2002. This work is a contribution to Geoscience Australia's "Law of the Sea Project".

1. INTRODUCTION

1.1 Some caveats

While argon analyses are technically feasible, submarine volcanic samples present several problems which may limit the success of $^{40}Ar/^{39}Ar$ geochronology. A brief summary of these limiting factors is given here as a background to the results presented below.

1. Alteration – Submarine volcanics are typically partially affected by hydrothermal alteration, which may involve addition of K and/or partial loss of radiogenic argon, and result in measured ages significantly younger than the age of extrusion.
2. Excess Argon – Previous studies have found that argon dissolved in basaltic magma may not be outgassed at the time of extrusion, particularly where extrusion has occurred at large water-depths (>1400 m) where hydrostatic pressure is sufficient to inhibit efficient outgassing (Dalrymple & Moore, 1968; Noble & Naughton, 1968). Argon trapped in this manner will tend to produce anomalously old ages relative to the time of extrusion. This effect is likely to be particularly problematic for whole-rock or glass samples.
3. Low Potassium content – Since the $^{40}Ar/^{39}Ar$ method is based on the natural decay of ^{40}K to ^{40}Ar, the low K content of most basalts requires that relatively large samples are required to produce measureable Ar signals. This requirement exacerbates the problem of finding and preparing sufficient fresh material which is free of argon loss (see point 1 above).
4. High Ca/K ratios – In addition to being low in potassium, basalts exhibit high Ca relative to K. The $^{40}Ar/^{39}Ar$ method involves irradiation of sample material by fast neutrons in order to convert a proportion of ^{39}K atoms to ^{39}Ar atoms. However, in addition to the desired $^{39}K(n,p)^{39}Ar$ reaction, several nuclear reactions on Ca also produce Ar isotopes; $^{40}Ca(n, n\alpha)^{36}Ar$, $^{40}Ca(n, \alpha)^{37}Ar$, $^{42}Ca(n, \alpha)^{39}Ar$. Thus, for samples with high Ca/K, correction for nucleogenic Ar from Ca becomes important. These corrections are made by irradiating CaF_2 salt together with sample materials and measuring the production of Ca-derived ^{36}Ar and ^{39}Ar relative to ^{37}Ar which is essentially solely Ca-derived. Corrections can then be made to measurements of unknowns by subtracting an appropriate proportion of measured ^{36}Ar and ^{39}Ar based on the measured ^{37}Ar.

1.2 Data Presentation

The data are graphically presented on both isochron and age spectrum diagrams. The form of the isochron used here plots $^{36}Ar/^{40}Ar$ versus $^{39}Ar/^{40}Ar$ and is sometimes known as the inverse isochron. In this diagram age is not proportional to the slope of a line, as in conventional isochron plots, but is inversely proportional to the x-axis intercept ($^{39}Ar/^{40}Ar$). The y-intercept ($^{36}Ar/^{40}Ar$) represents the isotopic composition of the non-radiogenic component of gas in the sample. The extent to which data define a straight line on this diagram gives an indication of how concordant in age and initial isotopic composition the different gas fractions are. An isochron age is necessarily a pooled age, involving a best fit through several data points.

In contrast, the age spectrum approach calculates an age for each individual gas fraction by assuming that any non-radiogenic gas has the argon isotopic composition of modern day atmosphere. On the inverse isochron plot this is equivalent to assuming a y-intercept of 0.003384 ($^{40}Ar/^{39}Ar = 295.5$ in modern atmosphere) and projecting from this point onto the x-axis to calculate an age from the $^{40}Ar/^{39}Ar$ ratio. Ages as plotted on an age spectrum are therefore "model" ages, and only as good as the assumption of any non-radiogenic argon being atmospheric in composition. The extent to which data

define an atmospheric $^{36}Ar/^{40}Ar$ value for the y-intercept on an inverse isochron plot provides a test of this assumption.

1.3 Analytical Methods

A comprehensive description of the $^{40}Ar/^{39}Ar$ method can be found in McDougall & Harrison (1999). Sample selection and mineral separation was carried out by Sebastien Meffre, at the University of Tasmania. Due to the low K content of the samples, and their relatively young age, severals tens to hundreds of milligrams of sample were required for argon measurement. Consequently all the supplied sample material was irradiated and analysed. Samples were packed in Al-foil and loaded, together with K-glass, CaF_2 salt, and the fluence monitor GA-1550 biotite, into Al canisters for irradiation for four days in position X33.3 in the HIFAR reactor at Lucas Heights, NSW. Cadmium shielding was used to reduce the problem of neutron-induced ^{40}Ar in the relatively high thermal neutron environment of HIFAR. The irradiation canister was inverted three times at exactly one quarter, one half, and three quarters through the irradiation period, to minimise the effect of neutron flux gradients along the length of the canister. Gas extraction for the fluence monitors, K-glass and CaF_2 salt was via argon-ion laser-fusion, with isotopic analysis in a VG3600 mass spectrometer. Step heating of unknowns was accomplished in a double vacuum tantalum furnace attached to a VG1200 mass spectrometer. Heating schedules involved holding the sample at the specified temperature for 15 minutes for each step. Active gas were removed with Zr-Al getters before admission into the mass spectrometer. Data treatment was via the Macintosh software "Noble". Neutron fluence, as given by the "J" parameter, was calculated for the positions of fluence monitors in the irradiation canisters assuming an age of 98.9 Ma for GA-1550 biotite (Renne *et al.* 1998; McDougall, unpublished), and estimated for the unknowns via curve fitting through the GA-1550 data. Similarly, correction factors used to account for K- and Ca-derived neutron-induced isotopes were calculated from analysis of K-glass and CaF_2 salt irradiated with the unknowns. The J values and correction factors are given in the data tables. Age uncertainties quoted in the data tables are at 1σ confidence level and include an estimated uncertainty in J of 0.5 %.

2. RESULTS

DR002B4 Plagioclase from Boninitic basalt

Gas was extracted in seven steps. The age spectrum (Fig. 1 a) is relatively flat over almost 90% of the gas release, but rises to significantly older ages over the final 10% of gas release. Steps 2 and 3 together comprise about 57% of the total gas and yield indistinguishable ages of 12.5 ± 0.5 Ma. Steps 5 and 6 are also indistinguishable from each other in age at ~30 Ma, although significantly less precise due to lower abundance of gas. It is noteworthy that the K/Ca ratio varies inversely with age, suggesting that the age variation is likely due to contamination of a more potassic phase with a very calcic plagioclase.

The total gas age, calculated by combining all gas fractions, is 12.9 ± 1.8 Ma and is clearly dominated by the younger age population associated with higher K/Ca. The inverse isochron plot (Fig 1 b) defines a line (MSWD = 23) with a y-intercept equivalent to a $^{40}Ar/^{36}Ar$ ratio of 303.5, close to the atmospheric value of 295.5, and with an x-intercept corresponding to an age of 11.1 ± 0.2 Ma. This age is largely controlled by steps two and three, which have the highest proportions of radiogenic argon, and as mentioned above are associated with relatively high K/Ca suggestive of potassic contamination.

Due to the likely presence of potassic alteration or contamination, little confidence is placed in the isochron age or the flat section of the age spectrum representing the time of basalt extrusion. Small proportions of potassic alteration with an argon age of ~10 Ma or younger, mixed with a calcic plagioclase with an age of ~30 Ma could explain the age pattern for this sample.

DR002B8 Plagioclase from Boninitic basalt

Gas was extracted in seven steps giving an age spectrum which rises from an age of ~13 Ma to a flat section defined by five consecutive steps constituting almost 60% of the gas release with a weighted mean age of 37.5 ± 0.8 Ma (Fig. 2 a). As noted for sample DR002B4 above, age varies inversely with K/Ca ratio, and the flat section in the age spectrum corresponds to very consistent values for K/Ca. The inverse isochron plot (Fig. 2 b) shows the final five gas fractions which form the flat section of the age spectrum lying along a rather poorly defined line (MSWD = 26) with a y-intercept corresponding to a $^{40}Ar/^{36}Ar$ ratio of ~321, slightly higher than the atmospheric value of 295.5, and an x-intercept giving an age of 36.2 ± 0.2 Ma.

The total fusion age of 29.4 ± 0.8 Ma reflects mixing between the two age populations seen in the age spectrum, and is not regarded as geologically meaningful. The data from this sample are consistent with calcic plagioclase having an age of ~37 Ma, contaminated by a minor amount of potassic alteration with an age of less than 15 Ma.

DR003A1 Plagioclase from Dolerite

Gas was extracted in seven steps with mostly discordant ages. Steps one, two and three all yield ages between 23 and 30 Ma, with steps 2 and 3 being indistinguishable within uncertainties (Fig. 3 a). Steps 4 and 5 yield significantly older ages of 81 and 103 Ma respectively, and are followed by intermediate ages of 47 and 65 Ma for steps 6 and 7. Ages do not vary with K/Ca in a consistent manner. Overall, K/Ca ratios for this sample are low compared with DR002B4 and DR002B8, suggesting that the potassic contamination postulated for the samples described above is not present in DR003A1.

The inverse isochron plot does not define a single line (Fig. 3 b). Steps one, two and three fall on a line with a y-intercept corresponding to a $^{40}Ar/^{36}Ar$ ratio of 288 and define an isochron age of 30.7 ± 0.4 Ma (1 σ). The subsequent four steps in the experiment fall significantly below this line, raising the possibility of a trapped or "excess" argon component with a higher $^{40}Ar/^{36}Ar$ ratio.

Geological interpretation of these data is problematic. The four highest temperature steps appear to be variably affected by excess argon, and are probably geologically meaningless. The first three steps are more consistent in age, and are likely to more closely approximate the time of plagioclase crystallisation. However, the competing effects of argon loss and excess argon cannot be ruled out, suggesting caution in interpretation.

DR003A2 Plagioclase from Dolerite

Gas was extracted in seven steps and defines an extremely discordant age spectrum (Fig. 4 a). Apparent ages range between 47 and 404 Ma with no two consecutive steps yielding concordant ages. There is no consistent variation of K/Ca with age. No meaningful trends can be distinguished on the inverse isochron plot (Fig. 4 b). This sample appears to be extensively affected by a trapped or "excess" argon component with $^{40}Ar/^{36}Ar$ much higher than the modern atmospheric value, making geological age interpretation impossible.

DR003B Basaltic Glass

Gas was extracted in six steps with approximately 70 % of the gas being released in step three. Steps three, four, five and six yield concordant ages at the 2σ level (Fig. 5 a) of ~23 Ma and together constitute over 95 % of the gas. Steps one and two represent only small proportions of the total gas and yield older ages, suggesting the presence of a small amount of loosely bound excess argon. The K/Ca ratio is very consistent for all steps, suggesting a homogeneous composition with little or no alteration. The inverse isochron plot (Fig. 5 b) shows all data, with the exception of step 2, falling on a well defined line (MSWD = 1.15) with an age of 23 ± 0.1 Ma, and a y-intercept corresponding to an essentially atmospheric $^{40}Ar/^{36}Ar$ ratio of 297. The concordance of four steps in the age spectrum, and the consistency of these ages with a well defined isochron age, gives confidence that the age of 23 Ma represents the time of isotopic closure of this glass, presumably corresponding to the age of extrusion.

3. SUMMARY

Five samples dredged from the sea floor in the vicinity of the Three Kings Ridge have been analysed by the $^{40}Ar/^{39}Ar$ step heating method. Plagioclase from sample DR002B8, while partially affected by argon loss associated with potassic alteration, yields a best estimate age for crystallisation of 37.5 ± 0.8 Ma. Plagioclase from the associated sample DR002B4 appears to have experienced more extensive alteration-related argon loss, but the final part of the age spectrum is suggestive of a crystallisation age of at least ~30 Ma, consistent with the results from DR002B8. Plagioclase from samples DR003A1 and DR003A2 contains significant proportions of excess argon, obscuring geological age information. Basaltic glass from DR003B yields a well-behaved age spectrum indicating an age of 23.0 ± 0.1 Ma for the timing of extrusion.

4. REFERENCES

Dalrymple, G. B. & Moore, J. M., 1968. ^{40}Ar excess in submarine pillow basalts from Kilauea Volcano, Hawaii. Science, 161, 1132 – 1135.

McDougall, I. & Harrison, T. M. Geochronology and thermochronology by the $^{40}Ar/^{39}Ar$ method. 2nd Edition, Oxford University Press, 1999.

Noble, C. S. & Naughton, J. J., 1968. Deep-ocean basalt: inert gas content and uncertainties in age dating. Science, 162, 265 – 267.

Renne, P. R., Swisher, C. C., Deino, A. L., Karner, D. B., Owens, T. L. and DePaolo, D. J., 1998. Intercalibration of standards, absolute ages and uncertainties in 40Ar/39Ar dating. Chemical Geology (Isotope Geoscience section), 145, 117 – 152.

Sample DR002B4 Plagioclase

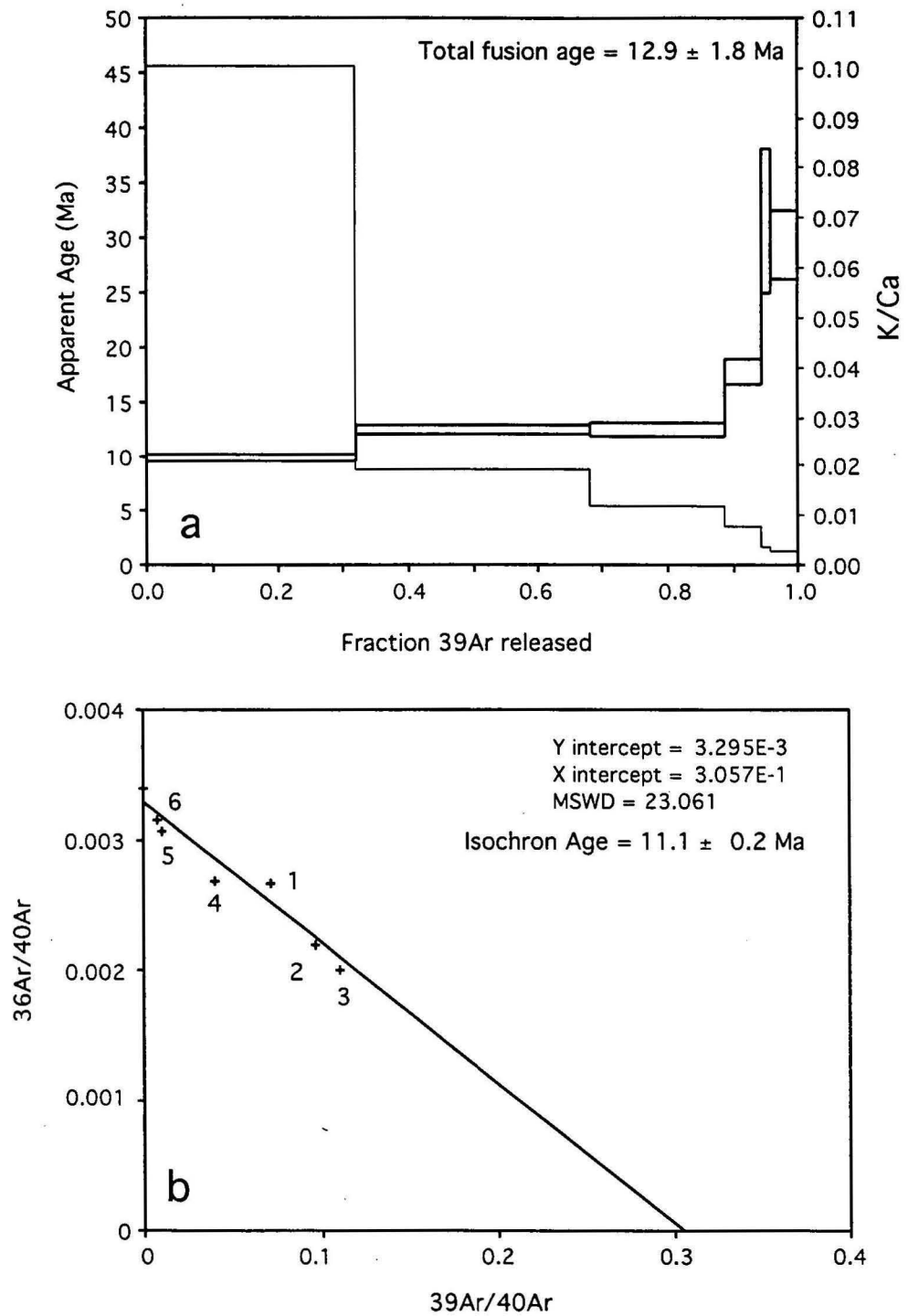

Figure 1. Argon isotopic data for sample DR002B4 Plagioclase.
a) Age spectrum shown in bold, and K/Ca values. b) inverse isochron plot. Numbers adjacent to data points refer to heating steps.

Sample DR002 B8 Plagioclase

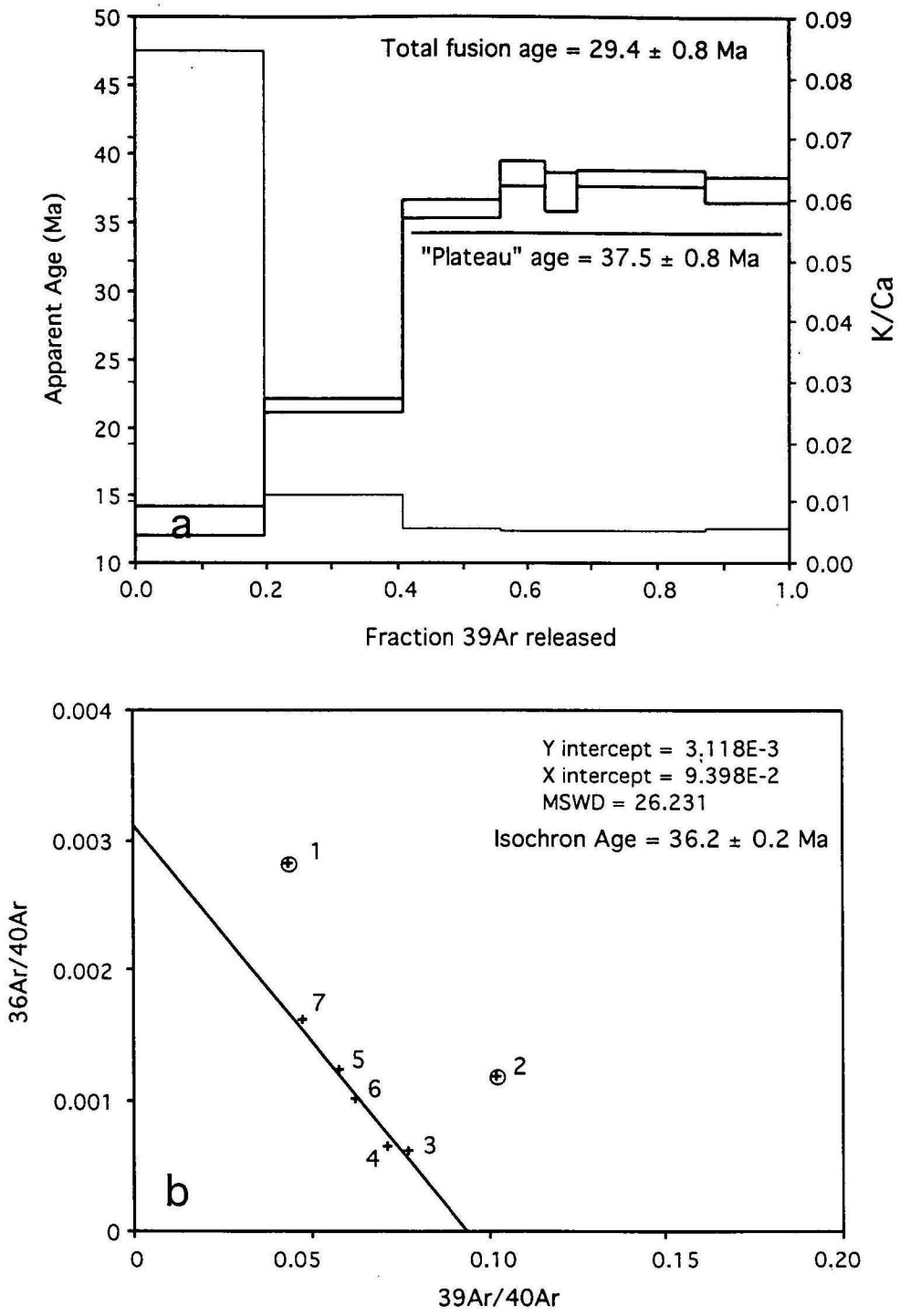

Figure 2. Argon isotopic data for sample DR002B8 Plagioclase.
a) Age spectrum shown in bold, and K/Ca values. b) inverse isochron plot. Numbers adjacent to data points refer to heating steps. Circled data points not included in regression to calculate isochron age.

Sample DR003A1 Plagioclase

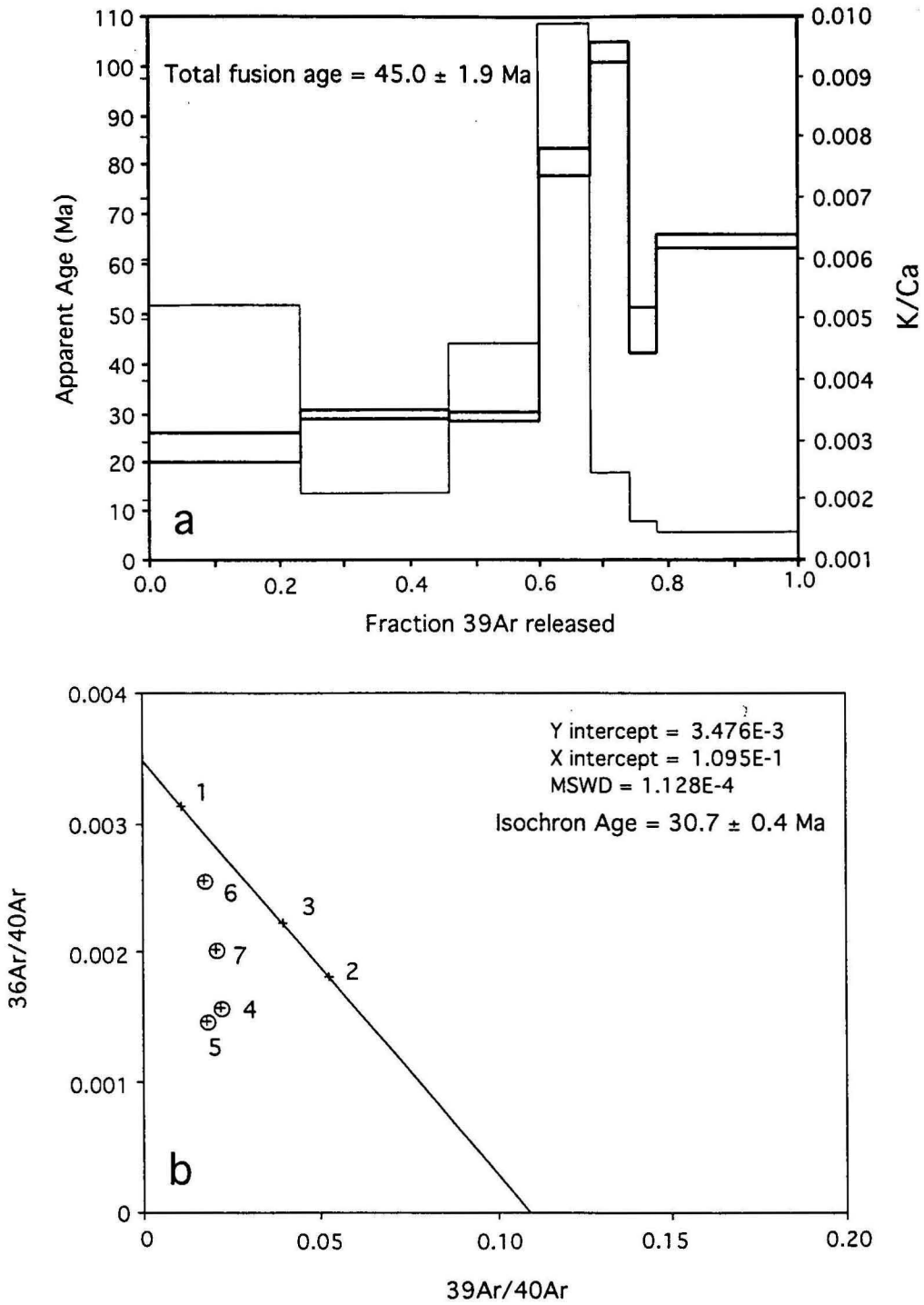

Figure 3. Argon isotopic data for sample DR003A1 Plagioclase.
a) Age spectrum shown in bold, and K/Ca values. b) Inverse isochron plot. Numbers adjacent to data points refer to heating steps. Circled data points not included in regression.

Sample DR003 A2 Plagioclase

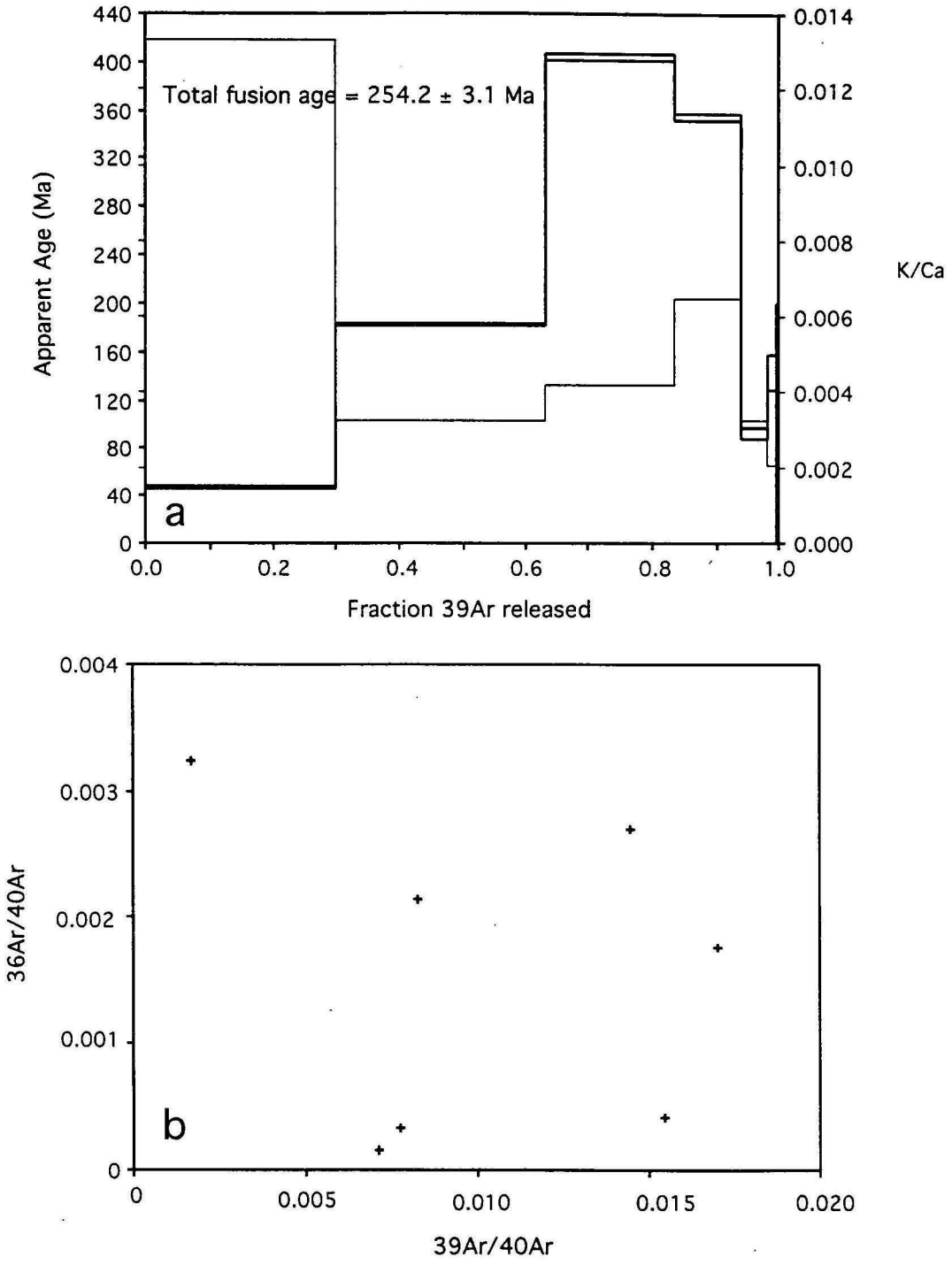

Figure 4. Argon isotopic data for sample DR003A2 Plagioclase.
a) Age spectrum shown in bold, and K/Ca values. b) Inverse isochron plot. Numbers adjacent to data points refer to heating steps. The scatter in these data do not allow for any meaningful regression.

Sample DR003B Glass

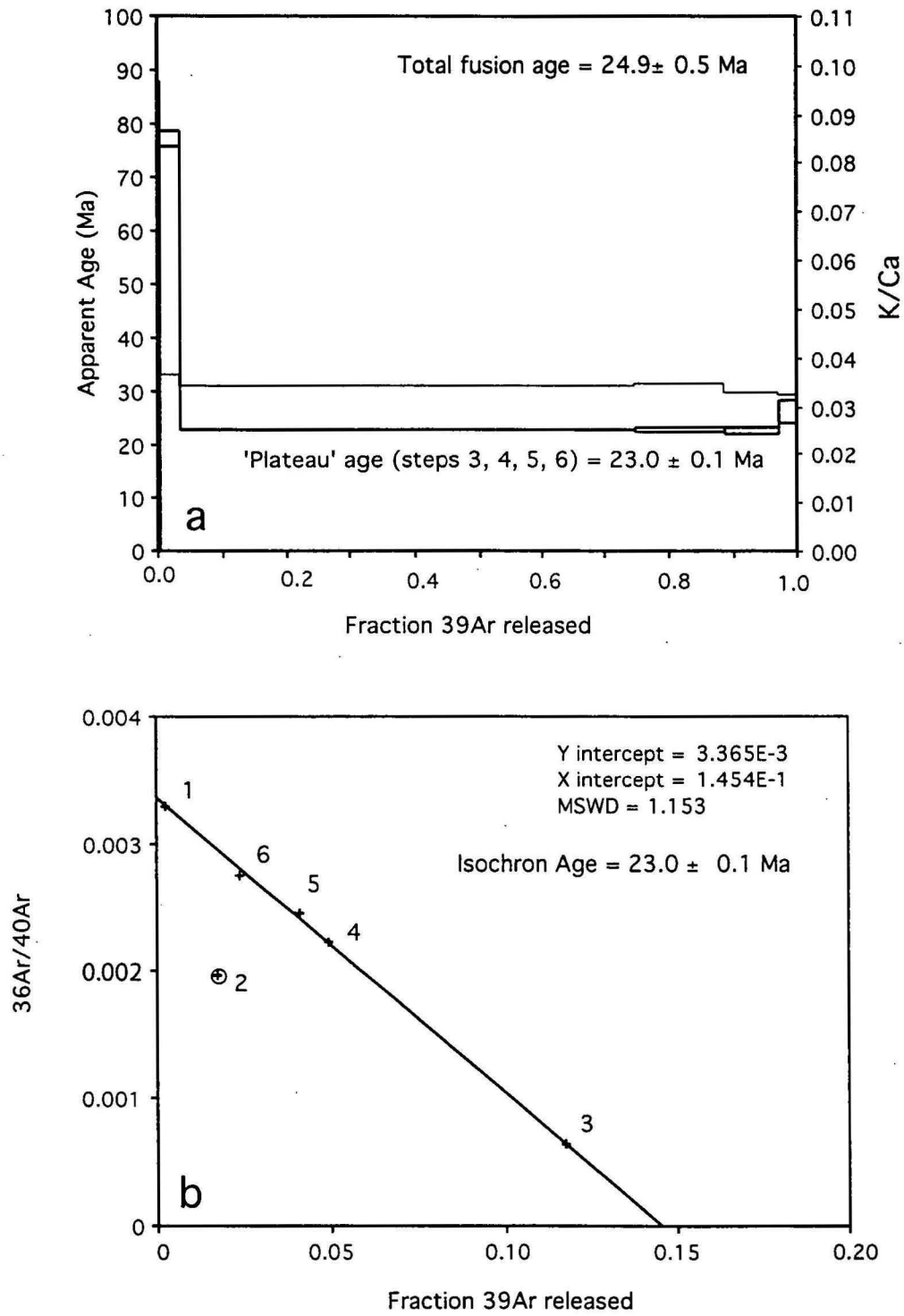

Figure 5. Argon isotopic data for sample DR003B Basaltic Glass.
a) Age spectrum shown in bold, and K/Ca values. b) Inverse isochron plot. Numbers adjacent to data points refer to heating steps. Step 2 was not included in the regression.

Table 1. Argon isotopic data for sample DR002B4 Plagioclase.

Temp (°C)	^{36}Ar 10^{-16} mol	^{37}Ar 10^{-13} mol	^{39}Ar 10^{-15} mol	^{40}Ar 10^{-13} mol	$\%^{40}Ar^*$	$^{40}Ar^*/^{39}Ar_K$	$^{39}Ar(\%)$	Age (Ma) ± 1 s.d.	Ca/K
DR002B4 Plagioclase, J = 1.887 x 10^{-3}									
700	9.34	1.25	23.90	3.35	20.9	2.944	31.91	10.0 ± 0.3	9.95
850	8.63	7.37	27.60	2.82	34.9	3.657	68.03	12.4 ± 0.4	52.00
950	5.12	6.96	16.10	1.41	40.6	3.686	88.8	12.5 ± 0.5	85.40
1050	3.74	2.75	4.41	1.06	20.8	5.266	94.38	17.8 ± 1.2	125.00
1150	3.37	1.38	1.10	0.95	9.6	9.362	95.69	31.6 ± 6.5	269.00
1250	14.50	6.40	3.68	3.93	6.9	8.713	99.85	29.4 ± 3.2	392.00
1400	14.40	0.23	0.13	4.23	0	0.001	100	0.0 ± 791.2	395.00
Total	59.10	26.30	76.90	17.70		3.805		12.9 ± 1.8	

Sample mass = 60 mg. Correction factors: $[^{36}Ar/^{37}Ar]_{Ca} = 3.31 \times 10^{-4}$; $[^{39}Ar/^{37}Ar]_{Ca} = 8.90 \times 10^{-4}$; $[^{40}Ar/^{39}Ar]_K = 3.0 \times 10^{-2}$

Table 2. Argon isotopic data for sample DR002B8 Plagioclase.

Temp (°C)	^{36}Ar 10^{-16} mol	^{37}Ar 10^{-13} mol	^{39}Ar 10^{-14} mol	^{40}Ar 10^{-13} mol	$\%^{40}Ar^*$	$^{40}Ar^*/^{39}Ar_K$	$^{39}Ar(\%)$	Age (Ma) ± 1 s.d.	Ca/K
DR002B8 Plagioclase, J = 1.905 x 10^{-3}									
700	9.97	0.92	1.48	3.41	16.5	3.823	19.5	13.1 ± 1.0	12
850	4.63	7.62	1.67	1.57	64.6	6.335	40.79	21.7 ± 0.5	90
1000	4.71	10.51	1.21	1.46	81.6	10.60	55.76	36.1 ± 0.7	177
1080	2.43	5.35	0.58	0.76	80.6	11.34	62.91	38.6 ± 0.9	188
1160	2.05	3.55	0.38	0.61	62.9	10.94	67.59	37.2 ± 1.4	191
1300	7.65	14.42	1.60	2.38	69.7	11.24	87.2	38.2 ± 0.6	186
1400	6.72	9.33	1.04	2.05	51.7	11.01	100	37.5 ± 1.0	184
Total	38.15	51.70	7.96	12.26		8.618		29.4 ± 0.8	

Sample mass = 119 mg. Correction factors: $[^{36}Ar/^{37}Ar]_{Ca} = 3.62 \times 10^{-4}$; $[^{39}Ar/^{37}Ar]_{Ca} = 8.13 \times 10^{-4}$; $[^{40}Ar/^{39}Ar]_K = 3.0 \times 10^{-2}$

Table 3. Argon isotopic data for sample DR003A1 Plagioclase.

Temp (°C)	^{36}Ar 10^{-16} mol	^{37}Ar 10^{-13} mol	^{39}Ar 10^{-15} mol	^{40}Ar 10^{-13} mol	$\%^{40}Ar^*$	$^{40}Ar^*/^{39}Ar_K$	$^{39}Ar(\%)$	Age (Ma) ± 1 s.d.	Ca/K
DR003A1 Plagioclase, J = 1.883 x10^{-3}									
700	29.09	8.92	9.59	8.29	7.3	6.839	23.15	23.1 ± 3.0	191.00
800	10.59	21.74	10.55	1.69	46.2	8.858	46.14	29.8 ± 0.9	469.00
920	5.16	6.15	5.85	1.36	34.2	8.69	60.12	29.3 ± 1.1	218.00
1050	2.75	1.62	3.16	1.39	53.2	24.289	68.02	80.7 ± 2.8	101.00
1150	3.51	4.81	2.65	1.25	56.5	31.179	73.93	102.9 ± 1.9	403.00
1250	4.29	5.39	2.10	0.95	24.4	13.899	78.28	46.6 ± 4.5	614.00
1400	18.58	30.23	10.73	4.02	40.2	19.369	100	64.6 ± 1.6	690.00
Total	73.96	78.86	44.62	18.95		13.408		45.0 ± 1.9	

Sample mass = 129 mg. Correction factors: $[^{36}Ar/^{37}Ar]_{Ca} = 3.46 \times 10^{-4}$; $[^{39}Ar/^{37}Ar]_{Ca} = 7.95 \times 10^{-4}$; $[^{40}Ar/^{39}Ar]_K = 3.0 \times 10^{-2}$

Table 4. Argon isotopic data for sample DR003A2 Plagioclase.

Temp (°C)	^{36}Ar 10^{-16} mol	^{37}Ar 10^{-13} mol	^{39}Ar 10^{-15} mol	^{40}Ar 10^{-13} mol	$\%^{40}Ar^*$	$^{40}Ar^*/^{39}Ar_K$	$^{39}Ar(\%)$	Age (Ma) ± 1 s.d.	Ca/K
DR003A2 Plagioclase, J = 1.875 x 10^{-3}									
700	13.69	2.70	7.04	4.71	20.3	13.99	29.74	46.7 ± 1.6	75.20
850	6.57	12.47	8.67	4.97	87.8	56.78	63.21	182.5 ± 1.1	308.00
950	3.12	5.87	5.16	6.59	95.5	133.94	83.67	404.2 ± 2.4	237.00
1050	1.72	1.93	2.53	3.06	90.1	115.68	94.03	354.2 ± 3.0	154.00
1150	1.56	1.54	1.08	0.57	47.6	27.97	98.23	92.2 ± 4.4	305.00
1250	1.11	0.80	0.38	0.38	36.4	44.06	99.6	143.2 ± 14.5	484.00
1400	1.82	0.16	0.10	0.54	4.4	26.28	100	86.8 ± 113.7	324.00
Total	29.60	25.48	24.96	20.82		64.445		205.8 ± 2.5	

Sample mass = 49 mg. Correction factors: $[^{36}Ar/^{37}Ar]_{Ca} = 3.63 \times 10^{-4}$; $[^{39}Ar/^{37}Ar]_{Ca} = 7.85 \times 10^{-4}$; $[^{40}Ar/^{39}Ar]_K = 3.0 \times 10^{-2}$

Table 5. Argon isotopic data for sample DR003B Glass.

Temp (°C)	^{36}Ar 10^{-16} mol	^{37}Ar 10^{-13} mol	^{39}Ar 10^{-15} mol	^{40}Ar 10^{-13} mol	$\%^{40}Ar^*$	$^{40}Ar^*/^{39}Ar_K$	$^{39}Ar(\%)$	Age (Ma) ± 1 s.d.	Ca/K
DR003B Glass, J = 1.863 x 10^{-3}									
700	8.69	0.03	0.68	2.64	2.9	11.33	0.4	37.67 ± 50.37	8.8
800	5.71	0.71	4.99	2.78	41.6	23.47	3.6	77.18 ± 1.49	27.4
950	11.22	16.86	111.90	9.40	80.8	6.89	74.6	23.01 ± 0.09	29.1
1050	11.04	3.36	22.49	4.49	34.1	6.90	88.9	23.05 ± 0.47	28.8
1150	8.31	2.02	12.91	3.14	27.5	6.79	97.1	22.66 ± 0.72	30.2
1250	5.56	0.74	4.66	1.94	18.6	7.85	100.0	26.20 ± 2.18	30.6
Total	50.52	23.72	157.60	24.38		7.46		24.88 ± 0.52	

Sample mass = 59 mg. Correction factors: $[^{36}Ar/^{37}Ar]_{Ca} = 3.10 \times 10^{-4}$; $[^{39}Ar/^{37}Ar]_{Ca} = 9.90 \times 10^{-4}$; $[^{40}Ar/^{39}Ar]_K = 3.0 \times 10^{-2}$